LASER SELF FOCUSING AND RELATED PHENOMENA IN PLASMAS

L. A. PATEL

DEPARTMENT OF PHYSICS
INDIAN INSTITUTE OF TECHNOLOGY, DELHI

LASER SELF FOCUSING AND RELATED PHENOMENA IN PLASMAS

Thesis submitted to the
Indian Institute of Technology, New Delhi
for the award of the degree of
Doctor of Philosophy

Lalitbhai Atmaram PATEL

Department of Physics
Indian Institute of Technology, New Delhi
May, 1978

ACKNOWLEDGEMENTS

No word would suffice to express my deep regards for Professor M.S.Sodha without whose guidance my Ph.D. work would not have even started. I am much indebted to Dr. D.P.Tewari and Dr. V.K.Tripathi who catalysed the work. I take this opportunity to thank Professor A.K. Ghatak and Professor C.L. Mehta for keen interest in my work, and to Dr. R.P.Sharma and Dr. S.C.Kaushik for guidance at several stages of the work.

I am very much thankful to my colleagues in the Electrophysics Laboratory for providing me with a stimulating academic environment, and to Mr. T.N.Gupta for elegant typing of the present thesis. I am thankful to the National Council of Educational Research & Training (India) for financial assistance.

I am grateful to my maternal and other relatives for helping me in various ways, to Laxmi for L , and to parents for parental care. I dedicate this thesis to my grandmother in the fond memories of my grandfather.

Lalit A. Patel
1978 05 21

(Lalit A. Patel)

ABSTRACT

The present thesis is devoted to a theoretical study of various aspects of laser self focusing and effect of self focusing on parametric excitations and ion acoustic solitons in plasmas. The first two chapters present an analysis of self focusing of a laser beam (or pulse) in a plasma whose concentration may vary in time and space. The effect of appropriate boundary conditions and temperature-dependence of the thermal conduction process is seen to be quite significant. New criteria for monotonic and oscillatory defocusing of the laser beam have been derived. Nonlinearity in the absorption is seen to enhance the possibility of focusing of the beam. The direct coupling between the left and right circularly polarized modes, in the presence of an axial static magnetic field, leads to axial asymmetry of the intensity-profiles of the two modes. In the final two chapters, the effect of self focusing has been analysed. The expression for the temporal growth rate of a parametric excitation is seen to be modified, and moreover, the excitation is seen to become considerably nonuniform on account of self focusing of the pump laser beam. It is seen that the ion-acoustic solitons, in order to get destabilized, require a very inhomogeneous and intense electromagnetic field.

CONTENTS

PREFACE

In the presence of a high power laser beam, a large number of nonlinear phenomena - e.g. self focusing[1-5], parametric excitations[6-10], soliton formation[11-15] - can occur in a plasma. These phenomena constitute a class of nonlinear physics[16-18] - a subject of much activity in recent years. Apart from academic interest, these phenomena also have some relevance to thermonuclear fusion[19] and ionospheric modifications[20]. The self focusing[1-5] can concentrate energy of the laser beam into smaller regions of the plasma and can influence several other processes. Parametric excitations[6-10] generate electrostatic waves which eventually heat the plasma through their Landau damping. The presence of solitons[11-15] can also influence heating of the plasma. The present thesis is devoted to the study of various aspects of laser self focusing and effect of the laser self focusing on parametric excitations and ion acoustic solitons in plasmas. In the following, a brief survey of the relevant literature and a chapterwise summary of the present thesis have been presented.

Self Focusing in Plasmas

The dielectric constant of a plasma[3,4], irradiated by a laser beam (of nonuniform distribution) generally

increases with the intensity of the beam. For a beam of radially Gaussian intensity distribution, the phase velocity of various parts of the wavefront decreases with the radial distance. The wavefront attains a curvature and tends to converge the beam. This process is accompanied by the diffraction-divergence of the beam. When the intensity of the beam is high enough, the nonlinear self-convergence predominates over the diffraction - divergence and the beam gets self focused. The threshold intensity for self focusing is usually quite low (much lower than most of the other nonlinear phenomena), and hence laser self focusing can occur very easily[1-5].

The nonlinearity in (i.e. intensity-dependence of) the dielectric constant of a plasma arises due to a variety of reasons: (1) relativistic increase in the electron mass[21-23], (2) redistribution of the plasma by the ponderomotive force[1,24-28], and (3) redistribution of the plasma due to the nonuniform heating of electrons[4,29-35]. The first mechanism is operative instantaneously; however, the corresponding nonlinearity is weak. The second mechanism is operative on a time scale $\tau_p \sim r_0 / c_s$ (where r_0 is the initial laser beamwidth and c_s is the ion acoustic speed); the corresponding nonlinearity is moderate. The last mechanism, which leads to the strongest nonlinearity, is operative on larger time scale

$\tau_\epsilon \sim M/m\nu$ (where M is the mass of an ion or a neutral, m is the electron mass and ν is the electron collision frequency). All these mechanisms of nonlinearity have been widely discussed in the earlier literature.

There exist several approaches[1,36-39] to the problem of laser self focusing. The approach due to Akhmanov et al.[1] is the most widely used[1-5], because it is very straightforward and yet gives reasonable results in the paraxial region. Earlier analyses[4,40,41] have shown that if the initial beamwidth exceeds the mechanism-dependent critical beamwidth, there exist two values of the initial axial intensity E_o^2 (called lower and upper self trapping intensities E_{stl}^2 and E_{stu}^2) for which the beam becomes self trapped. The beam experiences monotonic defocusing, oscillatory focusing or oscillatory defocusing depending upon whether $E_o^2 < E_{stl}^2$, $E_{stl}^2 < E_o^2 < E_{stu}^2$ or $E_o^2 > E_{stu}^2$.

Experiments[5] on the propagation of laser pulses in nonlinear media had observed that the laser pulse propagates like a self trapped filament. This was interpreted on the basis of the concept of 'moving foci'[5,36]. Several other aspects of the experimental observations[42-45] on self focusing of laser pulses in plasmas have been touched upon in recent theories[46-48]. A recent numerical analysis[49] of the problem of transient self focusing has revealed that

the time-dependence of the intensity-profile of a laser pulse undergoes qualitative changes as the pulse propagates.

It has been observed that an intense laser beam can penetrate much farther than the normal skin depth[50,51] in an overdense plasma[52-56] (i.e. a plasma whose plasma frequency exceeds the laser frequency). This kind of anomalous penetration has been explained[41] in terms of the plasma-redistribution caused by the ponderomotive force.

Many experiments[53-56] have observed that a laser beam propagates like a self trapped filament after travelling for a certain distance. Independent of these experiments, a numerical analysis[57] and another analytical investigation[58,59] have revealed that the laser absorption can lead to damping of oscillations of the laser beamwidth.

Though the phenomenon of laser self focusing has already been investigated very intensively, earlier analyses of the phenomenon suffer from a variety of limitations. A few of them are as follows:-

1) In evaluating[32-35] the heating of electrons limited by thermal conduction (i.e. in solving the heat-conduction equation), the electron collision frequency[50] and thermal conductivity[60,61] of the plasma have been assumed to be independent of the electron temperature and

moreover, appropriate boundary conditions[62,63] have not been taken into account.

2) The criteria for monotonic and oxillatory defocusing[40,41] have not been derived completely and rigorously.

3) The pulse-shape distortion[49] which accompanies transient self focusing has not been analysed satisfactorily well; an analytical explanation for the numerical reveala-tion has not been presented.

4) Anomalous penetration[41] has not been analysed in detail; earlier analyses were restricted to some particular situations.

5) The observed[53-56] propagation of a laser beam like a self trapped filament has not been interpreted reasonably well.

6) The intensity-dependence[36] of the imaginary part of the dielectric constant (i.e. nonlinearity in the laser absorption) has not been taken into account.

Self Focusing in Magnetoplasmas

Many of the plasmas in which laser self focusing is investigated are immersed in static magnetic fields[64,65]. For electromagnetic plane waves propagating along the directionof astatic magnetic field, left and right circularly polarized modes are the normal modes of propa-gation[4,66-68]. However, in the case of a nonuniform laser

beam, these two modes are coupled[4] in two ways: (1) directly, on account of the anisotropy induced by the static magnetic field, and (2) indirectly, on account of the intensity-dependence of the dielectric constant. In all of the experimental investigations[53-56,69] and many of the theoretical investigations[4,40], only one mode has been considered to be present. Sodha et al.[70] have shown that the indirect coupling leads to cross-focusing of the two modes. The direct coupling has so far not been treated adequately. Effect of nonuniformity[64] in the plasma temperature and static magnetic field on laser self focusing has so far not been analysed.

Parametric Excitations

A parametric excitation[6-10] is a three-wave-interaction in which a pump wave is converted into a signal wave and an idler wave. In a plasma irradiated by a laser beam, the ponderomotive force[71,72] gives rise to a coupling (when appropriate phase-matching conditions are fulfilled) between an electromagnetic wave of the laser beam, an electrostatic wave present in the plasma and another electromagnetic or electrostatic scattered wave. When the laser-energy exceeds energies of the other two waves, the laser beam parametrically excites the electrostatic and scattered waves. Depending upon the combination of electrostatic and scattered waves under

consideration, there are different types of parametric excitations possible in a plasma. In the stimulated Raman scattering, a photon (electromagnetic wave) gives rise to a plasmon (electron plasma wave) and gets scattered as another photon. In the stimulated Brillouin scattering, a photon gives rise to a phonon (ion acoustic wave) and gets scattered as another photon. In the two-plasmon decay, a photon decays into two plasmons. In the plasmon-phonon decay, a photon decays into a plasmon and a phonon.

It has been shown that the temporal growth of these parametric excitations is very much influenced by the inhomogeneity[6,7,73-77], turbulence[78,79] and boundedness[80] of the plasma. It is apparent[81-87] that the phenomenon of laser self focusing can influence parametric excitations in a plasma, since it makes the plasma and laser-beam inhomogeneous. Sodha et al. have shown that the yield of the third harmonic electromagnetic waves[84] and electron plasma waves[85] in a plasma is considerably enhanced if the pump laser beam is self focused. Earlier analyses[6,81-87] of the effect of self focusing on the temporal growth of parametric excitations have been less rigorous and restricted to a certain particular manifestation of the phenomenon of self focusing.

Solitons

A soliton[11-14,88-90] is a disturbance which propagates without suffering any distortion in its shape, and can exist when the nonlinear effects exactly cancel out the dispersive effects of the medium. A clear understanding of the effect of external perturbations on solitons is very essential in order to point out similarities and differences between solitons and particles[15,91,92]. Recently some investigations[93,94] have been carried out in this direction.

In a plasma[95], a variety of solitons can exist[13]. Ion acoustic solitons[96-99] are solitons in the ion fluid of a plasma and have been widely investigated. Effects of multidimensionality[100-102], ion temperature[103], inhomogeneity[104-106], static magnetic field[107] and electromagnetic field[108-110] on ion acoustic solitons have been analysed. The effect of an electromagnetic field on the stability of ion acoustic solitons has, however, not been analysed in sufficient detail.

Summary of the Thesis

In the present thesis, the phenomena of laser self focusing, parametric excitations and ion acoustic solitons in plasmas have been investigated so as to eliminate the aforementioned limitations of the earlier investigations. A chapterwise summary of the thesis is as follows:-

CHAPTER 1: LASER SELF FOCUSING IN PLASMAS

This chapter presents an analysis of self focusing of a Gaussian laser beam (which may be in the form of a pulse) in a plasma whose electron concentration may vary in time and space. The laser absorption is allowed to vary with the laser intensity. The nonlinearity in the dielectric constant arises on account of the plasma-redistribution by the ponderomotive force or nonuniform heating of electrons. Electron-heating limited by thermal conduction has been rederived. Following Akhmanov 'et al.'s approach, the beamwidth parameter and hence the laser intensity and frequency shift (i.e. time derivative of the phase) of the laser pulse have been evaluated as functions of time and the distance of propagation. The following conclusions are drawn:

1) The temperature-dependence of the collision frequency and thermal conductivity and the boundary effects cannot be ignored when the nonuniform heating of electrons is limited by thermal conduction.

2) A laser beam in a (quiescent, homogeneous, nonabsorbing) plasma undergoes oscillatory divergence when the initial axial intensity E_o^2 is less than the lower self trapping intensity E_{stl}^2 but larger than a "linear" self trapping intensity E_L^2 predicted by the low-field expansion of the dielectric constant.

3) On account of the saturation of the dielectric constant at high laser intensity (or in other words, the double valuedness of the self trapping intensity), time-dependence of the axial intensity of a laser pulse changes appreciably as the pulse propagates.

4) Anomalous penetration of a laser beam in an overdense plasma depends upon the plasma-inhomogeneity and initial laser intensity.

5) In an axially inhomogeneous plasma, the laser beamwidth tends to attain a constant value depending upon the plasma-inhomogeneity and initial laser intensity.

6) Tendency of a laser beam to become self trapped (as represented by damping of oscillations of the beam-width parameter) increases if the laser absorption decreases with the laser intensity.

7) Consideration of nonlinearity in absorption predicts focusing of a laser beam (under certain conditions) even when the linear-absorption approximation would predict defocusing of the beam.

CHAPTER 2: LASER SELF FOCUSING IN A MAGNETOPLASMA

This chapter presents an analysis of self-focusing (and cross-focusing) of the left and right circularly polarized modes of a laser beam in a magnetoplasma. Following an extended version of Akhmanov's approach, the

beamwidth parameters and hence intensities of the two modes have been evaluated as functions of the distance of propagation. The calculations correspond to the case in which the carrier-redistribution is caused by the ponderomotive force; however, analysis of the problem is equally valid for any other mechanism of the intensity-dependence of the dielectric tensor . It is seen that the radial nonuniformity in the (initial) electron concentration, (initial) electron temperature and static magnetic field has considerable influence on self focusing of the two modes. The direct coupling between the two modes leads to axial asymmetry of the intensity profiles of the two modes. The direct coupling has, however, little effect on the cross-focusing phenomenon which is governed by the indirect coupling between the two modes.

CHAPTER 3: TEMPORAL GROWTH OF A PARAMETRIC EXCITATION BY A SELF FOCUSED LASER BEAM

This chapter consists of two parts. In PART 3A (MODIFIED EXPRESSION), the effect of self focusing of the pump laser beam on the temporal growth of an arbitrary parametric excitation has been analysed in the paraxial region. The two equations for the signal and idler modes have been decoupled by assuming the near self trapping condition and a linearly varying phase mismatch.

A modified expression for the temporal growth rate of the parametric excitation has been derived by employing the WKB approximation to solve the eigenvalue equation. In PART 3B (LOCAL CALCULATIONS), the mean beamwidth and self focusing length of the pump have been assumed to be so large that the modification in the expression for the temporal growth rate of a parametric excitation may be neglected. The temporal growth rates of stimulated Raman and Brillouin scattering of a laser beam in a plasma have been evaluated when the laser beam is self focused on account of the carrier-redistribution caused by the collision-dominated heating of electrons. The calculations predict a considerable spatial nonuniformity in the scattering on account of self focusing of the pump laser beam.

CHAPTER 4: ION ACOUSTIC SOLITONS IN AN ELECTROMAGNETICALLY IRRADIATED MAGNETOPLASMA

This chapter presents an analysis of the stability of ion acoustic solitons in the presence of an electromagnetic field and a static magnetic field. A modified Korteweg deVries equation has been derived in which the electromagnetic field plays the role of a source term. A one dimensional perturbation analysis shows that the static magnetic field influences only the transverse shape of the solitons. A homogeneous electromagnetic beam does

not destabilize the solitons; it reduces the amplitude, but not the velocity, of the solitons. However, any inhomogeneity in the electromagnetic field intensity does destabilize the ion acoustic solitons. An illustration considering a self focused laser beam shows that the destabilization is not appreciable - thereby, implying stability of solitons against external perturbations.

Relevant Publications

The theoretical investigations reported in the present thesis have resulted in the following publications/communications:-

1. Ion acoustic solitons in an electromagnetically irradiated magnetoplasma (L.A.Patel) Journal of Plasma Physics 18 (1977 Dec.) 381-389.

2. Effect of self focusing on scattering of a laser beam in a collisional plasma (L.A.Patel) Journal of Physics D 11 (1978 March)347-354.

3. Self focusing of a laser beam in a transient plasma (M.S.Sodha, D.P.Tewari and L.A.Patel) Journal of Plasma Physics 19 (1978 April).

4. Temporal growth of a parametric excitation by a self focused laser beam (L.A.Patel) Optical and Quantum Electronics 10 (1978 May).

5. Effect of nonlinear absorption on self focusing of a laser beam in a plasma (M.S.Sodha, L.A.Patel and R.P.Sharma) Journal of Applied Physics 49 (1978 June).

6. Self focusing of a laser beam in an inhomogeneous plasma (M.S.Sodha, L.A.Patel and S.C.Kaushik) Plasma Physics (1978).

7. Self focusing of a laser beam in a magnetoplasma (M.S.Sodha and L.A.Patel) Communicated.

The following publication has only a side-relation with the present thesis:

8. Self induced transparency of a two frequency pulse (L.A.Patel) Optik 50 (1978 March)243-247.

CHAPTER 1

LASER SELF FOCUSING IN PLASMAS

This chapter presents an analysis of self focusing[1-4] of a Gaussian laser beam (or pulse) in a plasma[4]; the initial electron concentration is allowed to vary in time and space, and the absorption coefficient[36] for the laser beam is allowed to vary with the laser intensity. In Sec.1.1, the expressions for the dielectric constant[4] have been presented for various cases of interest. In Sec.1.2, the wave equation for the linearly polarized electric field[1-4] of the laser beam (or pulse) has been solved under the paraxial and WKB approximations, and following Akhmanov et al.'s approach[1]. The laser intensity and frequency shift (time derivative of the phase) have been expressed in terms of the beamwidth parameter. An equation for the beamwidth parameter has been derived and its implications have been discussed. Numerical calculations have been carried out for several illustrative cases. In Sec.1.3, numerical results along with a discussion have been presented. The main conclusions from the present chapter are as follows:-

1) The temperature-dependence of the collision frequency[50] and thermal conductivity[60,61] and the boundary effects[62,63] cannot be ignored when the non-uniform heating of electrons is limited by thermal conduction.

2) A laser beam in a (quiescent, homogeneous, nonabsorbing) plasma undergoes oscillatory divergence[40] when the initial axial intensity E_o^2 is less than the lower self trapping intensity E_{stl}^2 but larger than the "linear" self trapping intensity E_L^2 predicted by the low-field expansion of the dielectric constant[3,4].

3) On account of saturation of the dielectric constant at high intensity (or in other words, the double valuedness of the self trapping intensity)[40,41], time-dependence of the axial intensity of a laser pulse changes[49] appreciably as the pulse propagates.

4) Anomalous penetration[41] of a laser beam in an overdense plasma[52-56] depends upon the plasma-inhomogeneity and initial laser intensity.

5) In an axially inhomogeneous plasma, the laser beamwidth tends to attain a constant value depending upon the plasma-inhomogeneity and initial laser intensity.

6) The tendency of a laser beam to become self trapped (as represented by damping of oscillations of the beamwidth parameter) increases if the laser absorption decreases with the laser intensity[57-59].

7) Consideration of nonlinearity in absorption predicts focusing of a laser beam (under certain conditions) even when the linear-absorption approximation[57] would predict defocusing of the beam. The effect of

nonlinear absorption is most significant when the electron collisions are predominantly with the diatomic molecules[4].

It is inferred from the present chapter that the axial inhomogeneity of the plasma and nonlinear/linear absorption of the laser radiation may be responsible for the observed[53-56] self trapping of a laser beam after a certain distance of propagation. However, the self trapping on account of the plasma-inhomogeneity or laser-absorption is seen to be partial - in the sense that the oscillations of the beamwidth parameter are only damped (but not completely eliminated) and that the laser beam starts diverging[57] after a certain extent of propagation like a self-trapped filament. It is suggested that further experiments should be carried out to check whether the laser self trapping is partial as mentioned above.

1.1: Dielectric Constant

The dielectric constant of a nonrelativistic plasma at frequency ω much greater than the electron collision-frequency ν is given by[3,4]

$$\epsilon = 1 - (\omega_p^2/\omega^2)(N/N_0) - i(\omega_p^2\nu_0/\omega^3)(N\nu/N_0\nu_0), \qquad (1\text{-}1)$$

where $\omega_p = (4\pi N_0 e^2/m)^{1/2}$, N_0, ν_0 are the plasma frequency, electron concentration and electron collision

frequency respectively in the absence of the laser beam; N and ν are the electron concentration and electron collision frequency respectively in the presence of the laser beam; m is the electron mass (whose relativistic variation has been neglected) and e is the electron charge. The ratios ω_p^2/ω^2 and $\omega_p^2\nu_o/\omega^3$ may vary in time and space if the plasma is nonsteady and inhomogeneous in the absence of the laser beam. The ratios N/N_o and $N\nu/N_o\nu_o$ depend upon the laser intensity $\vec{E}^*\cdot\vec{E}$ as discussed in the following.

As shown in Sec.1.2, the radial intensity-distribution of an initially Gaussian laser beam may be expressed[1-4] as

$$\vec{E}^*\vec{E} = E_a^2 \exp\left(-r^2/r_o^2 f^2\right), \qquad (1.2)$$

where the axial intensity E_a^2 and the beamwidth parameter f vary with the distance of propagation z and time t; r is the radial coordinate of the cylindrical coordinate system and r_o is the initial laser beamwidth. In an axially symmetric plasma, ω_p^2/ω^2 and $\omega_p^2\nu_o/\omega^3$ are even functions of r. Then in the paraxial region ($r \ll r_o f$), ϵ may be expressed by making the Maclaurin series expansion[62,63] in powers of $r^2/r_o^2 f^2$. The expansion upto the first power of $r^2/r_o^2 f^2$ gives

$$\epsilon \simeq (\epsilon_{ar} - i\epsilon_{ai}) - (\epsilon_{2r} + i\epsilon_{2i})\, r^2/r_o^2 f^2 , \qquad (1.3)$$

where

$$\epsilon_{ar} = 1 - \left[(\omega_p^2/\omega^2)(N/N_o)\right]_{(r=0)} , \qquad (1.4)$$

$$\epsilon_{ai} = \left[(\omega_p^2 \nu_o/\omega^3)(N\nu/N_o\nu_o)\right]_{(r=0)} , \qquad (1.5)$$

$$\epsilon_{2r} = \left[\frac{\partial}{\partial(r^2/r_o^2 f^2)}\left(\frac{\omega_p^2}{\omega^2}\frac{N}{N_o}\right)\right]_{(r=0)} , \qquad (1.6)$$

$$\epsilon_{2i} = \left[\frac{\partial}{\partial(r^2/r_o^2 f^2)}\left(\frac{\omega_p^2 \nu_o}{\omega^3}\frac{N\nu}{N_o\nu_o}\right)\right]_{(r=0)} . \qquad (1.7)$$

1.1a : Absence of nonlinearity

In order to understand the difference between the self focusing[1-5] and induced focusing[58,111] (as in an optical fiber), it is instructive to consider a "hypothetical" case in which the laser beam does not induce any modifications in the plasma. In this case,

$$N/N_o = 1 , \qquad (1.8\,a)$$

$$N\nu/N_o\nu_o = 1 . \qquad (1.9\,a)$$

Consequently

$$\epsilon_{ar} = 1 - (\omega_p^2/\omega^2)_{(r=0)} , \qquad (1.10\,a)$$

$$\epsilon_{ai} = (\omega_p^2 \nu_o / \omega^3)_{(r=0)} , \qquad (1.11\,a)$$

$$\epsilon_{2r} = r_o^2 f^2 \left[\frac{\partial}{\partial r^2} \left(\frac{\omega_p^2}{\omega^2} \right) \right]_{(r=0)} , \qquad (1.12\,a)$$

$$\epsilon_{2i} = r_o^2 f^2 \left[\frac{\partial}{\partial r^2} \left(\frac{\omega_p^2 \nu_o}{\omega^3} \right) \right]_{(r=0)} . \qquad (1.13\,a)$$

1.1b : Ponderomotive force

In a plasma, irradiated by a nonuniform laser beam, the electrons experience a ponderomotive force[3,4,24-28]

$$\vec{F}_{ponderm.} = -(e^2/2m\omega^2)\,\nabla(\vec{E}^* \cdot \vec{E}) . \qquad (1.14)$$

This leads to ambipolar diffusion[3,4] and consequent redistribution of electrons and ions. On small time scales ($t < \tau_p \sim r_o/c_s$), the electron-temperature does not rise appreciably and hence the carrier-redistribution on account of nonuniform heating[3,4] of electrons can be neglected. Dynamics[112] of the ponderomotive force (and

dynamics of the consequent redistribution) may be neglected if the time scales of variations of the electron concentration N_o and laser intensity $\vec{E}^* \cdot \vec{E}$ are much larger than the time required for the redistribution by the ponderomotive force. Effect of the plasma boundaries[27,113] on the redistribution by the ponderomotive force is negligible if the boundaries are located far away from the z axis (r=0). Under these conditions, it can be shown that

$$N / N_o = \exp\left(-\beta_b \vec{E}^* \cdot \vec{E}\right), \qquad (1.8b)$$

$$N\nu / N_o \nu_o \simeq (N / N_o)^b = \exp\left(-b\beta_b \vec{E}^* \cdot \vec{E}\right), \qquad (1.9b)$$

where

$$\beta_b = e^2 / 4 m K_B T_o \omega^2, \qquad (1.15b)$$

K_B is the Boltzmann constant, T_o is the plasma temperature (in the absence of the laser beam), and

$$b = 2 \text{ or } 1 \qquad (1.16)$$

depending upon whether the electron collisions are with ions or neutrals[50]. Consequently

$$\epsilon_{ar} = 1 - (\omega_p^2/\omega^2)_{(r=0)} \exp(-\beta_b E_a^2), \qquad (1.10b)$$

$$\epsilon_{ai} = (\omega_p^2 \nu_o/\omega^3)_{(r=0)} \exp(-b\beta_b E_a^2), \qquad (1.11b)$$

$$\epsilon_{2r} = r_o^2 f^2 \left[\frac{\partial}{\partial r^2}\left(\frac{\omega_p^2}{\omega^2}\right)\right]_{(r=0)} \exp(-\beta_b E_a^2) + \left(\frac{\omega_p^2}{\omega^2}\right)_{(r=0)} \beta_b E_a^2 \exp(-\beta_b E_a^2), \qquad (1.12b)$$

$$\epsilon_{2i} = r_o^2 f^2 \left[\frac{\partial}{\partial r^2}\left(\frac{\omega_p^2 \nu_o}{\omega^3}\right)\right]_{(r=0)} \exp(-b\beta_b E_a^2) + \left(\frac{\omega_p^2 \nu_o}{\omega^3}\right)_{(r=0)} b\beta_b E_a^2 \exp(-b\beta_b E_a^2). \qquad (1.13b)$$

1.1c : Electron-heating without thermal conduction

On large time scales ($t > \tau_\epsilon$), the electrons are heated[4,29-35] by the laser beam. The pressure gradients generated on account of the nonuniform heating of electrons lead to redistribution of the plasma through ambipolar diffusion[3,4]. The nonlinearity due to ponderomotive force is negligible[3,4] as compared to that due to nonuniform heating of electrons. If the initial laser beamwidth is large ($r_o^2 \gg \kappa_o M/\nu_o m K_B N_o$, where κ_o is the thermal conductivity in the absence of the laser beam and M is the mass of ion/neutral),

contribution of thermal conduction to the electron-heating may be neglected[32] as compared to the contribution of the collisional energy-transfer (between electrons and ions/neutrals). It can then be shown that (cf. APPENDIX),

$$N/N_o = (1 + \beta_c \vec{E}^* \cdot \vec{E})^{s/2-1}, \qquad (1.8c)$$

$$N\nu/N_o\nu_o \simeq (N/N_o)^b (T/T_o)^{s/2} = (1+\beta_c \vec{E}^* \cdot \vec{E})^{bs/2-b} (1+2\beta_c \vec{E}^* \cdot \vec{E})^{s/2}, \qquad (1.9c)$$

where

$$\beta_c = Me^2/6m^2 k_B T_o \omega^2, \qquad (1.15c)$$

M is the mass of an ion (or a neutral scatter), and

$$s = -3 \text{ or } 1 \text{ or } 2 \qquad (1.17)$$

depending upon whether the electron collisions are with ions or nondiatomic molecules or diatomic molecules[4]. Consequently

$$\epsilon_{ar} = 1 - (\omega_p^2/\omega^2)_{(r=a)} (1+\beta_c E_a^2)^{s/2-1}, \qquad (1.10c)$$

$$\epsilon_{ai} = (\omega_p^2 \nu_o/\omega^3)_{(r=a)} (1+\beta_c E_a^2)^{bs/2-b} (1+2\beta_c E_a^2)^{s/2}, \qquad (1.11c)$$

$$\epsilon_{2r} = r_o^2 f^2 \left[\frac{\partial}{\partial r^2}\left(\frac{\omega_p^2}{\omega^2}\right)\right]_{(r=0)} \left(1+\beta_c E_a^2\right)^{s/2-1} + \left(\frac{\omega_p^2}{\omega^2}\right)_{(r=0)} (1-s/2)\,\beta_c E_a^2 \left(1+\beta_c E_a^2\right)^{s/2-2}, \qquad (1.12c)$$

$$\epsilon_{2i} = r_o^2 f^2 \left[\frac{\partial}{\partial r^2}\left(\frac{\omega_p^2 \nu_o}{\omega^3}\right)\right]_{(r=0)} \left(1+\beta_c E_a^2\right)^{bs/2-b} \left(1+2\beta_c E_a^2\right)^{s/2} + \left(\frac{\omega_p^2 \nu_o}{\omega^3}\right)_{(r=0)} \left[\frac{(b-bs/2)}{(1+\beta_c E_a^2)} - \frac{s}{(1+2\beta_c E_a^2)}\right] \beta_c E_a^2 \times \left(1+\beta_c E_a^2\right)^{bs/2-b} \left(1+2\beta_c E_a^2\right)^{s/2}. \qquad (1.13c)$$

1.1d : Electron-heating limited by thermal conduction

As discussed in Sec.1.1c, on long time scales ($t > \tau_\epsilon$), the carrier-redistribution is caused by the nonuniform heating of electrons. If the initial laser beamwidth is small ($r_o^2 \ll \chi_o M / \nu_o m K_B N_o$), contribution of the collisional energy-transfer (between electrons and ions/neutrals) to the electron-heating may be neglected[33,34] as compared to the contribution of the thermal conduction. In APPENDIX, the heat conduction equation for this case has been solved by allowing the thermal conductivity[60,61] χ and electron collision frequency[50] ν to vary with

the electron temperature T and by employing the appropriate boundary conditions[62,63]. It has been shown that

$$N/N_o = \left\{ 1/2 + \left[1 + 2\sigma N_a^2 N_o^{-2} \beta_d E_a^2 \right.\right.$$
$$\left.\left. (gf^2 - r^2/r_o^2) \right]^{1/\sigma} /2 \right\}^{s/2} - 1 , \qquad (1.8d)$$

$$N\nu/N_o\nu_o \simeq (N/N_o)^b (T/T_o)^{s/2}$$
$$= \left\{ 1/2 + \left[1 + 2\sigma N_a^2 N_o^{-2} \beta_d E_a^2 \right.\right.$$
$$\left.\left. (gf^2 - r^2/r_o^2) \right]^{1/\sigma} /2 \right\}^{bs/2} - b$$
$$\left[1 + 2\sigma N_a^2 N_o^{-2} \beta_d E_a^2 \right.$$
$$\left. (gf^2 - r_y^2/r_o^2) \right]^{s/2\sigma} , \qquad (1.9d)$$

where

$$\beta_d = N_o \nu_o e^2 r_o^2 / 8 \chi_o T_o m \omega^2 , \qquad (1.15a)$$

χ_o is the thermal conductivity of the plasma in the absence of the laser beam, N_a is the electron concentration on the axis in the presence of the laser beam,

$$\sigma = 1 + \ln (\chi \nu_o N_a / \chi_o \nu N_o) / \ln (T/T_o) \qquad (1.18)$$

is a parameter which characterizes the variation of the ratio χ/ν (of the thermal conductivity χ to the electron collision frequency ν) with the electron temperature T, and

$$g = \int_0^{b^2/r_o^2} [1 - \exp(-x)]\, x^{-1}\, dx \qquad (1.19)$$

is the boundary effect parameter determined[114] by the boundary r = b at which $T = T_o$. Consequently

$$\epsilon_{ar} = 1 - (\omega_p^2/\omega^2)_{(r=o)} \left\{ 1/2 + [1 + 2\sigma g N_a^2 N_o^{-2} \beta_d E_a^2 f^2]^{1/\sigma}/2 \right\}^{s/2-1}, \qquad (1.10d)$$

$$\epsilon_{ai} = (\omega_p^2 \nu_o/\omega^3)_{(r=o)} [1 + 2\sigma g N_a^2 N_o^{-2} \beta_d E_a^2 f^2]^{s/2\sigma} \left\{ 1/2 + [1 + 2\sigma g N_a^2 N_o^{-2} \beta_d E_a^2 f^2]^{1/\sigma}/2 \right\}^{bs/2-b}, \qquad (1.11d)$$

$$\epsilon_{2r} = r_o^2 f^2 \left[\frac{\partial}{\partial r^2}\left(\frac{\omega_p^2}{\omega^2}\right) \right]_{(r=o)} \left\{ 1/2 + [1 + 2\sigma g N_a^2 N_o^{-2} \beta_d E_a^2 f^2]^{1/\sigma}/2 \right\}^{s/2-1} +$$

$$(\omega_p^2/\omega^2)_{(x=0)}\ (1-S/2)\ N_a^2 N_0^{-2} \beta_d\ E_a^2\ f^2$$

$$[1 + 2\sigma g\ N_a^2 N_0^{-2} \beta_d\ E_a^2 f^2\ ]^{1/\sigma - 1}\ \{1/2 +$$

$$[1+ 2\sigma g\ N_a^2 N_0^{-2} \beta_d\ E_a^2 f^2\ ]^{1/\sigma}\ /2\ \}^{S/2-2},$$

(1-12 d)

$$\epsilon_{2i} = r_0^2 f^2 \left[\frac{\partial}{\partial r^2}\left(\frac{\omega_p^2 \nu_0}{\omega^3}\right)\right]_{(x=0)} [1 + 2\sigma g\ N_a^2 N_0^{-2}\ \beta_d\ E_a^2 f^2$$

$$]^{S/2\sigma} \{ 1/2 + [1+2\sigma g\ N_a^2 N_0^{-2} \beta_d\ E_a^2\ f^2\ ]^{1/\sigma}/2$$

$$\}^{b\,S/2-b} + \left(\frac{\omega_p^2 \nu_0}{\omega^3}\right)_{(x=0)} \{ [$$

$$\left(\frac{2b - bS}{1+[1+2\sigma g N_a^2 N_0^{-2} \beta_d E_a^2 f^2]^{1/\sigma}}\right) - \left(\frac{S}{[1+2\sigma g N_a^2 N_0^{-2} \beta_d E_a^2 f^2]^{1/\sigma}}\right)$$

$$] N_a^2 N_0^{-2} \beta_d E_a^2 f^2\ [1 + 2\sigma g N_a^2 N_0^{-2} \beta_d E_a^2 f^2$$

$$]^{S/2\sigma + 1/\sigma - 1} \} \{ 1/2 + [1 +$$

$$2\sigma g N_a^2 N_0^{-2} \beta_d E_a^2 f^2\ ]^{1/\sigma}/2\ \}^{bS/2-b}.$$

(1-13 d)

1.2 : Laser Propagation

1.2.1: Wave equation

If the laser radiation is linearly polarized and $\omega^2/c^2 \gg |\nabla^2 \ln \epsilon|$, the electric field $\vec{E}$ of the laser beam (or pulse) is governed by the scalar wave equation[1-4]

$$\frac{\partial^2 E}{\partial z^2} + \frac{1}{r}\frac{\partial}{\partial r} r \frac{\partial E}{\partial r} - \frac{1}{c^2}\frac{\partial^2 D}{\partial t^2} = 0, \qquad (1.20)$$

where $\vec{D}$ is the displacement vector. If the laser radiation is quasimonochromatic, the electric field $\vec{E}$ may be expressed as

$$E = \mathcal{E} \exp\left(i\omega t - i\omega c^{-1} \int_0^z \epsilon_{ar}^{1/2} dz \right), \qquad (1.21)$$

where the complex amplitude $\mathcal{E}$ varies slowly with time t and the distance of propagation z (but may vary rapidly with the radial coordinate r), and $\epsilon_{ar}^{1/2}\,\omega/c$ is the wavenumber under the assumption that $\epsilon_{ai} \ll \epsilon_{ar}$. If nonlocal effects in the plasma and time-dependence of the wavenumber are negligible, the displacement vector $\vec{D}$ is given by[3,4]

$$D = \left[\epsilon \mathcal{E} - i \frac{\partial \epsilon}{\partial \omega} \frac{\partial \mathcal{E}}{\partial t} \right] \exp(i\omega t). \qquad (1.22)$$

Upon substituting for **E** and D from Eqs. 1.21 and 1.22, neglecting the time-dependence of ϵ and employing the WKB approximation, Eq. 1.20 becomes[1-4]

$$\frac{-2i\omega\epsilon_{ar}^{1/2}}{c}\frac{\partial\mathcal{E}}{\partial z} - i\frac{\partial\epsilon_{ar}^{1/2}}{\partial z} + \frac{1}{r}\frac{\partial}{\partial r}\,r\frac{\partial\mathcal{E}}{\partial r} - \frac{\omega^2}{c^2}\left[i\epsilon_{ai} + (\epsilon_{2r}+i\epsilon_{2i})\frac{r^2}{x_0^2 f^2}\right]\mathcal{E} - \frac{2i\omega\epsilon^{1/2}}{c^2}\frac{\partial(\omega\epsilon^{1/2})}{\partial\omega}\frac{\partial\mathcal{E}}{\partial t} = 0 . \tag{1.23}$$

Time-derivative in Eq. 1.23 can be eliminated by using the concept of "reduced time"[2,3]. Thus the independent variables z and t are replaced by the new dimensionless independent variables

$$\xi = z\,c/\omega\,r_0^2 \tag{1.24}$$

and

$$\tau = \omega t - \frac{\omega}{c}\int_0^z \left[\frac{\epsilon^{1/2}}{\epsilon_{ar}^{1/2}}\frac{\partial(\omega\epsilon^{1/2})}{\partial\omega}\right] dz . \tag{1.25}$$

In the paraxial region, r dependence of τ may be neglected and hence the expression 1.25 reduces to

$$\tau = \omega t - \frac{\omega}{c}\int_0^z \frac{\partial(\omega\epsilon_{ar}^{1/2})}{\partial\omega}\,dz . \tag{1.25'}$$

In terms of ξ and τ, Eq.1.23 reduces to the parabolic equation

$$-2i\epsilon_{ar}^{1/2}\frac{\partial \mathcal{E}}{\partial \xi} - i\frac{\partial \epsilon_{ar}^{1/2}}{\partial \xi}\mathcal{E} + \frac{r_o^2}{r}\frac{\partial}{\partial r}\, r\frac{\partial \mathcal{E}}{\partial r} - \frac{r_o^2\omega^2}{c^2}\left[i\epsilon_{ai} + (\epsilon_{2r}+i\epsilon_{2i})\frac{r^2}{r_o^2 f^2}\right] = 0 . \tag{1.26}$$

1.2.2: Solution of the parabolic equation

The initial (z=0) electric field will be taken to be Gaussian in the form

$$\mathcal{E} = E_o \exp(-r^2/r_o^2). \tag{1.27'}$$

Then following Akhmanov et al.[1], the solution of Eq.1.26 can be expressed as

$$\mathcal{E} = E_a \exp(-r^2/2r_o^2 f^2)\exp i(\theta - \varphi r^2/r_o^2), \tag{1.27}$$

where the axial electric field amplitude E_a, beamwidth parameter f, axial phase θ and offaxial phase coefficient φ are real and vary with ξ and τ but not with r. The expression 1.2 is consistent with the expression 1.27. Substituting for $\mathcal{E}$ from Eq.1.27 into Eq.1.26, and then equating the coefficients of

$2\epsilon_{ar}^{1/2}$, $2i\epsilon_{ar}^{1/2}$, $-2\epsilon_{ar}^{1/2} r^2/r_o^2$, $-2i\epsilon_{ar}^{1/2} r^2/r_o^2 f3$

on both sides of the resulting equation, the following four equations are obtained. (Treating the coefficients of r^0 and r^2 independently in this way is an approximation to the Fourier-series-orthogonalization condition and is justified only in the paraxial region)

$$\frac{\partial\theta}{\partial\xi} - \frac{1}{\epsilon_{ar}^{1/2} f3} = 0 , \qquad (1.28)$$

$$\frac{\partial \ln E_a}{\partial\xi} + \frac{\partial \ln \epsilon_{ar}^{1/4}}{\partial\xi} + \frac{2\varphi}{\epsilon_{ar}^{1/2}} + \frac{r_o^2\omega^2\epsilon_{ai}}{2c^2\epsilon_{ar}^{1/2}} = 0 , \qquad (1.29)$$

$$\frac{\partial\varphi}{\partial\xi} + \frac{2\varphi^2}{\epsilon_{ar}^{1/2}} - \frac{1}{2\epsilon_{ar}^{1/2} f4} + \frac{r_o^2\omega^2\epsilon_{2r}}{2c^2 f^2 \epsilon_{ar}^{1/2}} = 0 , \qquad (1.30)$$

$$\frac{\partial f}{\partial\xi} - \frac{2\varphi f}{\epsilon_{ar}^{1/2}} + \frac{r_o^2\omega^2 f\,\epsilon_{2i}}{2c^2\epsilon_{ar}^{1/2}} = 0 . \qquad (1.31)$$

Equations 1.28 and 1.31 give

$$\theta = \int \frac{d\xi}{\epsilon_{ar}^{1/2} f^2} , \qquad (1.32)$$

$$\varphi = \frac{\epsilon_{ar}^{1/2}}{2} \frac{\partial \ln f}{\partial\xi} + \frac{r_o^2\omega^2\epsilon_{2i}}{4c^2} . \qquad (1.33)$$

Substituting for φ from Eq. 1.33 into Eq. 1.29 and then integrating it gives the following expression for the axial intensity.

$$E_a^2 = \frac{E_o^2}{f^2} \frac{\epsilon_{ar(\xi=0)}^{1/2}}{\epsilon_{ar}^{1/2}} \exp\left[-\left(\frac{r_o^2\omega^2}{c^2}\right)\int\left(\frac{\epsilon_{ai}+\epsilon_{2i}}{\epsilon_{ar}^{1/2}}\right)d\xi\right], \tag{1.34}$$

where $E_o^2 = E_a^2(\xi=0)$ is the initial axial intensity.

Substituting for φ from Eq.1.33 into Eq. 1.30 gives

$$\frac{\partial^2 f}{\partial \xi^2} + \left[\frac{\partial \ln \epsilon_{ar}^{1/2}}{\partial \xi} + \left(\frac{r_o^2\omega^2}{c^2}\right)\frac{\epsilon_{2i}}{\epsilon_{ar}^{1/2}}\right]\frac{\partial f}{\partial \xi} =$$

$$\left[\frac{1}{\epsilon_{ar} f^3} - \left(\frac{r_o^2\omega^2}{c^2}\right)\frac{\epsilon_{2r}}{\epsilon_{ar} f} - \left(\frac{r_o^2\omega^2}{c^2}\right)^2 \frac{\epsilon_{2i}^2 f}{4\epsilon_{ar}}\right.$$

$$\left. - \left(\frac{r_o^2\omega^2}{c^2}\right)\frac{f}{2\epsilon_{ar}^{1/2}}\frac{\partial \epsilon_{2i}}{\partial \xi}\right]. \tag{1.35}$$

The boundary conditions for Eq.1.35, corresponding to a plane wavefront are[1-4]

$$f(\xi=0) = 1, \tag{1.36}$$

$$\left[\partial f / \partial \xi\right]_{(\xi=0)} = 0. \tag{1.37}$$

1.2.3: Frequency shift

The frequency shift normalized by the laser frequency ω is defined as[3]

$$\Delta = \frac{d\theta}{d\tau} - \frac{d\varphi}{d\tau}\,\frac{r^2}{r_0^2} \quad . \qquad (1.38)$$

It is convenient to express Δ as

$$\Delta = \left[\frac{d\theta}{d(\beta E_0^2)}\,\frac{\partial(\beta E_0^2)}{\partial(\omega t)} + \frac{d\theta}{d(\omega_p^2/\omega^2)}\,\frac{\partial(\omega_p^2/\omega^2)}{\partial(\omega t)}\right] - \left[\frac{d\varphi}{d(\beta E_0^2)}\,\frac{\partial(\beta E_0^2)}{\partial(\omega t)} + \frac{d\varphi}{d(\omega_p^2/\omega^2)}\,\frac{\partial(\omega_p^2/\omega^2)}{\partial(\omega t)}\right]\frac{r^2}{r_0^2} \quad , \qquad (1.39)$$

where β is arbitrary, β_b, β_c or β_d depending upon whether the case under consideration is (a) absence of nonlinearity, (b) ponderomotive force, (c) electron-heating without thermal conduction or (d) electron-heating limited by thermal conduction. The quantities $\partial(\beta E_0^2)/\partial(\omega t)$ and $\partial(\omega_p^2/\omega^2)/\partial(\omega t)$ are known beforehand. In the assumed absence of explicit time-dependence of the dielectric constant, the quantities $d\theta/d(\beta E_0^2)$, $d\theta/d(\omega_p^2/\omega^2)$, $d\varphi/d(\beta E_0^2)$ and $d\varphi/d(\omega_p^2/\omega^2)$ depend only on ξ, βE_0^2 and ω_p^2/ω^2. This fact greatly simplifies the evaluation of Δ at any reduced time τ.

1.2.4: Behaviour of E_a^2 and f

Equation 1.35 can be solved numerically by the Runge-Kutta method[115]. It would be helpful to have a qualitative idea regarding the variations of the axial intensity E_a^2 and beamwidth parameter f with the distance

of propagation ξ .

In the absence of nonlinearity, absorption and axial inhomogeneity (in the absence of the laser beam), Eqs. 1.34 and 1.35 reduce to[111]

$$E_a^2 = \frac{E_0^2}{f^2} \quad , \tag{1.40}$$

$$\frac{\partial^2 f}{\partial \xi^2} = \frac{1}{\epsilon_{ar}} \left[\frac{1}{f^3} - \frac{I_0 4\omega^2 f}{c^2} \left(\frac{\partial}{\partial r^2} \frac{\omega_p^2}{\omega^2} \right)_{(r=0)} \right] . \tag{1.41}$$

The two terms on the right hand side of Eq.1.41 represent the diffraction and induced focusing respectively. The beam experiences monotonic defocusing (i.e. f keeps increasing with ξ), oscillatory defocusing (i.e. f oscillates between 1 and $f_{max} > 1$), trapping (i.e. f=1) and oscillatory focusing (i.e. f oscillates between 1 and $f_{min} < 1$) depending upon whether $\left(\frac{\partial}{\partial r^2} \frac{\omega_p^2}{\omega^2} \right)_{(r=0)}$ is < 0, > 0 but < 1, $= 1$ and > 1. This case has been investigated (analytically) intensively in the context of optical fibers.

In the absence of nonlinearity and absorption, Eqs.1.34 and 1.35 reduce to[111]

$$E_a^2 = \frac{E_0^2}{f^2} \frac{\epsilon_{ar(\xi=0)}^{1/2}}{\epsilon_{ar}^{1/2}} \quad , \tag{1.42}$$

$$\frac{\partial^2 f}{\partial \xi^2} + \frac{\partial \ln \epsilon_{ar}^{1/2}}{\partial \xi} \frac{\partial f}{\partial \xi} = \frac{1}{\epsilon_{ar}} \left[\frac{1}{f^3} - \frac{r_0^4 \omega^2 f}{c^2} \left(\frac{\partial}{\partial r^2} \frac{\omega_p^2}{\omega^2} \right)_{(r=0)} \right]. \tag{1.43}$$

The second term on the left hand side of Eq. 1.43 gives rise to growth or decay of the oscillations of f (i.e. f_m, which is f_{max} in the case of oscillatory defocusing and f_{min} in the case of oscillatory focusing, becomes ξ dependent in such a way that $|f_m - 1|$ increases or decreases with ξ) depending upon whether $\partial \ln \epsilon_{ar}^{1/2} / \partial \xi$ is $<$ or >0 (i.e. whether the electron concentration N_o increases or decreases with ξ). The criteria for defocusing/focusing are slightly modified according to the value of $\left(\partial^2 \epsilon_{ar} / \partial \xi^2 \right)_{(\xi=0)}$. The present WKB analysis fails in the region where $\epsilon_{ar} \simeq 0$.

In the absence of nonlinearity and axial inhomogeneity, Eqs. 1.34 and 1.35 reduce to[111]

$$E_a^2 = \frac{E_o^2}{f^2} \exp\left[-\left(\frac{r_o^2 \omega^2}{c^2} \right) \int \left(\frac{\omega_p^2 \nu_o}{\omega^3} + r_o^2 f^2 \frac{\partial}{\partial r^2} \frac{\omega_p^2 \nu_o}{\omega^3} \right)_{(r=0)} \frac{d\xi}{\epsilon_{ar}^{1/2}} \right], \tag{1.44}$$

$$\frac{\partial^2 f}{\partial \xi^2} + \frac{r_o^4 \omega^2 f^2}{c^2 \epsilon_{ar}^{1/2}} \left(\frac{\partial}{\partial r^2} \frac{\omega_p^2 \nu_o}{\omega^3} \right)_{(r=0)} \frac{\partial f}{\partial \xi} = \frac{1}{\epsilon_{ar}} \left[\frac{1}{f^3} - \frac{r_o^4 \omega^2 f}{c^2} \left(\frac{\partial}{\partial r^2} \frac{\omega_p^2}{\omega^2} \right)_{(r=0)} - \frac{r_o^8 \omega^4 f^5}{4 c^4} \left(\frac{\partial}{\partial r^2} \frac{\omega_p^2 \nu_o}{\omega^3} \right)^2_{(r=0)} \right]. \tag{1.45}$$

The criteria for defocusing/focusing of f are greatly modified by the radial nonuniformity in the absorption as represented by the last term on the right hand side of Eq.1.45. Oscillations of f grow or decay depending upon whether $\left(\frac{\partial}{\partial r^2}\frac{\omega_p^2\nu_0}{\omega^3}\right)_{(r=0)}$ is < 0 or > 0 (i.e. whether $N_0\nu_0$ increases or decreases with r). A similar result had been obtained by Marcuse[58] and Yuen.[59]

In the absence of radial nonuniformity, absorption and axial inhomogeneity and if the laser-induced axial inhomogeneity is negligible, then Eq.1.34 reduces to Eq.1.40 and Eq.1.35 reduces to[40,41]

$$\frac{\partial^2 f}{\partial \xi^2} = \frac{1}{\epsilon_{2r}}\left[\frac{1}{f^3} - \left(\frac{\gamma_0^2\omega_p^2}{c^2}\right)\frac{\epsilon_{2r1}}{f}\right], \qquad (1.46)$$

where

$$\epsilon_{2r1} = \epsilon_{2r}\left(\frac{\partial}{\partial r^2}\frac{\omega_p^2}{\omega^2}=0\right)\Big/\left(\frac{\omega_p^2}{\omega^2}\right) . \qquad (1.47)$$

The two terms on the right hand side of Eq.1.46 represent the diffraction and self-focusing respectively. The self trapping intensity according to the low-field expansion[3] of the dielectric constant, called "linear" self trapping intensity, E_L^2 is given by the relation

$$\lim_{f\to\infty}\left[f^2\,\epsilon_{2r1}\left(E_a^2 = E_L^2/f^2\right)\right] = c^2/\gamma_0^2\omega_p^2 . \qquad (1.48)$$

Equations 1.13 and 1.48 give

$$E_L^2 = c^2 / \beta_b r_0^2 \omega_p^2 \qquad (1.49b)$$

in the case of ponderomotive force,

$$E_L^2 = c^2 / (1-s/2) \beta_c r_0^2 \omega_p^2 \qquad (1.49c)$$

in the case of electron-heating without thermal conduction, and

$$E_L^2 = 0 \qquad (1.49d)$$

in the case of electron-heating limited by thermal conduction. The actual self trapping intensity E_{st}^2 is given by the relation

$$\epsilon_{2r1} (E_a^2 = E_{st}^2) = c^2 / r_0^2 \omega_p^2 . \qquad (1.50)$$

No analytical expression for E_{st}^2 exists. However, it can be seen[40] that Eq.1.50 has no root if $r_0^2\omega_p^2/c^2 < (r_0^2\omega_p^2/c^2)_{crit.}$ and it has two roots if $r_0^2\omega_p^2/c^2 > (r_0^2\omega_p^2/c^2)_{crit.}$; the lower and upper of the two roots (i.e. lower self trapping intensity E_{stl}^2 and upper self trapping intensity E_{stu}^2) decreasesand increases respectively as $r_0^2\omega_p^2/c^2$ increases. It can be shown that the beam experiences monotonic defocusing, oscillatory defocusing, trapping and oscillatory focusing depending

upon whether $E_o^2 \leq E_L^2$, $E_L^2 < E_o^2 < E_{stl}^2$ or $E_o > E_{stu}^2$, $E_o^2 = E_{stu}^2$ and $E_{stl}^2 < E_o^2 < E_{stu}^2$. In the light of these new criteria for monotonic and oscillatory defocusing, the earlier criteria[1-4,40,41] are incomplete and approximate.

In the absence of radial nonuniformity, absorption and axial inhomogeneity, the beamwidth parameter oscillates between its initial value of unity and another maximum/minimum value f_m. The case of monotonic defocusing has no real value for f_m; oscillatory defocusing, trapping and oscillatory focusing correspond to $f_m > 1$, $f_m = 1$ and $0 < f_m < 1$ respectively. Multiplying both sides of Eq.1.46 by $2\,\partial f/\partial \xi$ and then integrating once gives[3,40]

$$\left(\frac{\partial f}{\partial \xi}\right)^2 = \frac{1}{\epsilon_{ar}}\left[1 - \frac{1}{f^2} - \left(\frac{r_o^2\omega_p^2}{c^2}\right)\int_1^{f^2} \epsilon_{2r1}\,\frac{df^2}{f^2}\right]. \qquad (1.51)$$

At $f = f_m$, $\partial f/\partial \xi = 0$ and hence Eq. 1.51 gives

$$\left(r_o^2\omega_p^2/c^2\right)\int_1^{f_m^2} \epsilon_{2r1}\, f^{-2}\, df^2 = 1 - f_m^{-2}. \qquad (1.52)$$

It can then be shown that

$$\left(r_o^2\omega_p^2/c^2\right)\left[\exp\left(-\beta_b E_o^2/f_m^2\right) - \exp\left(-\beta_b E_o^2\right)\right] = 1 - f_m^{-2}. \qquad (1.53\,b)$$

in the case of ponderomotive force, and

$$(r_0^2\omega_p^2/c^2)\left[(1+\beta_c E_0^2/f_m^2)^{s/2-1} - (1+\beta_c E_0^2)^{s/2-1}\right] = 1 - f_m^{-2} \qquad (1.53c)$$

in the case of electron-heating without thermal conduction. It may be argued that

$$\partial^2 f/\partial \xi^2 = 0 \quad \text{at} \quad f \simeq (1+f_m)/2 . \qquad (1.54)$$

This gives an approximate analytical expression for f_m:

$$f_m = 2\left[\beta_b E_0^2 / \ln(\beta_b E_0^2 r_0^2 \omega_p^2/c^2)\right]^{1/2} - 1 \qquad (1.55b)$$

in the case of ponderomotive force, and

$$f_m = 2\left[\beta_c E_0^2 / \left\{\left[(1-\gamma/2)\beta_c E_0^2 r_0^2 \omega_p^2/c^2\right]^{1/(2-s/2)} - 1\right\}\right]^{1/2} - 1 \qquad (1.55c)$$

in the case of electron-heating without thermal conduction.

In the absence of radial nonuniformity and absorption, Eq.1.34 reduces to Eq.1.40 and Eq.1.35 reduces to[41]

$$\frac{\partial^2 f}{\partial \xi^2} + \frac{\partial \ln \epsilon_{ar}^{1/2}}{\partial \xi}\frac{\partial f}{\partial \xi} = \frac{1}{\epsilon_{ar}}\left[\frac{1}{f^3} - \left(\frac{r_0^2\omega_p^2}{c^2}\right)\frac{\epsilon_{2r1}}{f}\right] . \qquad (1.56)$$

The discussion following Eq.1.43 applies in the present case also.

In the absence of radial nonuniformity, nonlinear (i.e. intensity-dependent) absorption and axial inhomogeneity

and if the laser-induced axial inhomogeneity is negligible, then Eq.1.35 reduces to Eq.1.46 and Eq.1.34 reduces to[57]

$$E_a^2 = \frac{E_o^2}{f^2} \exp\left[-\left(\frac{r_o^2 \omega_p^2 \nu_o}{c^2 \omega}\right) \int \frac{\epsilon_{ai1}}{\epsilon_{ar}^{1/2}} d\xi \right], \quad (1.57)$$

where

$$\epsilon_{ai1} = \epsilon_{ai} / \left(\omega_p^2 \nu_o / \omega^3\right). \quad (1.58)$$

The dependence of ϵ_{2r1} on E_a^2 and the decrease of E_a^2 with ξ (on account of the linear absorption) lead to decay of the oscillations of f till E_a^2 becomes so small that f starts defocusing monotonically[57].

In the absence of radial nonuniformity and axial inhomogeneity and if the laser-induced axial inhomogeneity is negligible, then Eqs.1.34 and 1.35 reduce to

$$E_a^2 = \frac{E_o^2}{f^2} \exp\left[-\left(\frac{r_o^2 \omega_p^2 \nu_o}{c^2 \omega}\right) \int \frac{(\epsilon_{ai1} + \epsilon_{2i1})}{\epsilon_{ar}^{1/2}} d\xi \right], \quad (1.59)$$

$$\frac{\partial^2 f}{\partial \xi^2} + \left(\frac{r_o^2 \omega_p^2}{c^2}\right) \frac{\epsilon_{2i1}}{\epsilon_{ar}^{1/2}} \frac{\partial f}{\partial \xi} = \frac{1}{\epsilon_{ar}} \left[\frac{1}{f^3} - \left(\frac{r_o^2 \omega_p^2}{c^2}\right) \frac{\epsilon_{2r1}}{f} - \left(\frac{r_o^2 \omega_p^2}{c^2}\right)^2 \frac{\epsilon_{2i1}^2 f}{4}\right], \quad (1.60)$$

where

$$\epsilon_{2i1} = \epsilon_{2i} \left(\frac{\partial}{\partial r^2} \frac{\omega_p^2 \nu_o}{\omega^3} = 0\right) / \left(\frac{\omega_p^2 \nu_o}{\omega^3}\right). \quad (1.61)$$

The presence of the last term on the right hand side of Eq.1.60 implies that nonlinearity (i.e. intensity-dependence and hence r dependence) of the absorption increases the possibility of focusing of the beam. The presence of the second term on the left hand side of Eq.1.60 implies that the positive valued ϵ_{2i1} (i.e. decrease of the absorption with the laser intensity) gives rise to an additional decay of the oscillations of f. Thus the number of oscillations of f possible before f starts defocusing monotonically is greater in the case of $\epsilon_{2i1} > 0$ than in the case of linear absorption (i.e. $\epsilon_{2i1} = 0$).

Above-mentioned conclusions (regarding the behaviour of E_a^2 and f) are valid for a laser beam in a quiescent (i.e. time independent) plasma. The conclusions may also be applied to a laser pulse in a transient (i.e. time-dependent) plasma[46-49]; various parameters appearing in the conclusions then refer to an instantaneous reduced time τ .

1.3: Results and Discussion

1.3.1: Absence of nonlinearity

Figures 1.1 and 1.2 illustrate the variations of the beamwidth parameter f and the axial intensity E_a^2 with the distance of propagation ξ in the absence of nonlinearity. Figure 1.1 is for such a small value of

$\left(\frac{\partial}{\partial r^2}\frac{\omega_p^2}{\omega^2}\right)_{(r=0)}$ that $f > 1$, whereas Fig.1.2 is for such a large value of $\left(\frac{\partial}{\partial r^2}\frac{\omega_p^2}{\omega^2}\right)_{(r=0)}$ that $f < 1$. In each of these two figures, three typical cases have been considered: (A) absence of both absorption and axial inhomogeneity, (B) axially increasing concentration without absorption, and (C) radially increasing absorption without axial inhomogeneity. The results presented here are consistent with the analytical results. It is, moreover, seen that the decay of the oscillations of f can occur on account of the axially increasing concentration as well as on account of the radially increasing absorption[58,59].

1.3.2: Intensity-dependence of various quantities

Figure 1.3 shows that the dependence of the functions $(N/N_0)_{(r=0)}$, $\epsilon_{ai1} = (N\nu/N_0\nu_0)_{(r=0)}$, $\epsilon_{2r1} = -\left[\frac{\partial(N/N_0)}{\partial(r^2/r_0^2f^2)}\right]_{(r=0)}$ and $\epsilon_{2i1} = -\left[\frac{\partial(N\nu/N_0\nu_0)}{\partial(r^2/r_0^2f^2)}\right]_{(r=0)}$ on the axial intensity E_a^2 in the (a) absence of nonlinearity, (b) case of ponderomotive force, and (c) case of electron-heating without thermal conduction. This figure is very helpful in determining the extent of focusing and absorption of the beam and growth/decay of oscillations of f. This figure shows that the intensity-dependence of the imaginary part ϵ_i of the dielectric constant is as strong as that of the real part ϵ_r, and hence the

linear-absorption approximation[57] is doubtful. In the case (c) with S=2, ϵ_r is intensity-independent whereas ϵ_{ai} and ϵ_{2i} increase and decrease respectively linearly with E_a^2.

Figure 1.4 illustrates the variations[40] of the "linear" self trapping intensity E_L^2 and "actual" self trapping intensities E_{st}^2 in various cases, with the dimensionless parameter $r_o^2\omega_p^2/c^2$. The labels L and A to the curves in this figure refer to "linear" and "actual" self trapping intensities respectively. The suffixes b, c, d_1 and d_5 to the labels L and A refer to the ponderomotive force, electron-heating with S=0 without thermal conduction, electron-heating with S=0 limited by thermal conduction with σ=1 and electron-heating with S=0 limited by thermal conduction with σ=5 respectively. In a homogeneous nonabsorbing plasma, the beam experiences monotonic defocusing, oscillatory defocusing, trapping or oscillatory focusing[40] depending upon whether the values chosen for $r_o^2\omega_p^2/c^2$ and E_o^2 lie below (or on) the curve L, in between the curves L and A, on the curve A or above the curve A.

1.3.3: Thermal conduction

Figure 1.5 illustrates the variations of the beam-width parameter f with the dimensionless distance of

propagation ξ when the carrier-redistribution is caused by the electron heating limited by thermal conduction, and the imaginary part of the dielectric constant is negligible. This figure reveals that the consideration of the temperature-dependence[50,60] of the ratio χ/ν (represented by $\sigma = 5$ instead of the usual $\sigma = 1$) and that of the boundary conditions[62,63] (represented by $g \gg 1$ instead of the usual $g = 1$) reduce focusing of the laser beam appreciably.

1.3.4: Extremum beamwidth parameter

The curves in the upper portion of Fig.1.6 illustrate the variation of the extremum[40] (i.e. maximum/minimum) value f_m of the beamwidth parameter with E_o^2 in the case of ponderomotive force, and when the imaginary part of the dielectric constant is negligible. The curves labelled with 35, 53 and 55 have been obtained by solving Eq.1.35 for f, solving Eq.1.53b for f_m and using the expression 1.55b for f_m respectively. Considering the approximations made in arriving at Eqs.1.53b and 1.55b, the agreement between the numerical results (plotted on the curve 35) and the analytical results (plotted on the curves 53 and 55) is very good. The curve in the lower portion of Fig.1.6 illustrates the variation of the dimensionless distance ξ_m at which f becomes f_m with

E_o^2 as obtained by solving Eq.1.35 for f in the case of ponderomotive force.

Figure 1.6 shows that f_m and ξ_m vary very rapidly with E_o^2 if $E_L^2 < E_o^2 < E_{stl}^2$ but very slowly if $E_o^2 > E_{stu}^2$. The variation of ξ_m with E_o^2 for $E_{stl}^2 < E_o^2 < E_{stu}^2$ implies, in the case of a laser pulse, an axial motion of the foci where the instantaneous axial intensity becomes maximum. The filamentary tracks observed[5] along the propagation of a laser pulse had been interpreted in terms of such an axial motion of the foci[5,36]. Such an interpretation would require the condition $d(\ln f_{min})/d(E_o^2) \ll d(\ln \xi_{min})/d(E_o^2)$ to be fulfilled for $E_{stl}^2 < E_o^2 < E_{stu}^2$. Figure 1.6, however, shows that generally $d(\ln f_{min})/d(E_o^2) \gg d(\ln \xi_{min})/d(E_o^2)$ for $E_{stl}^2 < E_o^2 < E_{stu}^2$. Hence the present investigation supports the concept of 'moving foci'[5,36] only partially.

1.3.5: Frequency shift

Figure 1.7 illustrates the variations of f with ξ in the case of ponderomotive force; the imaginary part of the dielectric constant has been neglected. The four curves correspond to: (1) $E_o^2 < E_L^2$, (2) $E_L^2 < E_o^2 < E_{stl}^2$, (3) $E_{stl}^2 < E_o^2 < E_{stu}^2$, (4) $E_o^2 > E_{stu}^2$. The shapes of these curves confirm the foregoing qualitative discussion on the behaviour of f.

Figures 1.8 and 1.9 illustrate the variations of the coefficients $\frac{d\theta}{d(\beta_b E_o^2)}$, $\frac{d\theta}{d(\omega_p^2/\omega^2)}$, $\frac{d\varphi}{d(\beta_b E_o^2)}$ and $\frac{d\varphi}{d(\omega_p^2/\omega^2)}$ (which appear in the expression 1.39 for the normalized frequency shift Δ) with ξ. On account of the negligible effect of the explicit temporal variation of the dielectric constant, the curves do not explicitly depend upon τ. As expected, the curves do not show any correlation with the variations of f represented in Fig.1.7. This figure is very useful in the calculation of the instantaneous frequency shift[3] for any type of time dependences of E_o^2 and N_o. Thus, for $\xi_o^2\omega^2/c^2=100$, $\omega_p^2/\omega^2=0.04$, $\beta_b E_o^2=1.0$, $\xi=3$, $r=0$, $\partial(\beta_b E_o^2)/\partial\tau = 10^{-10}$ and $\partial(\omega_p^2/\omega^2)/\partial\tau = 10^{-14}$, the third curves in Fig.1.8 imply that the normalized frequency shift is

$$\Delta \simeq (-0.93\times10^{-10} + 36\times10^{-14}) = -0.9264 \times 10^{-10}.$$

Thus, the frequency shift is in general negligibly small[3].

1.3.6: Pulse distortion

Figures 1.10 and 1.11 illustrate the variations of E_a^2 with τ/τ_o for $E_b^2 = E_{oo}^2 \exp(-\tau^2/\tau_o^2)$. In Fig. 1.10, $E_{oo}^2 = 1.5/\beta_b$ is less than the upper self trapping intensity E_{stu}^2; whereas in Fig.1.10, $E_{oo}^2 = 10/\beta_b > E_{stu}^2$. It is to be noted that the initial Gaussian time dependence of the laser intensity is distorted[49] to such an extent that in many cases the pulse shape develops

peaks. In the earlier analyses[46-48] restricted to small values of E_{oo}^2 and ξ, the development of peaks was not observed. A similar peak-development was revealed in an elaborate numerical analysis[49] by Feit and Fleck. The sort of pulse shape distortion observed in the present analysis can be easily interpreted on the basis of the double valuedness[40] of the self trapping intensity. For high enough values of ξ, the curves in Fig.1.11 show dips at $\tau = 0$ because E_{oo}^2 has been chosen to be greater than E_{stu}^2 in this case. This prediction (i.e. reversal of the Gaussian time dependence of the pulse) can be easily checked in experiments with very intense laser pulses propagating over long distances in plasmas.

In the calculations related to Figs.1.10 and 1.11, instantaneous values of various parameters have been used. Hence the initial symmetry of the time-dependence of the pulse is preserved. If the relaxation effects were included in the analysis, some asymmetry in the pulse-shape[49] would have been observed.

1.3.7: Axial inhomogeneity and anomalous penetration

Figures 1.12 - 1.15 illustrate the variations of f with ξ in the cases in which the carrier-redistribution is caused by (b) ponderomotive force and (c) electron-heating with S=0 without thermal conduction. Figures 1.12,

1.13, 1.14 and 1.15 correspond to a homogeneous plasma, an inhomogeneous plasma with exponentially decreasing electron concentration, linearly increasing concentration and periodically varying concentration respectively. The imaginary part of the dielectric constant has been neglected. Figure 1.12 confirms the foregoing discussion on the qualitative behaviour of f in a homogeneous plasma. The curves in Fig. 1.13 show that for the electron concentration decreasing with the distance of propagation, the diffraction effect tends to predominate over the nonlinear focusing effect and consequently the beam tends to diverge[3] monotonically even when E_0^2 exceeds E_L^2.

The curves in Figs.1.14 and 1.15 show that an intense laser beam can penetrate[41] in an overdense plasma[52-56] (for which $\omega_p > \omega$) and that the oscillations of f tend to damp out with the distance of propagation (i.e. the laser beam tends to become self trapped); the analysis being based on the WKB approximation[40,41] is not valid in the cutoff region where $\epsilon_{ar} \simeq 0$. A closer look at Fig.1.15 shows that the tendency of the laser beam to be self trapped and anomalous penetration[41] depend very much on the type of plasma-inhomogeneity and initial laser intensity. Figure 1.16 illustrates the variation of the depth of penetration ξ_p (i.e. the distance upto which

the laser beam can propagate "normally") with the initial axial intensity E_o^2, when the electron concentration increases linearly with ξ and the carrier-redistribution is caused by ponderomotive force. The results plotted in Fig.1.16 are more accurate than the ones reported previously[41] and show that the depth of penetration ξ_p increases sharply with the initial axial intensity E_o^2.

1.3.8: Nonlinear absorption

Figures 1.17 and 1.18 illustrate the variations of f and E_a^2 with ξ in the case of ponderomotive force. The magnitude of the ratio $\left(\frac{\omega_p^2 \nu_o}{\omega^3}\right)$, which determines the magnitude of absorption of the laser beam of given intensity, has been taken to be larger in Fig.1.18 than in Fig.1.17. These figures confirm the effect of absorption discussed in Sec.1.2.4. In addition, it is seen that stabilization in f does not necessarily imply stabilization in E_a^2 and that $(-df_{max}/d\xi) > (-df_{min}/d\xi)$ and $(-dE_{a\,max}^2/d\xi) > (-dE_{a\,min}^2/d\xi)$ when the variations of f (and hence E_a^2) damp with ξ.

Figures 1.19 - 1.21 illustrate the variations of f and E_a^2 with ξ in the case of electron-heating without thermal conduction; S = -3, 1 and 2 for Figs. 1.19, 1.20 and 1.21 respectively. As expected from similarity in the nature of the dielectric constant, it is seen that the

results in the cases of Figs. 1.19 and 1.20 are similar to the results in the case of Fig.1.18. Effect of increase in the value of S is seen to be quite appreciable; it (1) reduces the number of oscillations of f that can occur before f starts defocusing monotonically[57], (2) distorts the pattern of oscillations of f, and (3) increases the value of the effective absorption coefficient so that E_a^2 approaches zero more rapidly. Results shown in Fig.1.21 are even more interesting. The linear-absorption approximation predicts monotonic defocusing of a laser beam of any value of the initial axial intensity E_o^2 when S=2. Consideration of nonlinearity in the absorption, however, predicts focusing of the beam if E_o^2 fulfills certain conditions. These effects are obvious from the variations of $(N/N_o)_{(r=o)}$, ϵ_{a1i}, ϵ_{2r1} and ϵ_{2i1} depicted in Fig.1.3.

Figures 1.1 - 1.21

Fig.1.1 f and $\Lambda \log(E_a^2/E_o^2)$ versus ξ in the absence of nonlinearity. $r_o^2\omega^2/c^2 = 900$. $\omega_p^2/\omega^2 = 0.1$ $(1+0.001\ r^2/r_o^2)$ for (A&C) & $0.1(1+\xi)(1+0.001 r^2/r_o^2)$ for (B). $\omega_p^2 \nu_o/\omega^3 = 0$ for (A&B) & $0.01(1+0.002\ r^2/r_o^2)$ for (C). $\Lambda = 1$ for (A&B) & 0.04 for (C).

Fig.1.2 f and $\log(E_a^2/E_o^2)$ versus ξ in the absence of nonlinearity . $r_o^2\omega^2/c^2 = 900$. $\omega_p^2/\omega^2 = 0.1(1+r^2/r_o^2)$ for (A&C) & $0.1(1+\xi)(1+r^2/r_o^2)$ for (B). $\omega_p^2 \nu_o/\omega^3 = 0$ for (A&B) & $0.01(1+2r^2/r_o^2)$ for (C).

Fig.1.3 The functions $(N/N_o)_{(r=0)}$, $\Lambda_a \epsilon_{2i1}$, ϵ_{2r1} & $\Lambda_2 \epsilon_{2i1}$ versus $\log(\beta E_o^2)$ in the (a) absence of nonlinearity, (b) case of ponderomotive force with b=2, and (c) case of electron-heating without thermal conduction with S=-3 for ($c\bar{3}$) & 1 for (c1) & 2 for (c2). β = arbitrary for (a) & β_b for (b) and β_c for (c).
$\Lambda_a = 1$ for (a & b & $c\bar{3}$ & c1) & .0.1 for (c2).
$\Lambda_2 = 1$ for (a & b & $c\bar{3}$ & c1) & -0.1 for (c2).

Fig.1.4 $\Lambda r_o^2 \omega_p^2/c^2$ versus $\lambda\beta E_o^2$ for $E_o^2 = E_L^2$ for (L) & E_{st}^2 for (A). The case under consideration is ponderomotive force for (b), electron-heating with S=0 without thermal conduction for (c),

electron-heating with S=0 limited by thermal conduction with σ =1 for (d1), and electron-heating with S=0 limited by thermal conduction with σ =5 for (d5). Λ =1 for (L & Ab & Ac) & 1/g for (Ad1) & 1/20g for (Ad5). λ =1 for (L & Ab & Ac) & g for (Ad1 & Ad5).

Fig.1.5 f versus $\lambda\xi$ in the case of electron heating with S=0 limited by thermal conduction. σ = 1 for (1 & 1g) & 5 for (5 & 5g). g = 1 for (1 & 5) & 10 for (A1g &A5g) & 40 for (B1g & B5g). $r_o^2\omega^2/c^2$ = 470 for (A) & 160 for (B). ω_p^2/ω^2 = 0.25. $\beta_d E_o^2$ = 0.01 for (A) & 1 for (B). λ = 1 for (A) & 2 for (B).

Fig.1.6 f_m and ξ_m versus $\beta_b E_o^2$ as obtained by (35) solving Eq.1.35 for f in the case of ponderomotive force, (53) solving Eq.1.53c for f_m, and (55) using the expression 1.55c for f_m. $r_o^2\omega^2/c^2$ = 100. ω_p^2/ω^2 = 0.04.

Fig.1.7 f versus ξ in the case of ponderomotive force. $r_o^2\omega^2/c^2$ = 100. ω_p^2/ω^2=0.04. $\beta_d E_o^2$ = 0.1 for (1) & 0.34 for (2) & 1.0 for (3) & 3.4 for (4).

Fig.1.8 $\frac{d\theta}{\lambda_1 d(\beta_b E_o^2)}$ and $\frac{d\theta}{\lambda_2 d(\omega_p^2/\omega^2)}$ versus ξ for the case and parameters same as in Fig.1.7.

λ_1 = 1 for (1 & 3 & 4) & 20 for (2).

λ_2 = 1 for (1) & 100 for (2) & 20 for (3) & 10 for (4).

Fig.1.9 $\frac{d\varphi}{\lambda_3 d(\beta_b E_o^2)}$ and $\frac{d\varphi}{\lambda_4 d(\omega_p^2/\omega^2)}$ versus ξ for the case and parameters same as in Fig.1.7.

λ_3 = 1 for (1 & 2 & 3) & 1/4 for (4).

λ_4 = 1 for (1) & 5 for (2 & 4) & 10 for (3).

Fig.1.10 $\beta_b E_a^2$ versus τ/τ_o in the case of ponderomotive force. $r_o^2\omega^2/c^2 = 100$. $\omega_p^2/\omega^2 = 0.04$. $\beta_b E_o^2 = 1.5\exp(-\tau^2/\tau_o^2)$. ξ = 0 for (0) & 1 for (1) & 2 for (2) & 4 for (4).

Fig.1.11 $\beta_b E_a^2$ versus τ/τ_o in the case of ponderomotive force. $r_o^2\omega^2/c^2 = 100$. $\omega_p^2/\omega^2 = 0.04$. $\beta_b E_o^2 = 10\exp(-\tau^2/\tau_o^2)$. ξ = 0 for (0) & 1 for (1) & 3 for (3) & 5 for (5).

Fig.1.12 f versus $\lambda\xi$ in the case of (b) ponderomotive force and (c) electron-heating with S=0 without thermal conduction. $r_o^2\omega^2/c^2 = 16$ for (b) and 20 for (c). $\omega_p^2/\omega^2 = 0.25$. $\beta_b E_o^2$ =0.25 for (b1) & 0.3 for (b2) & 1.5 for (b3) & 3 for (b4) & 6 for (b5).

$\beta_c E_o^2 = 0.15$ for (c1) & 0.25 for (c2) & 1 for (c3) & 5 for (c4) & 10 for (c5). $\lambda = 1$ for (c) & 0.5 for (d).

Fig.1.13 f versus ξ for the case and parameters same as in Fig.1.12 except that $\omega_p^2/\omega^2 = 0.25 \exp(-\xi/2)$.

Fig.1.14 f versus ξ for the case and parameters same as in Fig.1.12 except that $\omega_p^2/\omega^2 = 0.25\ (1 + \xi/2)$.

Fig.1.15 f versus ξ for the case and parameters same as in Fig.1.12 except that $\omega_p^2/\omega^2 = 0.25\ (4 + \sin(\pi\xi/4))$.

Fig.1.16 ξ_p versus $\beta_b E_o^2$ in the case of ponderomotive force for $r_o^2\omega^2/c^2 = 20$ and $\omega_p^2/\omega^2 = 0.5(1 + \xi/2)$.

Fig.1.17 f and $\log(E_a^2/E_o^2)$ versus $\lambda\xi$ in the case of ponderomotive force with $h=2$. $r_o^2\omega^2/c^2 = 900$. $\omega_p^2/\omega^2 = 0.1$. $\omega_p^2\nu_o/\omega^3 = 0.001$ for (1) & 0.01 for (2) & 0.1 for (3). $\beta_b E_o^2 = 0.01$ for (1) & 1 for (2) & 10 for (3). $\lambda = 1$ for (1 & 2) & 0.1 for (3).

Fig.1.18 f versus $\Lambda \log(E_a^2/E_o^2)$ versus $\lambda\xi$ in the case of ponderomotive force with b=2. $r_o^2\omega^2/c^2 = 900$. $\omega_p^2/\omega^2 = 0.1$. $\omega_p^2\nu_o/\omega^3 = 0.01$ for (1) & 0.1 for (2) & 1 for (3). $\Lambda = 1$ for (1 & 2) & 10 for (3). $\lambda = 1$ for (1) & 10 for (2) & 0.1 for (3). $\beta_b E_o^2 = 10\ \omega_p^2\nu_o/\omega^3$.

Fig.1.19 f and $\log(E_a^2/E_o^2)$ versus $\lambda\xi$ in the case of electron-heating without thermal conduction. S=-3. $r_o^2\omega^2/k^2 = 900$. $\omega_p^2/\omega^2 = 0.1$. $\omega_p^2\nu_o/\omega^3 = 0.001$ for (1) & 0.01 for (2) & 0.1 for (3). $\beta_c E_o^2 = 0.1$ for (1) & 1 for (2) & 10 for (3). $\lambda = 1$ for (1 & 2) & 0.1 for (3).

Fig.1.20 f and $\log(E_a^2/E_o^2)$ versus $\lambda\xi$ for the same case and parameters as in Fig.1.19 except that S=1. $\lambda = 1$ for (1 & 2) & 4 for (3).

Fig.1.21 f and $\log(E_a^2/E_o^2)$ versus $\lambda\xi$ for the same case and parameters as in Fig.1.19 except that S=2. $\omega_p^2\nu_o/\omega^3 = 0.0001$ for (1) & 0.001 for (2) & 0.01 for (3). $\lambda = 1$ for (1 & 2) & 100 for (3).

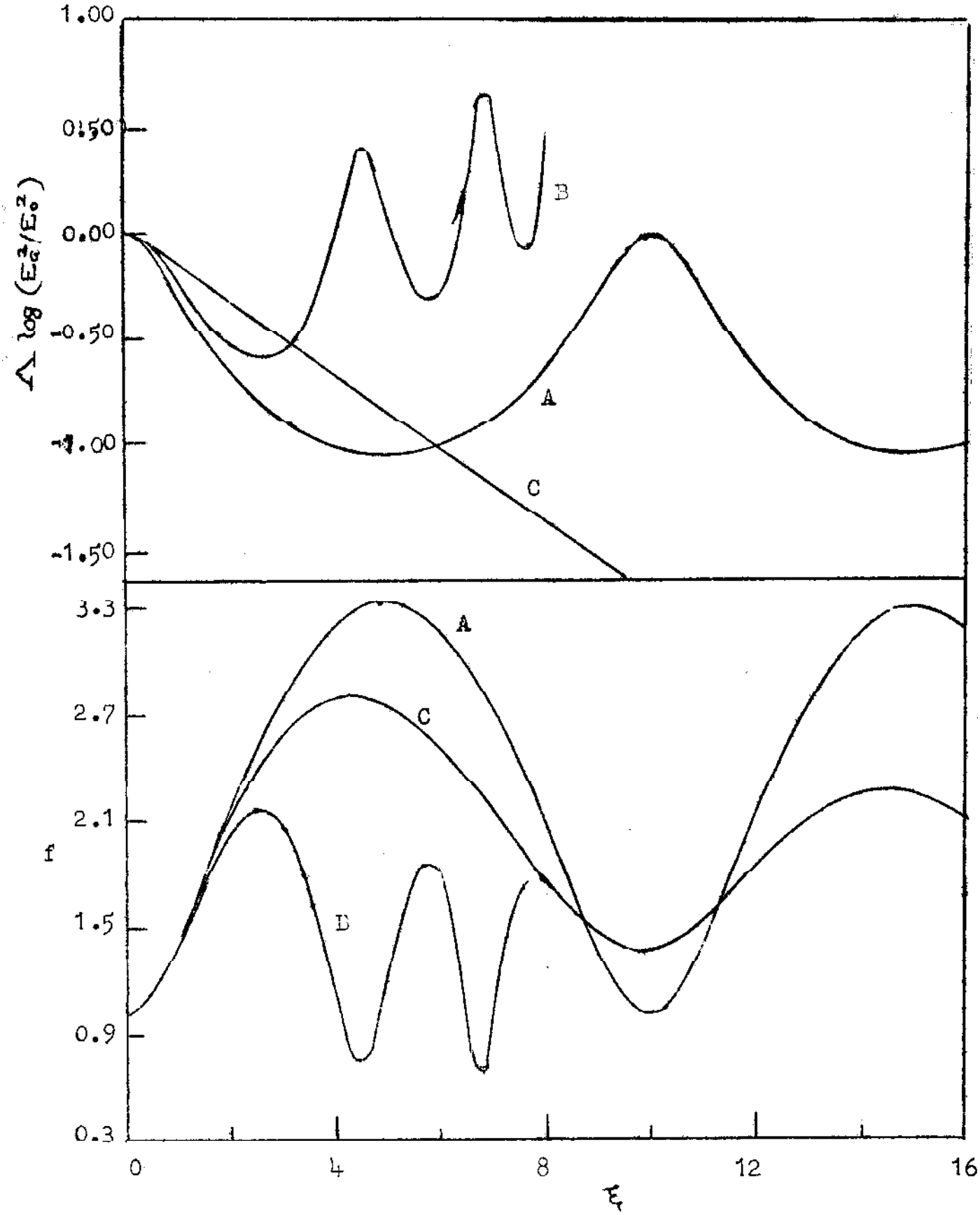
1.00
0.50
0.00
-0.50
-1.00
-1.50
Δ log (E_ξ²/E_0²)
A
B
C
3.3
2.7
2.1
1.5
0.9
0.3
f
A
C
B
0
4
8
12
16
ξ

Fig. 1.1

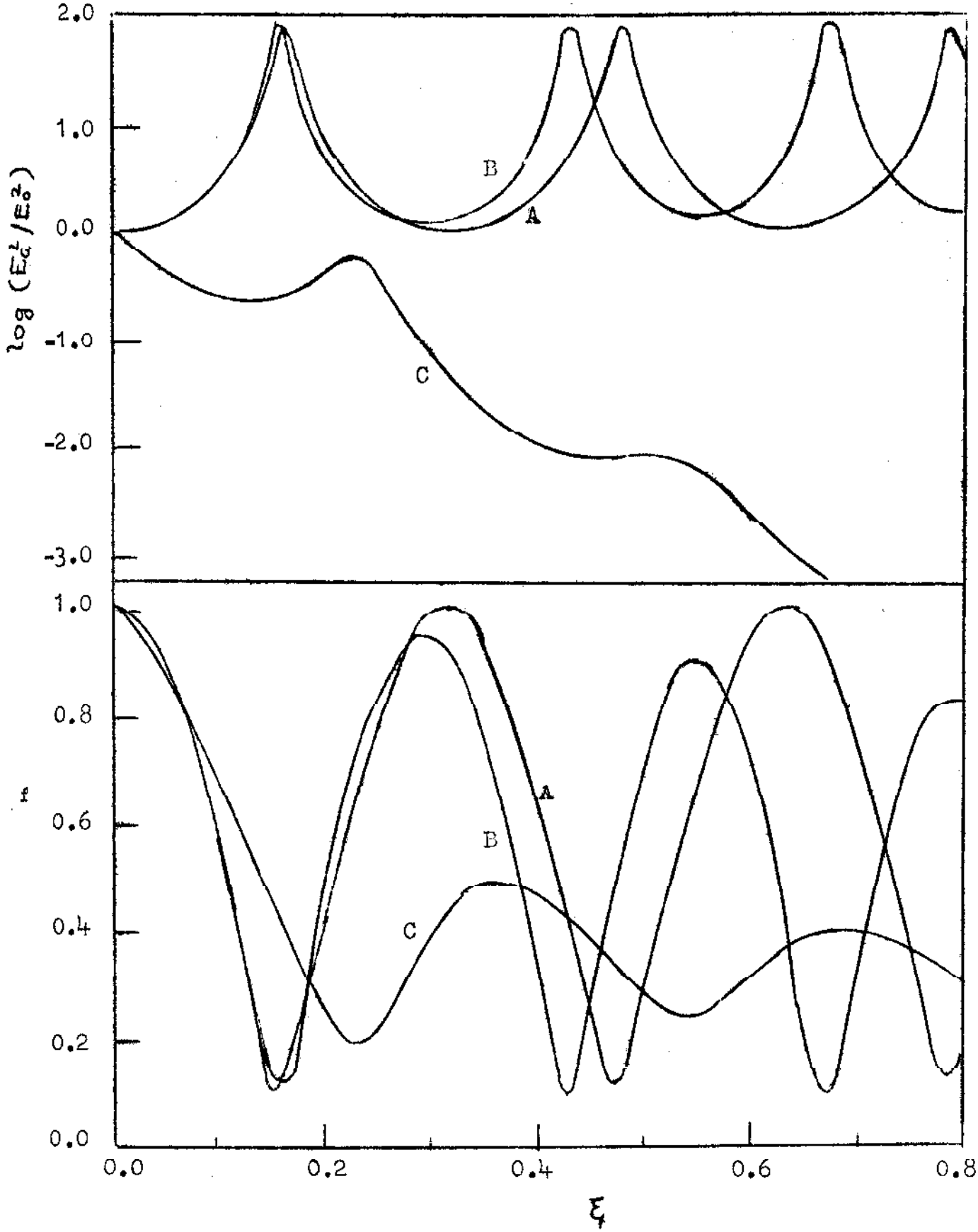
2.0
1.0
0.0
-1.0
-2.0
-3.0
log (E_c^2 / E_0^2)
A
B
C
1.0
0.8
0.6
0.4
0.2
0.0
f
A
B
C
0.0
0.2
0.4
0.6
0.8
ξ

Fig. 1.2

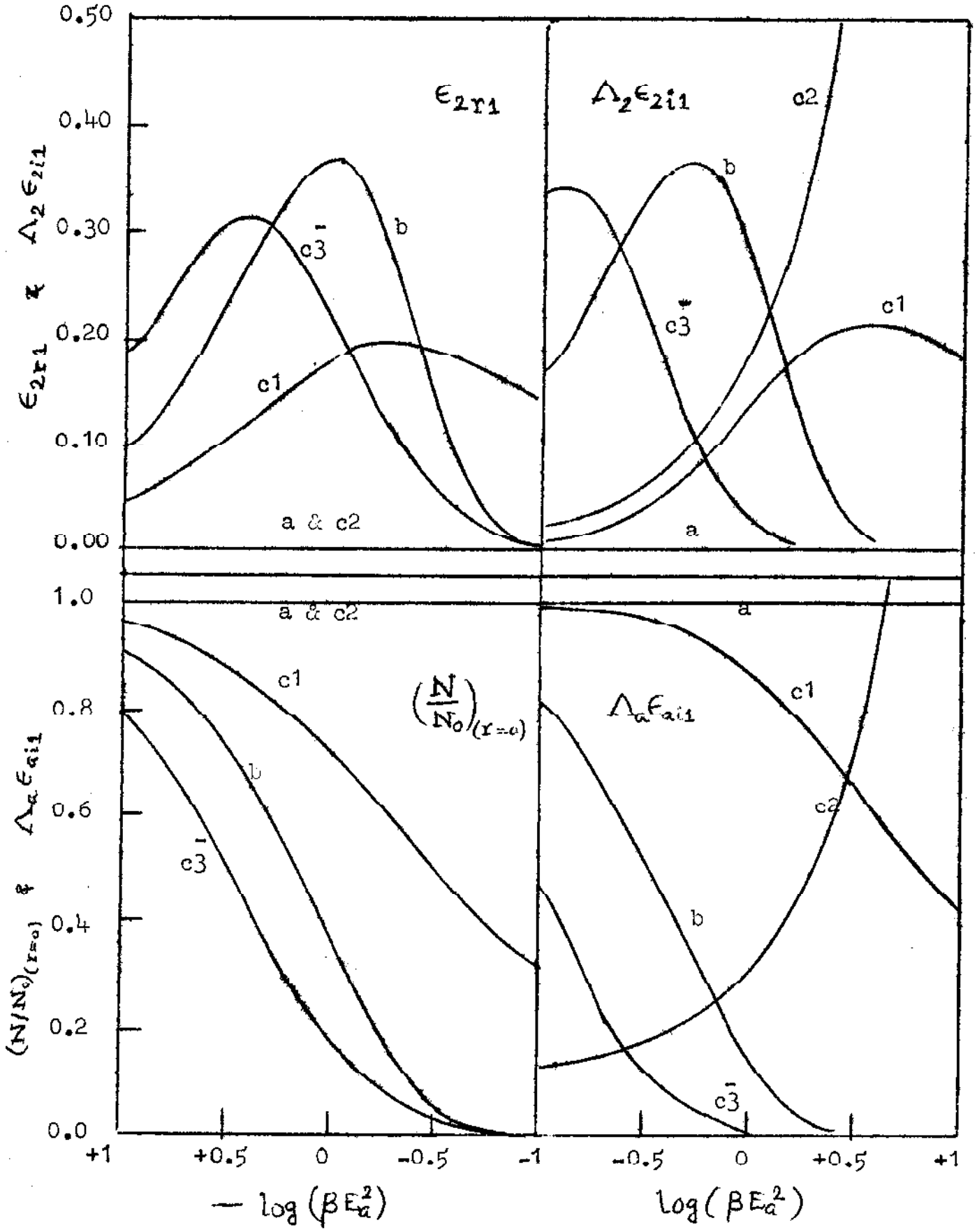
0.50
0.40
0.30
0.20
0.10
0.00
ϵ_{2r1} & $\Lambda_2\epsilon_{2i1}$
ϵ_{2r1}
$\Lambda_2\epsilon_{2i1}$
a & c2
a
b
c1
c2
c3
1.0
0.8
0.6
0.4
0.2
0.0
$(N/N_0)_{(r=a)}$ & $\Lambda_a\epsilon_{ai1}$
$\left(\frac{N}{N_0}\right)_{(r=a)}$
$\Lambda_a\epsilon_{ai1}$
+1
+0.5
0
-0.5
-1
$-\log(\beta E_a^2)$
$\log(\beta E_a^2)$

Fig. 1.3

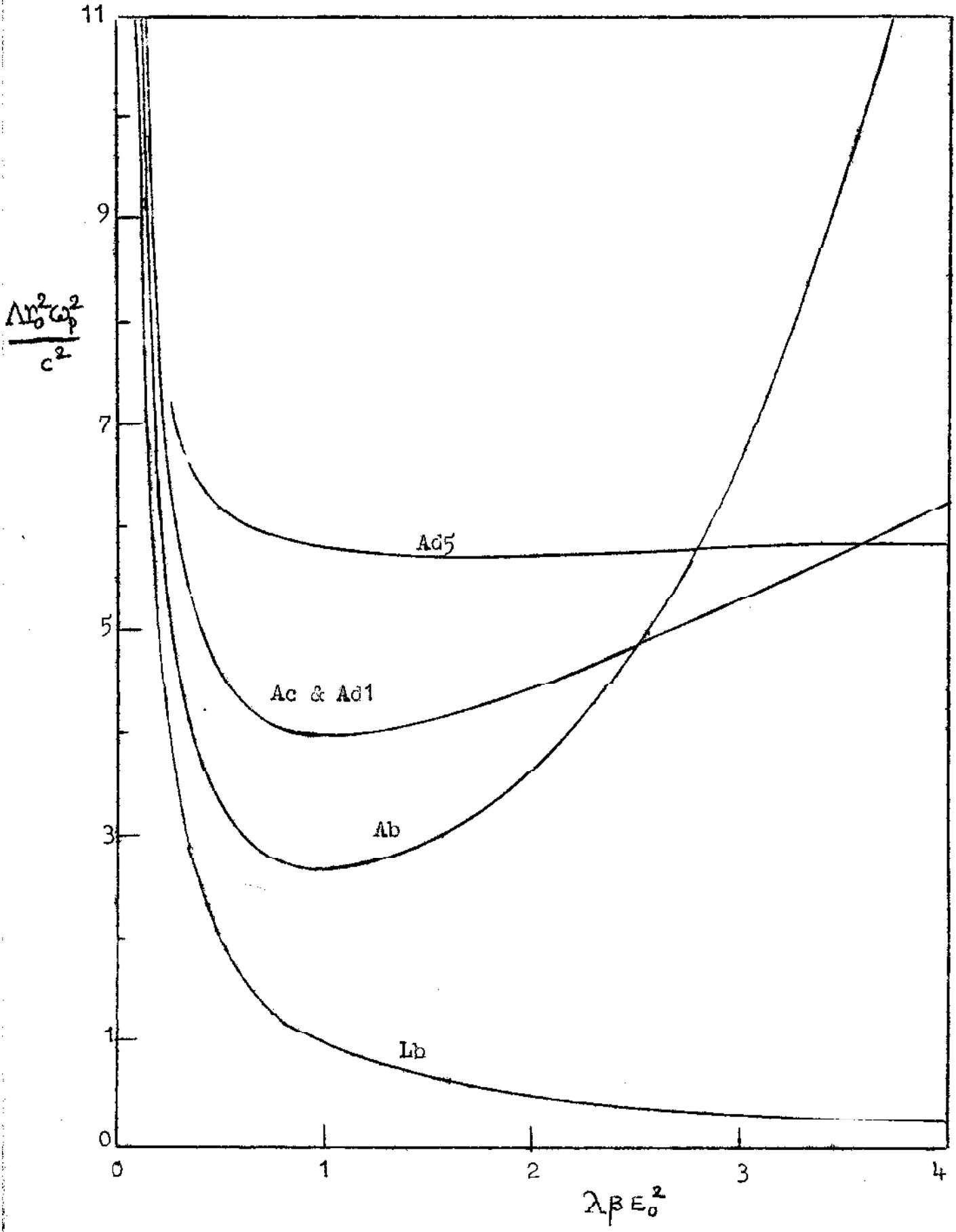
11
9
7
5
3
1
0
$\frac{\Lambda r_0^2 \omega_p^2}{c^2}$
Ad5
Ac & Ad1
Ab
Lb
0
1
2
3
4
$\lambda \beta \epsilon_0^2$

Fig. 1.4

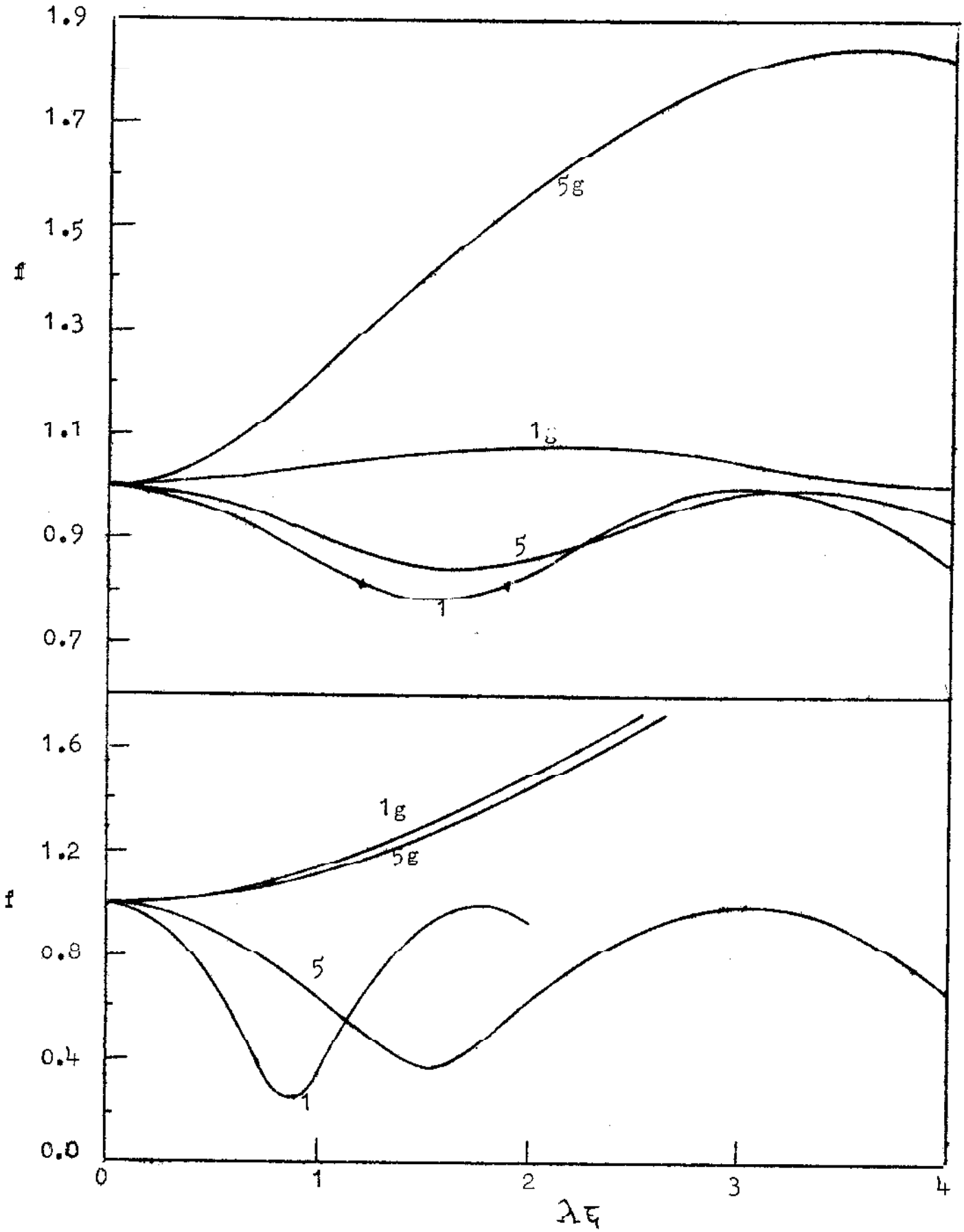

Fig. 1.5

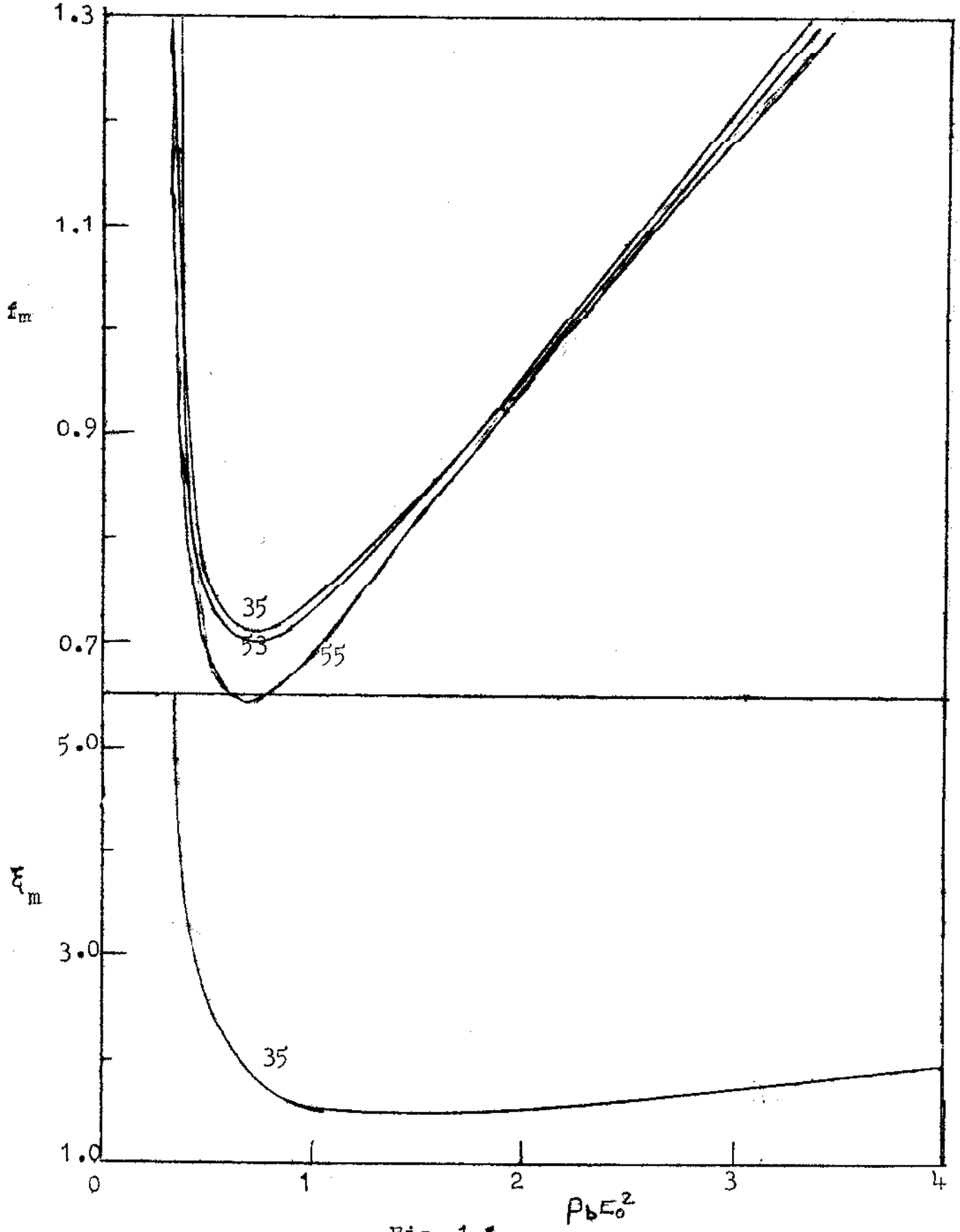

Fig. 1.6

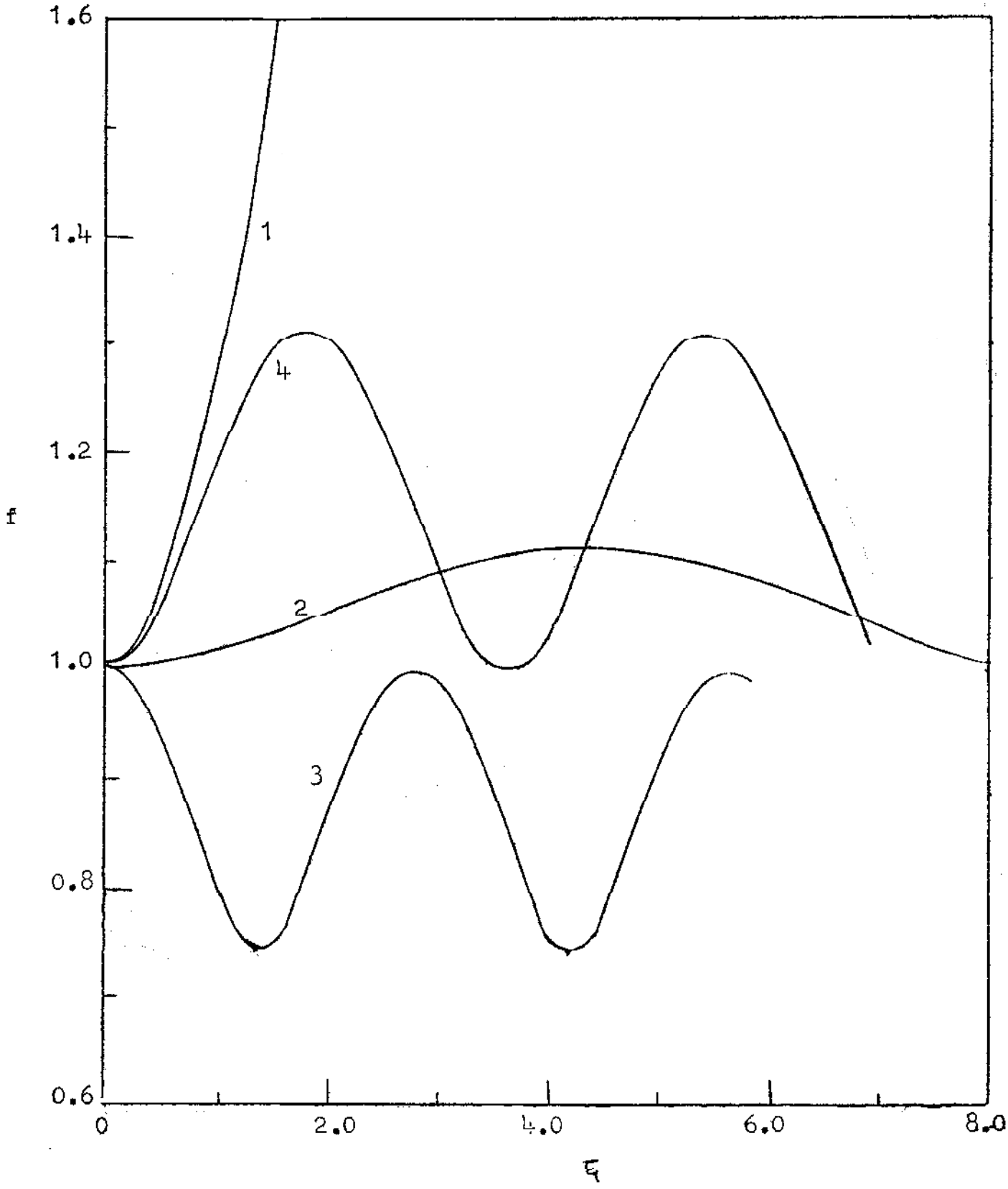

Fig. 1.7

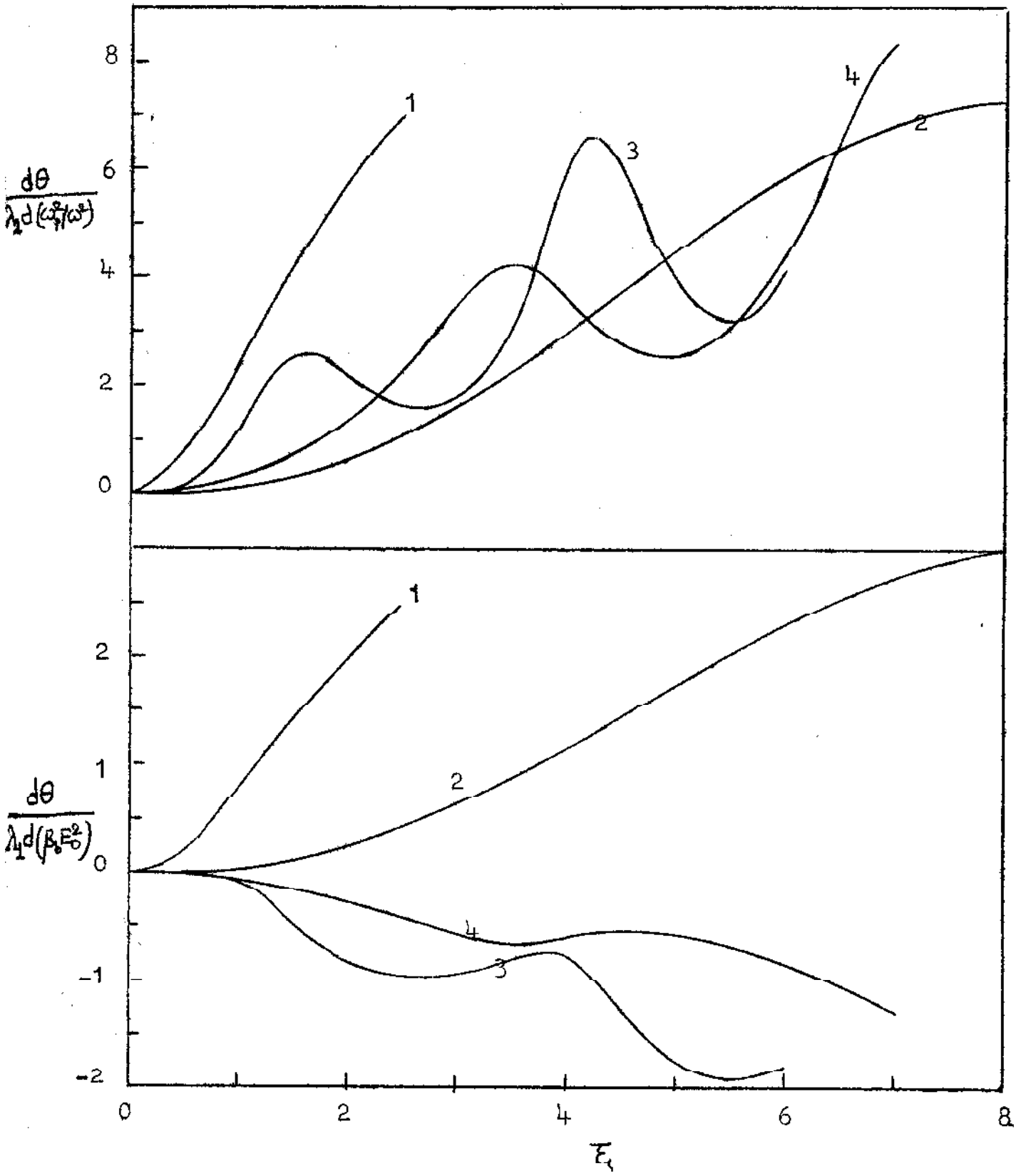
8
6
4
2
0
1
2
3
4
$\frac{d\theta}{\lambda_2 d(\omega_p^2/\omega^2)}$
2
1
0
-1
-2
$\frac{d\theta}{\lambda_1 d(\beta_0 E_0^2)}$
0
2
4
6
8
E_1

Fig. 1.8

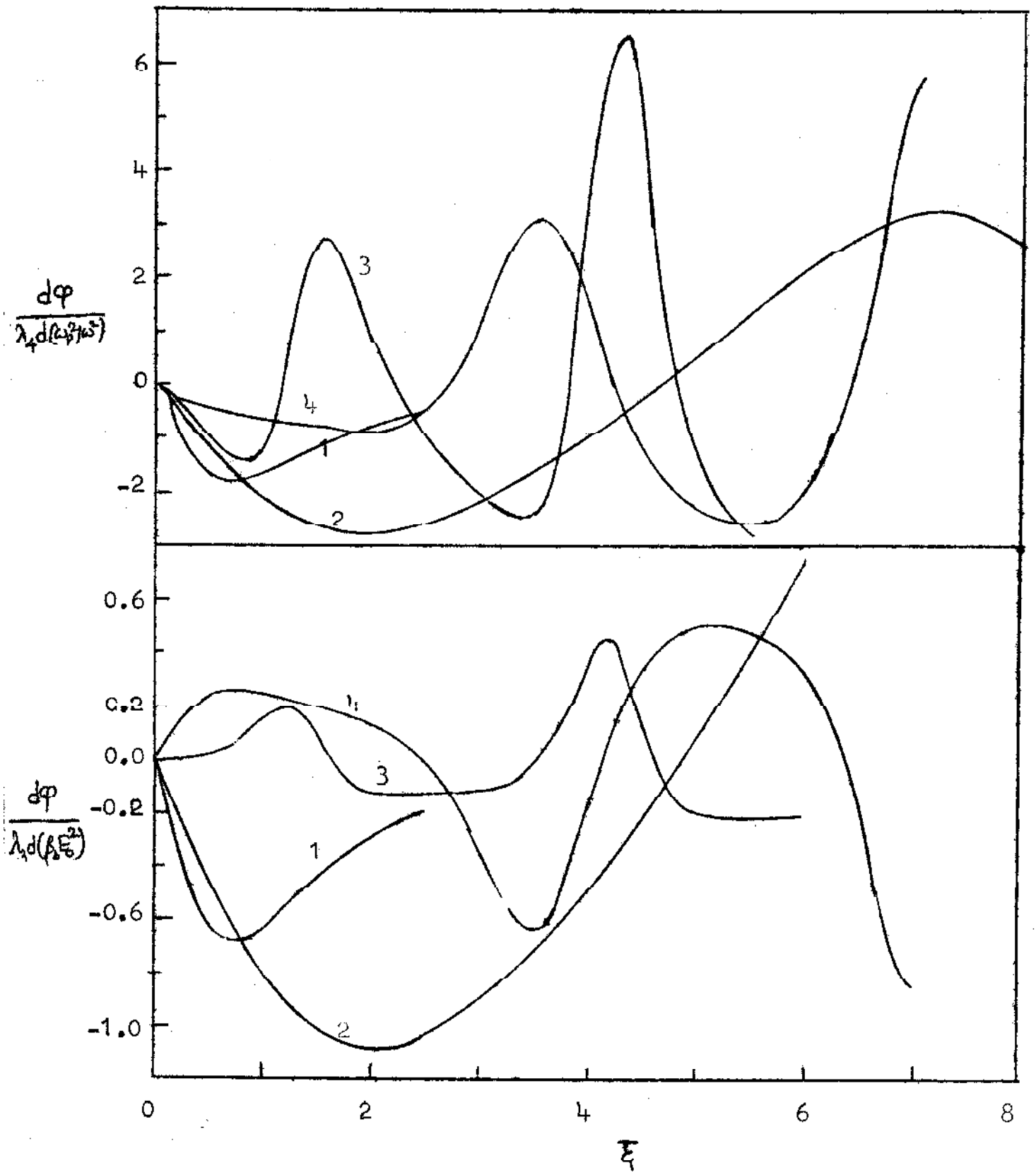
6
4
2
0
-2
3
4
1
2
$\frac{d\varphi}{\lambda_1 d(\omega_p^2/\omega^2)}$
0.6
0.2
0.0
-0.2
-0.6
-1.0
1
3
2
$\frac{d\varphi}{\lambda_1 d(\beta_2 E_0^2)}$
0
2
4
6
8
ξ

Fig. 1. 9

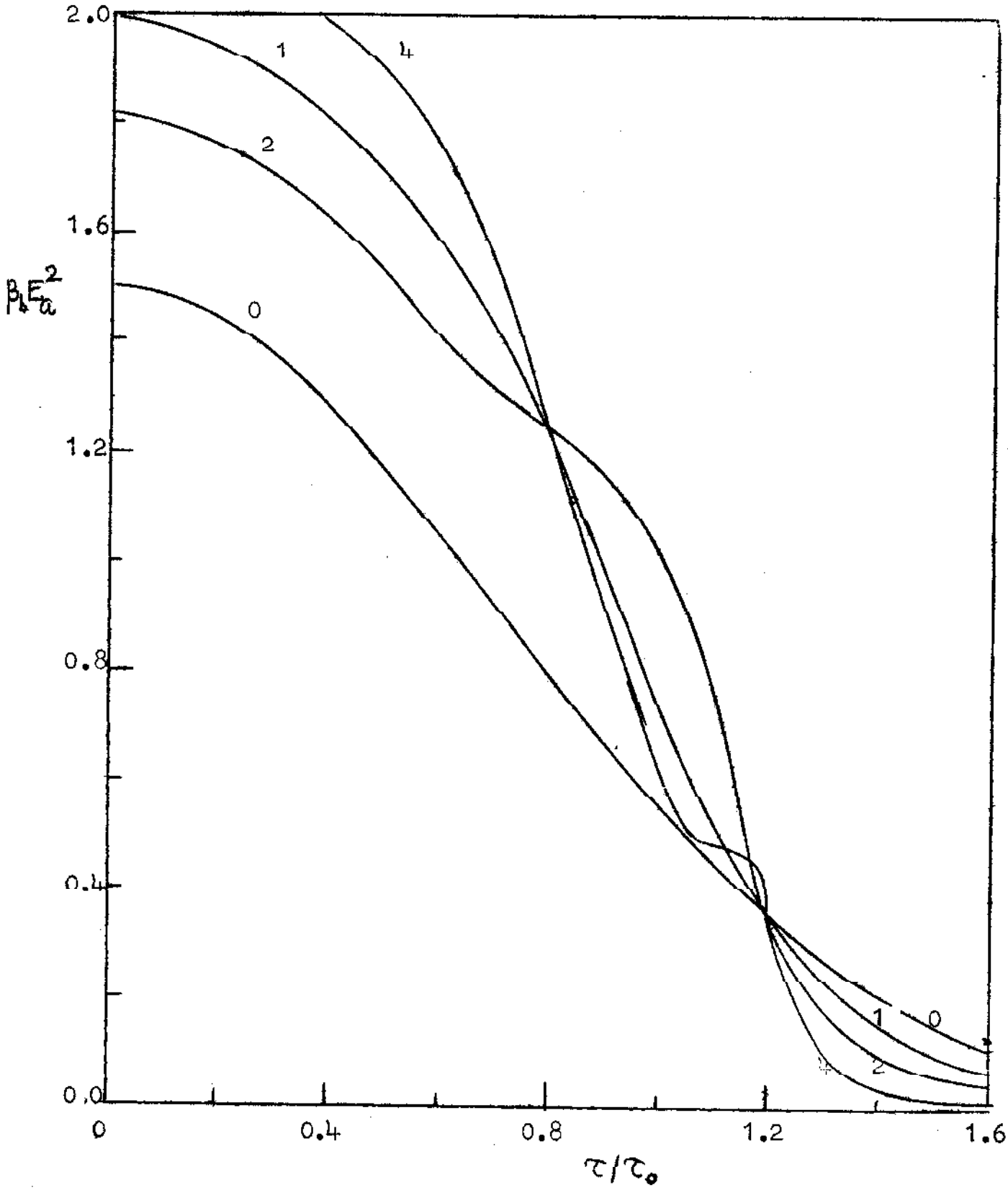

Fig. 1.10

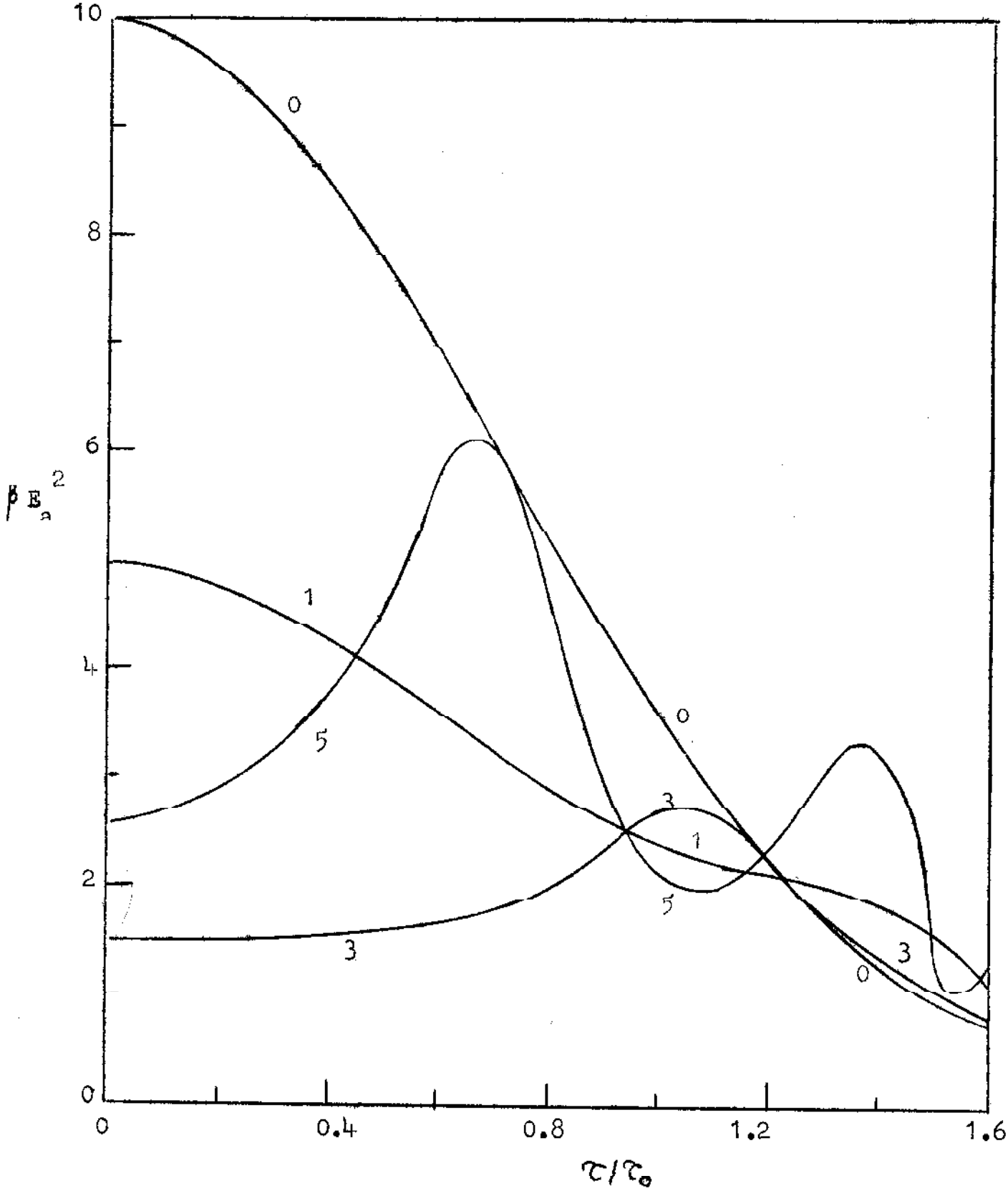

Fig. 1.11

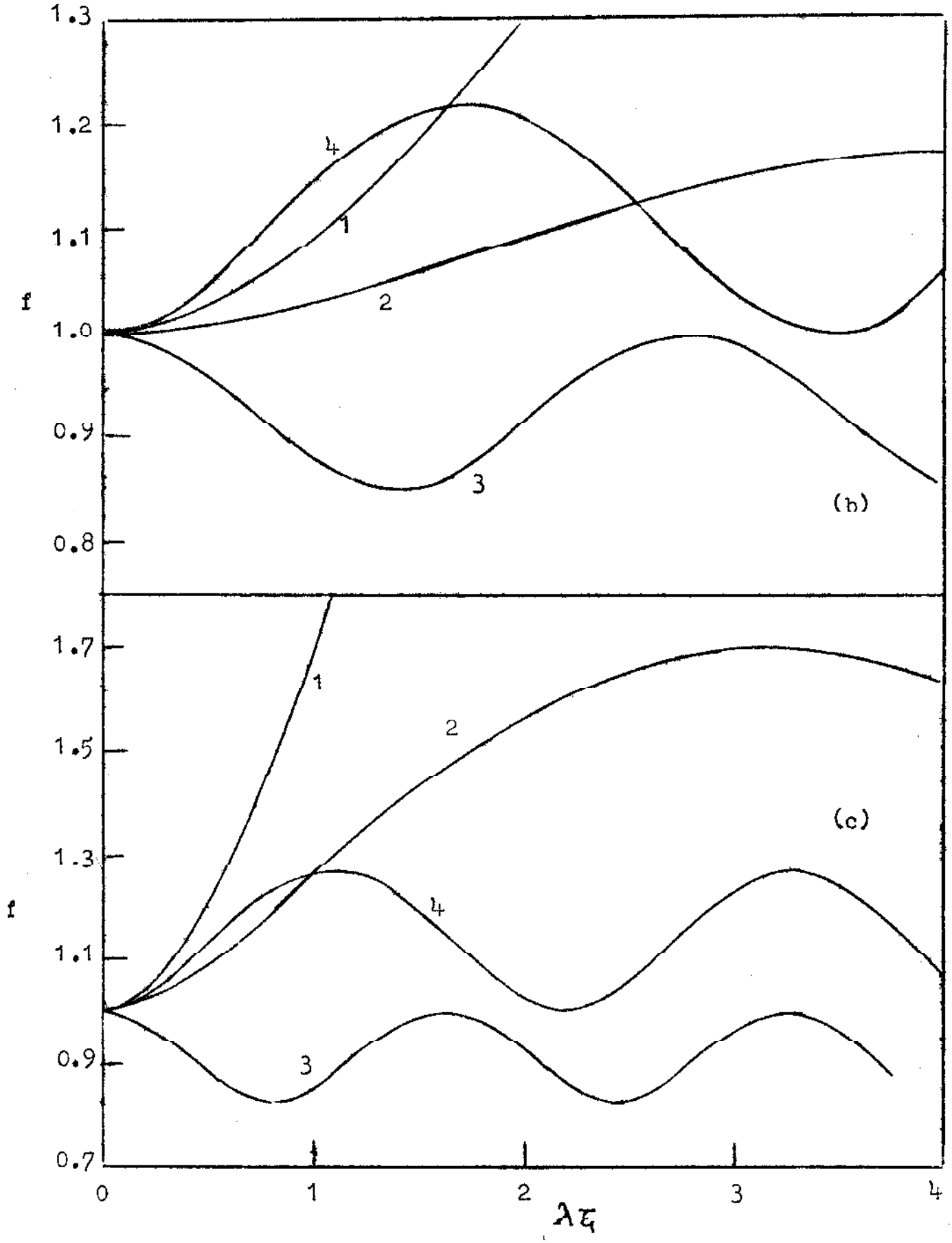

Fig. 1.12

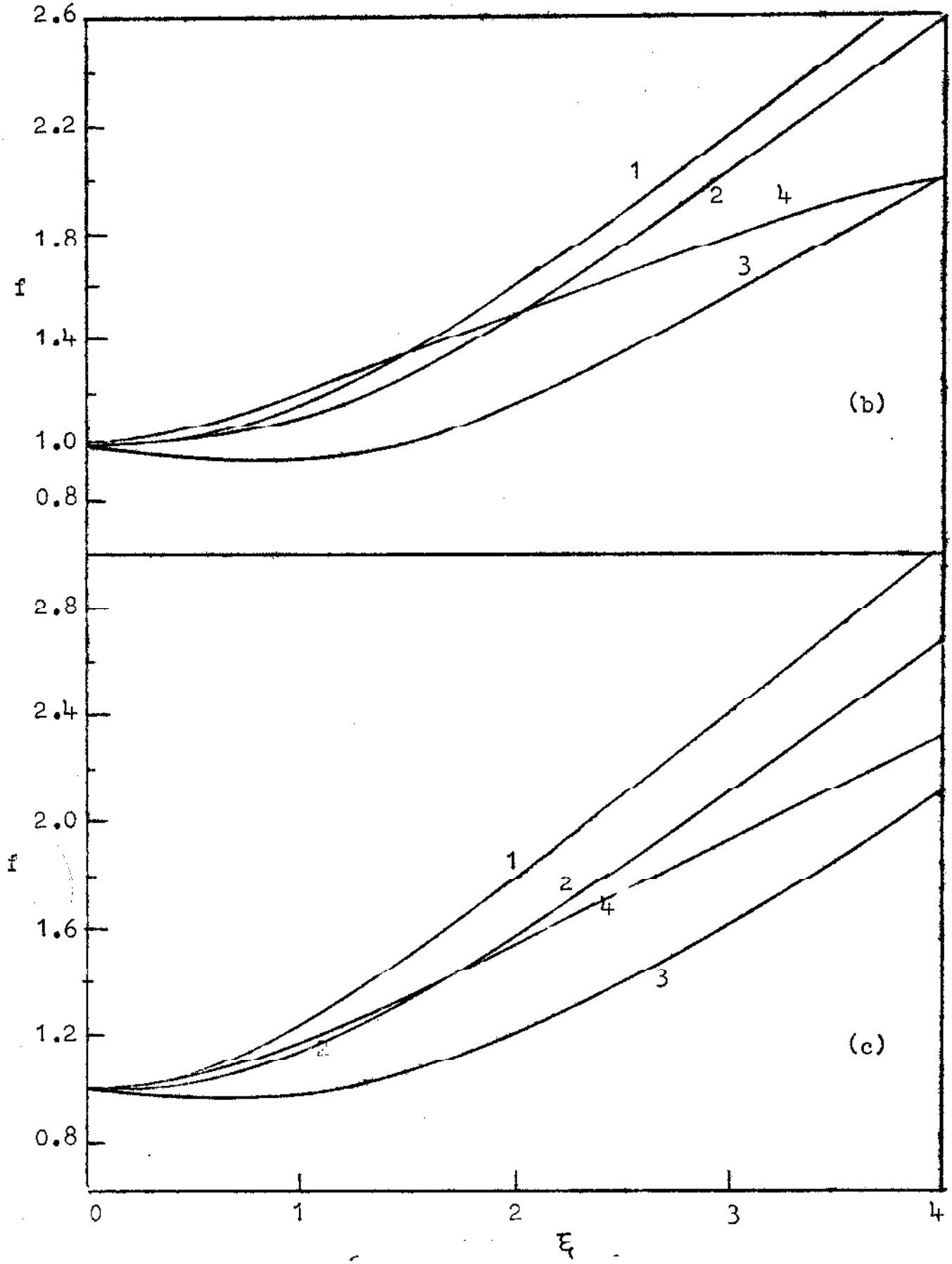

Fig. 1.13

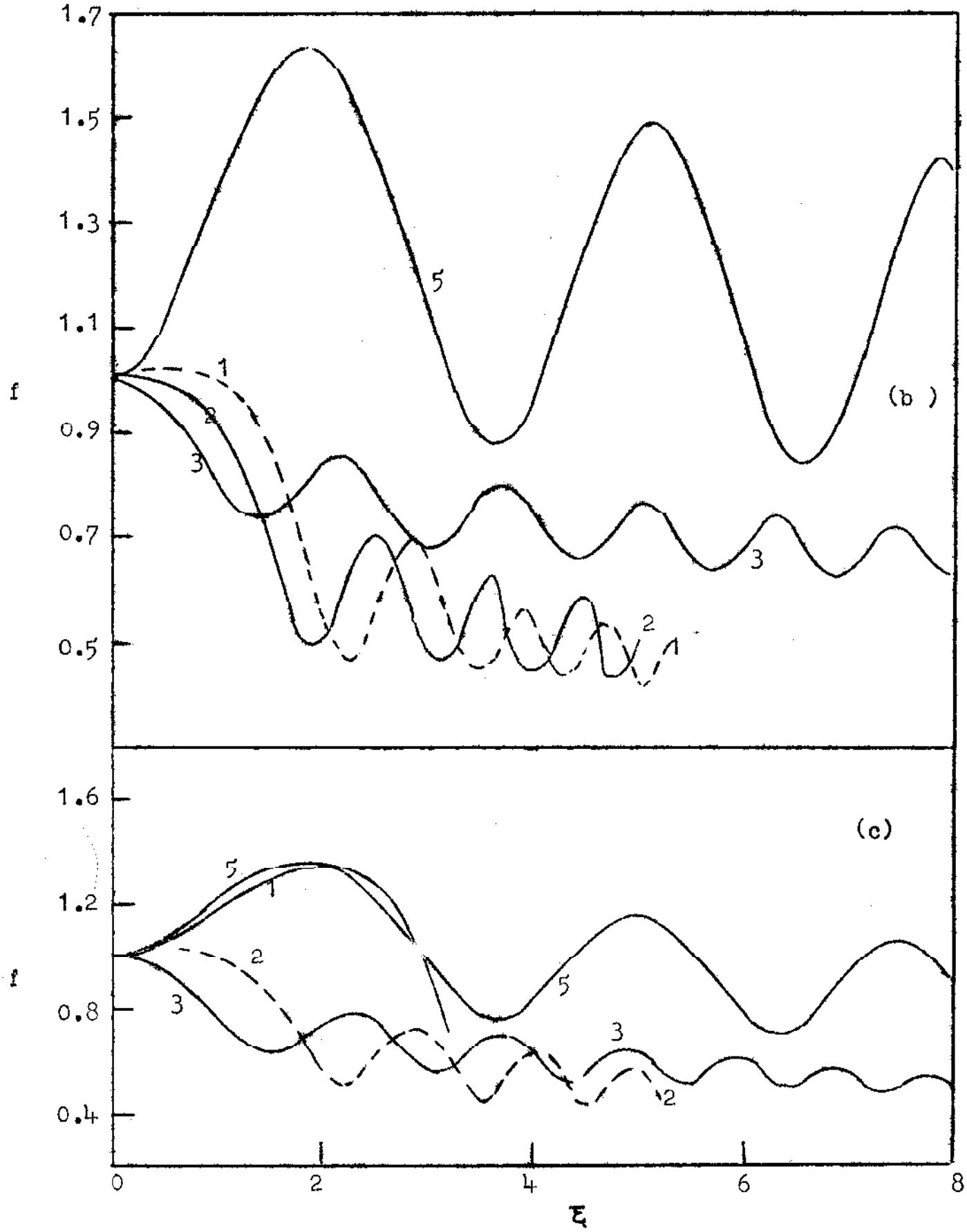

Fig. 1.14

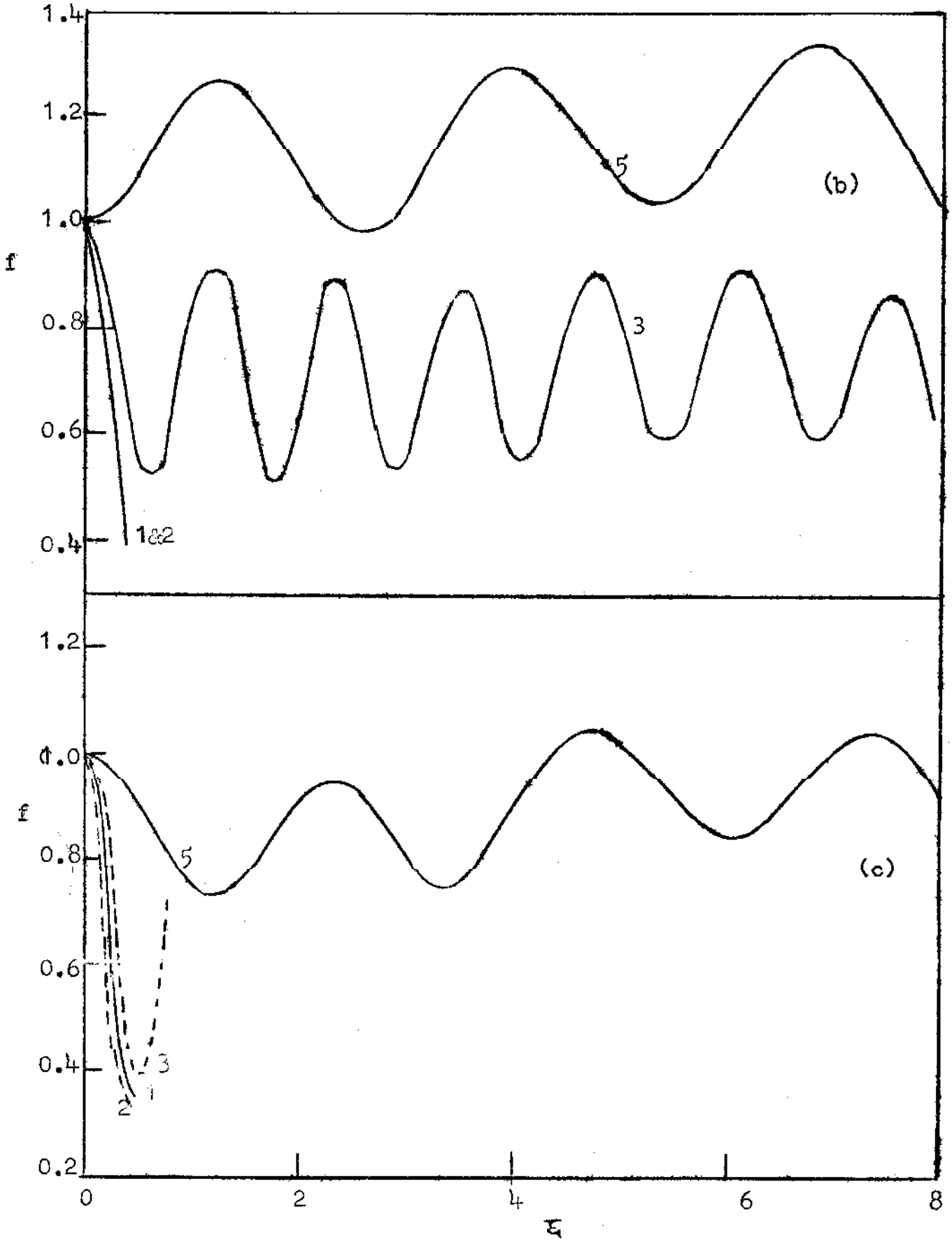

Fig. 1.15

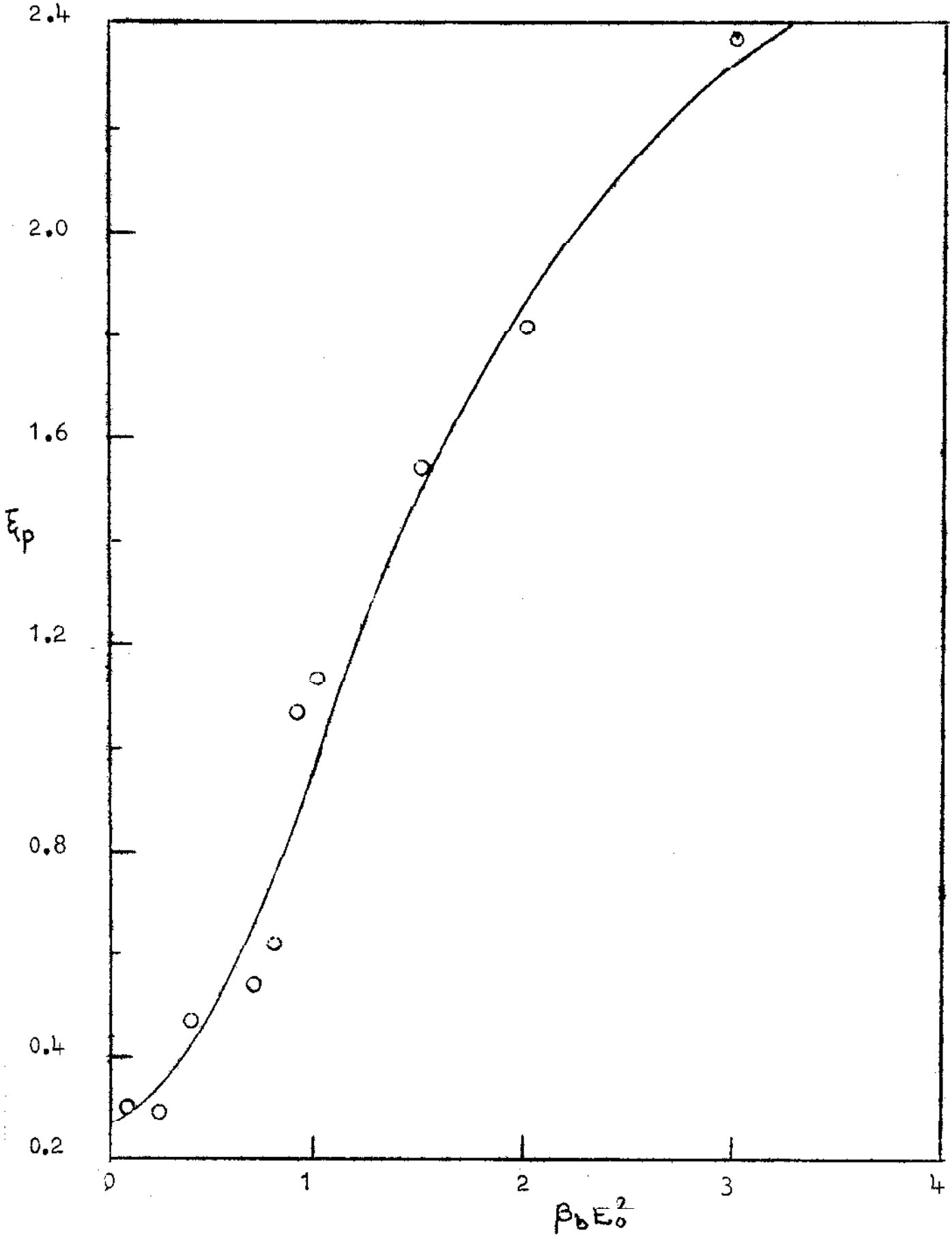

Fig. 1.16

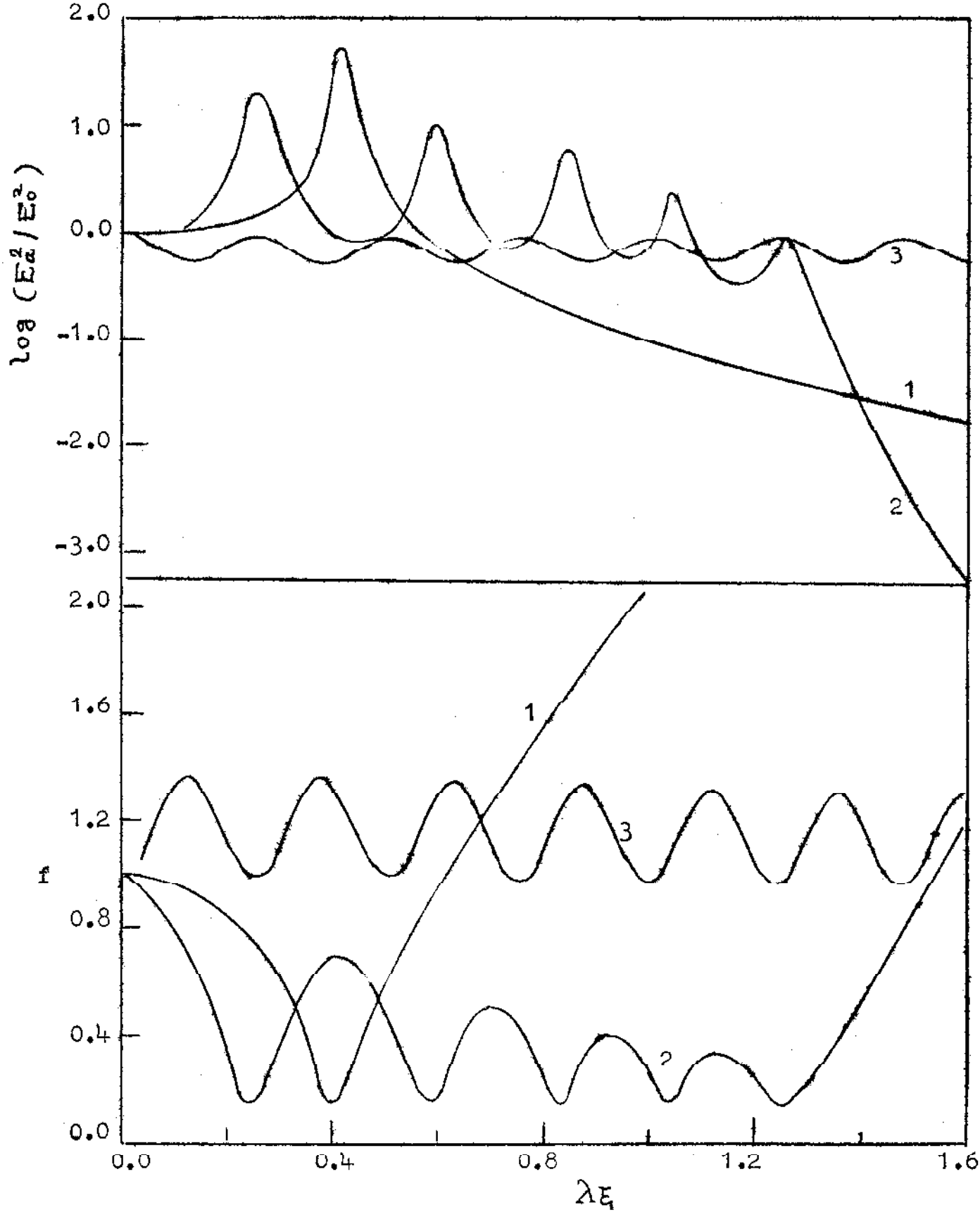
2.0
1.0
0.0
-1.0
-2.0
-3.0
log (E_d^2 / E_o^2)
1
2
3
2.0
1.6
1.2
0.8
0.4
0.0
f
1
2
3
0.0
0.4
0.8
1.2
1.6
λξ

Fig. 1.17

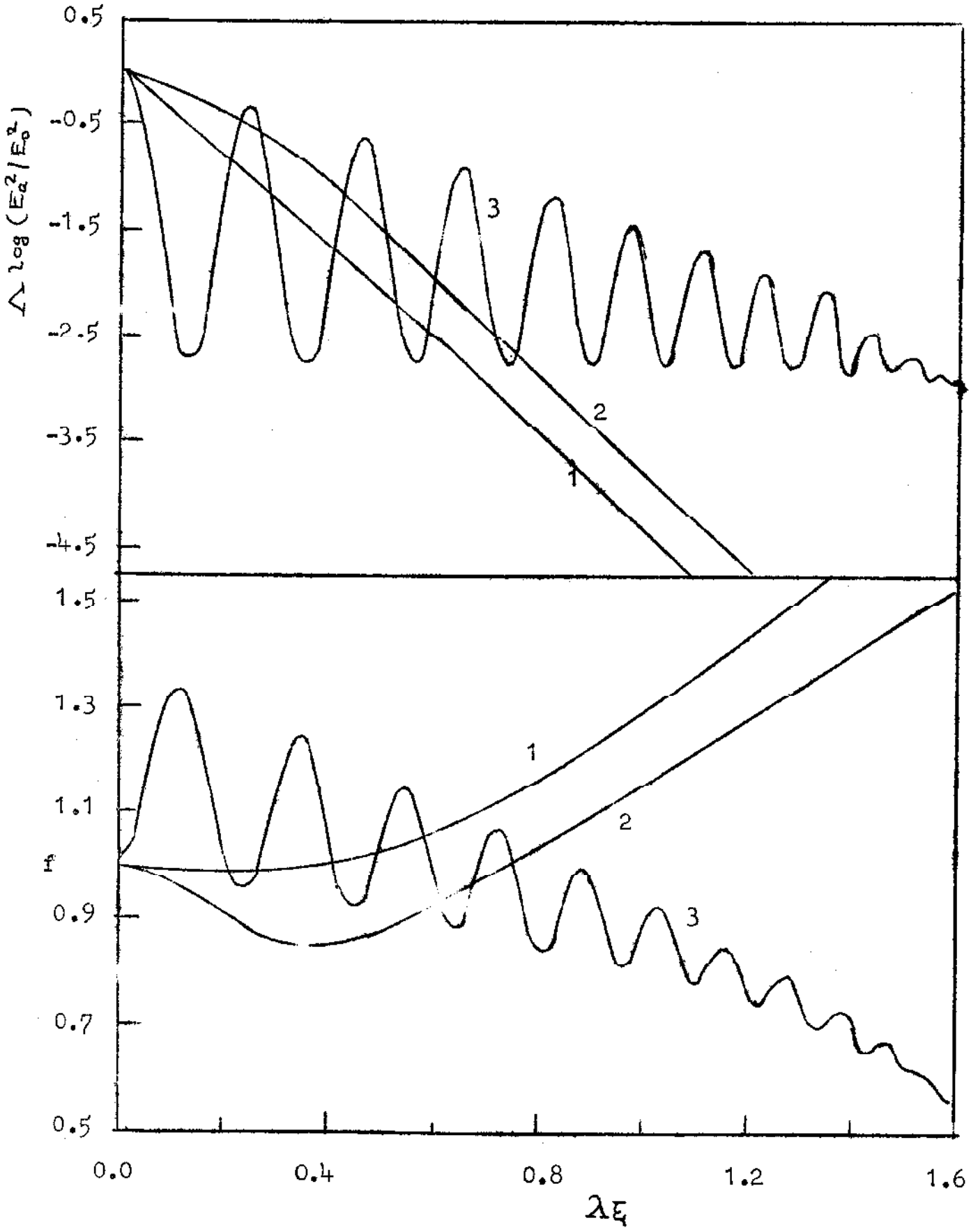
0.5
-0.5
-1.5
-2.5
-3.5
-4.5
Δ log (Ea²/Eo²)
3
2
1
1.5
1.3
1.1
0.9
0.7
0.5
f
1
2
3
0.0
0.4
0.8
1.2
1.6
λξ

Fig. 1.18

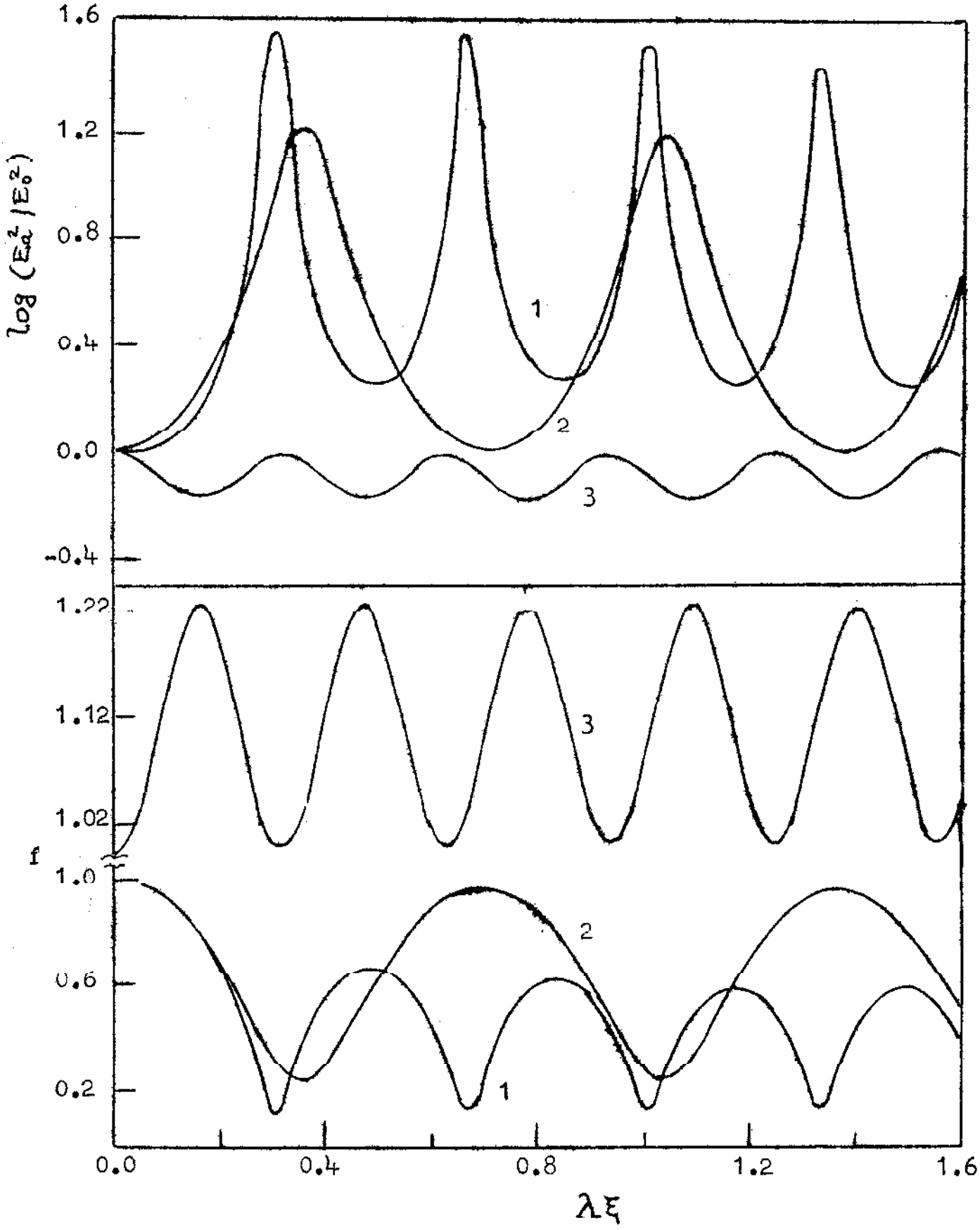
1.6
1.2
0.8
0.4
0.0
-0.4
log (Ea²/E₀²)
1
2
3
1.22
1.12
1.02
f
1.0
0.6
0.2
3
2
1
0.0
0.4
0.8
1.2
1.6
λξ

Fig. 1.19

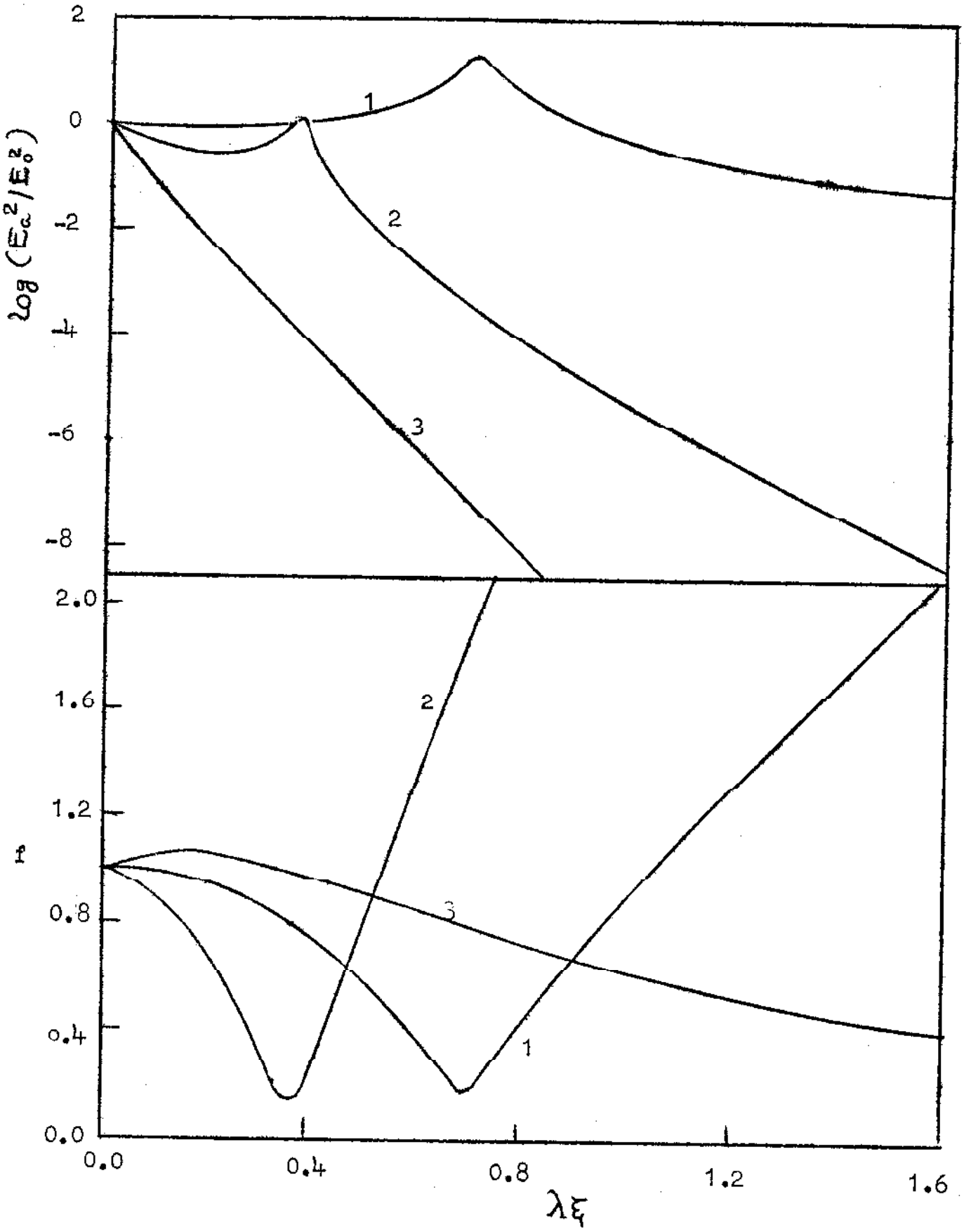

Fig. 1.20

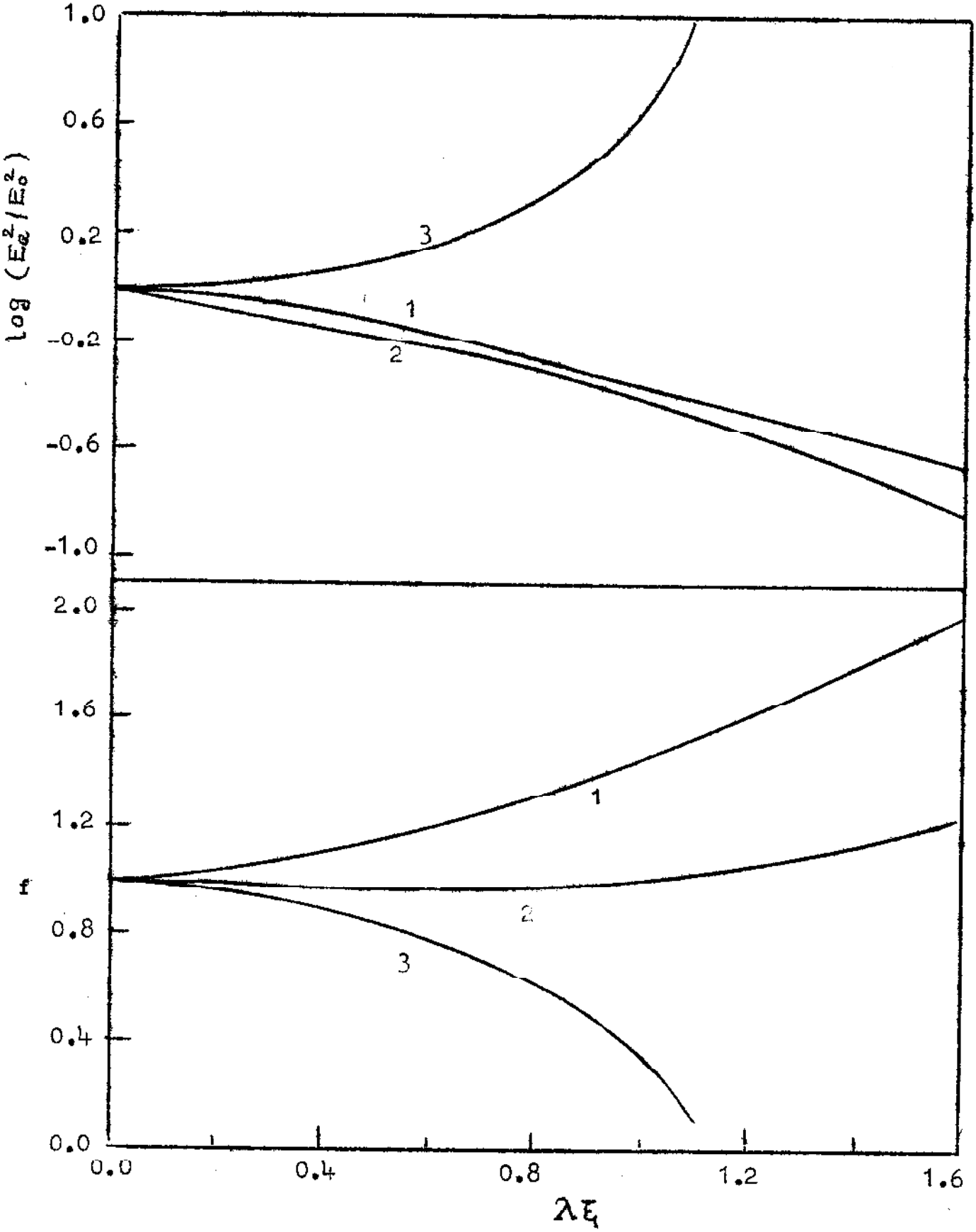
1.0
0.6
0.2
-0.2
-0.6
-1.0
log (E_ℓ²/E_o²)
3
1
2
2.0
1.6
1.2
0.8
0.4
0.0
f
1
2
3
0.0
0.4
0.8
1.2
1.6
λξ

Fig. 1.21

APPENDIX

ELECTRON-HEATING LIMITED BY THERMAL CONDUCTION

The drift velocity $\vec{v}$ and temperature T of electrons in a collisional plasma in the presence of a laser beam are governed by the following momentum and energy-balance equations[32-35].

$$m\frac{d\vec{v}}{dt} = -e\vec{E} - m\nu\vec{v} - N^{-1}\nabla_{\perp}(NK_B T), \qquad (A1)$$

$$\frac{3K_B}{2}\frac{dT}{dt} = -e\vec{v}\cdot\vec{E} - \frac{3m\nu K_B(T-T_o)}{M} + \frac{1}{Nr}\frac{\partial}{\partial r}\left(r\chi\frac{\partial T}{\partial r}\right), \qquad (A2)$$

where N, ν and χ are the electron concentration, electron collision frequency and thermal conductivity of the plasma respectively in the presence of the laser beam. The three terms on the right hand side of Eq.A2 correspond to the energy gained by electrons from the laser beam, energy transferred to heavy ions/neutrals in collisions, and energy lost through thermal conduction respectively. Since the ion/neutral mass M is much larger than the electron mass, T(ion/neutral) = T_o. Since the

characteristic lengths of axial variations of the laser intensity and electron concentration are much larger than the laser beamwidth, the axial variation of the electron temperature T has been neglected in writing Eq.A2. The convection loss[34], which is quite apparent in a flowing plasma, is negligible in the present case. The last term on the right hand side of Eq. A1 does not contribute to the oscillatory component of ν . Then in the steady state (i.e. when $dT/dt \simeq 0$), Eqs. A1 and A2 lead to

$$\frac{3mN\nu K_B(T-T_o)}{M} - \frac{1}{r}\frac{\partial}{\partial r}\left(r\chi\frac{\partial T}{\partial r}\right) = \frac{N\nu e^2 \vec{E}^* \cdot \vec{E}}{m\omega^2} \quad . \tag{A3}$$

If the initial laser beamwidth is so large that the condition[3,4]

$$r_o^2 \gg \chi_o M / \nu_o m K_B N_o \tag{A4}$$

is fulfilled, the second term in Eq. A3 may be neglected. Equation A3 then gives

$$T/T_o = 1 + 2\beta_c \vec{E}^* \cdot \vec{E} \quad , \tag{A5}$$

where

$$\beta_c = Me^2 / 6m^2 K_B T_o \omega^2 \quad . \tag{A6}$$

If the initial laser beamwidth is so small that the condition[32-34]

$$r_0^2 \ll \chi_0 M / \nu_0 m K_B N_0 \qquad (A7)$$

is fulfilled, the first term in Eq. A3 may be neglected. Equation A3 then gives

$$\frac{1}{r}\frac{\partial}{\partial r}\left(r\chi\frac{\partial T}{\partial r}\right) = -\frac{N\nu e^2 \vec{E}^* \cdot \vec{E}}{m\omega^2} \qquad (A8)$$

The condition A7 is satisfied mostly in strongly ionized plasmas in which collisions other than the electron-ion collisions are absent[50]. Thus $\nu \propto N$ in the present case. The temperature-dependences of χ and ν can be most conveniently represented in the forms[50,60,61]

$$\chi / \chi_0 = (T/T_0)^{n-1}, \qquad (A9)$$

$$\nu/\nu_0 = (N/N_0)(T/T_0)^{n-\sigma}, \qquad (A10)$$

where the subscript 0 refers to absence of the laser beam. Equation A8 then reduces to

$$\frac{1}{nT^{n-\sigma}}\frac{\partial}{\partial r}\left(r\frac{\partial T^n}{\partial r}\right) = -\frac{N^2\nu_0 T_0^{\sigma-1} e^2 \vec{E}^* \cdot \vec{E}}{N_0 \chi_0 m\omega^2}. \qquad (A11)$$

In order to simplify the solution of Eq. A11, the left hand side term may be approximated as $\frac{1}{\sigma r}\frac{\partial}{\partial r}\left(r\frac{\partial T^\sigma}{\partial r}\right)$. This approximation is justified, because the remainder

term

$$\frac{1}{nT^{n-\sigma}r}\frac{\partial}{\partial r}\left(r\frac{\partial T^{n}}{\partial r}\right)-\frac{1}{\sigma r}\frac{\partial}{\partial r}\left(r\frac{\partial T^{\sigma}}{\partial r}\right)=\frac{(\sigma-n)}{T^{\sigma}\sigma^{2}}\left(\frac{\partial T^{\sigma}}{\partial r}\right)^{2} \tag{A12}$$

is negligible in the paraxial region where T decreases linearly with r^2. Moreover, the radial variation of N appearing on the right hand side of Eq. A11 may be neglected and N may be replaced by the axial electron concentration N_a. With these approximations, Eq. A11 becomes

$$\frac{1}{r}\frac{\partial}{\partial r}\left(r\frac{\partial T^{\sigma}}{\partial r}\right)=-\frac{8\sigma N_a^2 T_o^{\sigma}\beta_d E_a^2}{N_o^2 r_o^2}\exp\left(-r^2/r_o^2 f^2\right), \tag{A13}$$

where the notation

$$\beta_d = N_o \nu_o e^2 r_o^2 / 8 \chi_o T_o m \omega^2 \tag{A15}$$

and the expression

$$\vec{E}^{*}\vec{E} = E_a^2 \exp\left(-r^2/r_o^2 f^2\right) \tag{A16}$$

have been introduced. Integrating Eq. A13 gives

$$\frac{\partial T^{\sigma}}{\partial r}=\frac{4\sigma N_a^2 T_o^{\sigma}\beta_d E_a^2 f^2}{N_o^2 r}\left[1-\exp\left(-r^2/r_o^2 f^2\right)\right]. \tag{A17}$$

As a boundary condition[62,63], it may be assumed that the plasma is not heated at and beyond the boundary located at

$r = b$, so that

$$T \text{ (at the boundary at } r = b) = T_o. \tag{A.18}$$

Integrating Eq. A17 gives

$$T^{\sigma} - T_o^{\sigma} = \frac{2\sigma N_a^2 T_o^{\sigma} \beta_d E_c^2 f^2}{N_o^2} \int_{r^2/r_o^2 f^2}^{b^2/r_o^2 f^2} \left[1 - \exp(-x)\right] x^{-1} dx . \tag{A19}$$

In the paraxial region ($r \ll r_o f$),

$$\int_0^{r^2/r_o^2 f^2} \left[1 - \exp(-x)\right] x^{-1} dx \simeq r^2/r_o^2 f^2 , \tag{A20}$$

and hence Eq. A19 leads to

$$T/T_o = \left[1 + 2\sigma N_a^2 N_o^{-2} \beta_d E_c^2 (g f^2 - r^2/r_o^2)\right]^{1/\sigma} , \tag{A21}$$

where

$$g = \int_0^{b^2/r_o^2 f^2} \left[1 - \exp(-x)\right] x^{-1} dx . \tag{A22}$$

For a large value of b^2/r_o^2, $dg/df \sim 0$ and hence g may be considered a z independent parameter evaluated at $f = 1$.

Using a kinetic treatment[4] for the pressure-balance condition[3,4], Sodha et al.[4] have shown that the electron concentration N varies with the electron temperature T

varies in the form

$$\frac{N}{N_o} = \left(\frac{T + T_o}{2T_o} \right)^{s/2 - 1} , \qquad (A23)$$

where

$$s = 2(n - \sigma) = -3 \text{ or } 1 \text{ or } 2 \qquad (A24)$$

depending upon whether the electron collisions are with ions or nondiatomic molecules or diatomic molecules[4]. Using the expressions for T as derived above, the following expressions are obtained:

$$N / N_o = (1 + \beta_e \vec{E}^* \cdot \vec{E})^{s/2-1} \qquad (A25)$$

when $r_o^2 \gg \chi_o M / \nu_o m K_B N_o$, and

$$N/N_o = \left\{ 1/2 + \left[1 + 2\sigma N_a^2 N_o^{-2} \beta_d E_a^2 (gf^2 - r^2/r_o^2) \right]^{1/\sigma} / 2 \right\}^{s/2-1} \qquad (A26)$$

when $r_o^2 \ll \chi_o M / \nu_o m K_B N_o$.

In the case of electron-ion collisions,

$$\sigma = 5 . \qquad (A27)$$

Earlier analyses[32-35] had implictly assumed $\sigma = 1$ since they had not considered the variations of the thermal conductivity of the plasma and electron collision frequency with the electron temperature. Since the plasma-boundary

$r = b$ is located much farther from the axis than the laser beamwidth at $r = r_o$, the boundary-effect parameter[114]

$$g \gg 1 \quad . \tag{A28}$$

Earlier analyses[32-35] had implicitly assumed g=1 since they had not considered the appropriate boundary conditions in solving the heat conduction equation. Moreover, unlike in the present analysis, the earlier analysis had assumed $N_a = N_o$ in solving the heat conduction equation. In this way, the earlier analyses[32-35] of the electron-heating limited by thermal conduction were very much approximate.

CHAPTER 2

LASER SELF FOCUSING IN A MAGNETOPLASMA

In Chapter 1, the analysis of laser self focusing was carried out in plasmas in the absence of any static magnetic field. Many of the plasmas are, however, immersed in (external or self-generated) static magnetic fields[64,65]. It is therefore important to understand how the presence of a static magnetic field influences the phenomenon of laser self focusing. This chapter presents an analysis of self focusing of a laser beam propagating along the direction of the static magnetic field in a magnetoplasma. The initial electron concentration and temperature and the static magnetic field are allowed to be nonuniform[64], and the laser absorption is allowed to vary with the laser intensity[36]. In Sec.2.1, the expressions for the components of the nonlinear dielectric[3,4,40] tensor of the plasma in the presence of left and right circularly polarized modes have been presented. Two cases of nonlinearity have been considered[3,4,40], viz. (1) the redistribution is caused by the ponderomotive force and (2) the redistribution is caused by the nonuniform heating of electrons. In Sec.2.2, the coupled wave equations[3,4,40] for the left and right circularly polarized modes of the laser have been solved under the paraxial and WKB approximations and following a

slightly modified version of Akhmanov et al.'s[1] approach. Equations for the beamwidth and "crosswidth" parameters and corresponding expressions for the intensities of the two modes have been derived. Numerical calculations have been carried out for typical sets of parameters corresponding to the case in which the redistribution is caused by the ponderomotive force.

It is seen that the radial nonuniformity[64] in the initial electron concentration, initial electron temperature and static magnetic field have considerable influence on self focusing of the two modes. The direct coupling[70] (which arises due to the magnetic-field induced anisotropy) between the two modes leads to axial asymmetry of the intensity profiles of the two modes. The indirect coupling[70] (which arises due to intensity-dependence of the dielectric tensor) between the two modes leads to cross-focusing of the two modes; the direct coupling has little effect on the cross-focusing.

2.1: Dielectric Tensor

The effective dielectric functions for the left and right circularly polarized modes of a laser beam (of frequency ω) propagating along the direction of the static magnetic field in a (nonrelativistic) magnetoplasma (with the collision frequency $\nu \ll$ the laser frequency

ω) are given by[3,4,40]

$$\epsilon_{\pm} = 1 - (\omega_p^2/\omega^2)(N/N_0)/(1 \mp \omega_c/\omega) - i(\omega_p^2 \nu_0/\omega^3)(N\nu/N_0\nu_0)/(1 \mp \omega_c/\omega) , \quad (2.1)$$

where $\omega_p = (4\pi N_0 e^2/m)^{1/2}$, N_0 and ν_0 are the plasma frequency, electron concentration and electron collision frequency respectively in the absence of the laser beam; N and ν are the electron concentration and electron collision frequency respectively in the presence of the laser beam; $\omega_c = |e| B_0/mc$, $B_0\hat{z}$, c, m and e are the cyclotron frequency, static magnetic field, light-speed in vacuum, electron mass and electron charge respectively. The ratios ω_p^2/ω^2 , $\omega_p^2\nu_0/\omega^3$ and ω_c/ω will be considered to be time-independent but they may vary in space[64]. The ratios N/N_0 and $N\nu/N_0\nu_0$ depend upon the electric field intensities $\vec{E}_{\pm}^{*} \cdot \vec{E}_{\pm}$ of the two modes.

As shown in Sec.2.2, the intensities $\vec{E}_{\pm}^{*} \cdot \vec{E}_{\pm}$ of the two modes are expressed as

$$\vec{E}_{\pm}^{*} \cdot \vec{E}_{\pm} = E_{a\pm}^2 \exp\left(-x^2/r_0^2 f_{x\pm}^2 - y^2/r_0^2 f_{y\pm}^2 - h_{\pm} x y/r_0^2\right) , \quad (2.2)$$

where the axial intensities $E_{a\pm}^2$, the beamwidth parameters $f_{x,y\pm}$ and the "cross width" parameters $h_{\pm}$ vary with the distance of propagation z; x and y are the transverse Cartesian coordinates, and r_0 is a suitably chosen constant

parameter. In an axially symmetric plasma, ω_p^2/ω^2, $\omega_p^2\nu_0/\omega^3$ and ω_c/ω are even functions of x and y. In the paraxial region ($x \ll r_0 f_{x\pm}$, $y \ll r_0 f_{y\pm}$), $\epsilon_\pm$ may be expanded as the Maclaurin series[62,63] in powers of x^2/r_0^2, y^2/r_0^2 and xy/r_0^2; the terms containing odd powers of x/r_0 and y/r_0 separately are negligible. The series-expansions upto the first powers give

$$\epsilon_\pm \simeq (\epsilon_{ar\pm} - i\epsilon_{ai\pm}) - (\epsilon_{xr\pm} + i\epsilon_{xi\pm})\, x^2/r_0^2 - (\epsilon_{yr\pm} + i\epsilon_{yi\pm})\, y^2/r_0^2 - (\epsilon_{cr\pm} + i\epsilon_{ci\pm})\, xy/r_0^2 , \tag{2.3}$$

where

$$\epsilon_{ar\pm} = 1 - \left[(\omega_p^2/\omega^2)(N/N_0)/(1 \mp \omega_c/\omega)\right]_{(x=y=0)} , \tag{2.4}$$

$$\epsilon_{ai\pm} = \left[(\omega_p^2\nu_0/\omega^3)(N\nu/N_0\nu_0)/(1 \mp \omega_c/\omega)\right]_{(x=y=0)} , \tag{2.5}$$

$$\epsilon_{xr\pm} = \left[\frac{\partial}{\partial(x^2/r_0^2)}\left\{\frac{\omega_p^2}{\omega^2}\frac{N}{N_0}\Big/(1 \mp \omega_c/\omega)\right\}\right]_{(x=y=0)} , \tag{2.6}$$

$$\epsilon_{xi\pm} = \left[\frac{\partial}{\partial(x^2/r_0^2)}\left\{\frac{\omega_p^2\nu_0}{\omega^3}\frac{N\nu}{N_0\nu_0}\Big/(1 \mp \omega_c/\omega)\right\}\right]_{(x=y=0)} , \tag{2.7}$$

$$\epsilon_{yr\pm} = \epsilon_{xr\pm}\left[x^2/r_0^2 \longrightarrow y^2/r_0^2\right] , \tag{2.8}$$

$$\epsilon_{yi\pm} = \epsilon_{xi\pm}\left[x^2/r_0^2 \longrightarrow y^2/r_0^2\right] , \tag{2.9}$$

$$\epsilon_{cr\pm} = \left[\left\{ \frac{\omega_p^2}{\omega^2} \Big/ (1 \mp \omega_c/\omega) \right\} \frac{\partial}{\partial (xy/r_o^2 f^2)} \left(\frac{N}{N_o} \right) \right]_{(x=y=0)} , \tag{2.10}$$

$$\epsilon_{ci\pm} = \left[\left\{ \frac{\omega_p^2 \nu_o}{\omega^3} \Big/ (1 \mp \omega_c/\omega) \right\} \frac{\partial}{\partial (xy/r_o^2 f^2)} \left(\frac{N\nu}{N_o \nu} \right) \right]_{(x=y=0)} . \tag{2.11}$$

2.1b: Ponderomotive force

On short time scale ($t < \tau_p \sim r_o/c_s$), the electron temperature remains almost unaltered in the presence of the laser beam, and the plasma-redistribution is governed by the ponderomotive force[4,24-28]. In the steady state, dynamics[112] of the ponderomotive force is unimportant. If the plasma-boundaries[27,112] are located far away from the axis (x=y=0), their effect on the plasma-redistribution caused by the ponderomotive force may be neglected. In the presence of the static magnetic field, the expression 1.8b ceases to be valid. It can be shown that[4,40]:

$$N/N_o = \exp \left[-\beta (1 - \omega_c/2\omega) \sum_{\pm} (1 \mp \omega_c/\omega)^{-2} \vec{E}_{\pm}^{*} \vec{E}_{\pm} \right] , \tag{2.12b}$$

$$N\nu/N_o\nu_o = (N/N_o)^b = \exp \left[-b\beta (1 - \omega_c/2\omega) \sum_{\pm} (1 \mp \omega_c/\omega)^{-2} \vec{E}_{\pm}^{*} \vec{E}_{\pm} \right] , \tag{2.13b}$$

where

$$\beta_b = e^2 / 4 m K_B T_o \omega^2 , \qquad (2.14\,b)$$

K_B is the Boltzmann constant, T_o is the plasma temperature in the absence of the laser beam, and

$$b = 2 \text{ or } 1 \qquad (2.15)$$

depending upon whether the electron collisions are with ions or neutrals. Consequently

$$\epsilon_{ar\pm} = 1 - (\omega_p^2/\omega^2)_{(x=y=0)} \exp\left[-\beta_{ob}(1-\omega_c/2\omega)\sum_{\pm} (1\mp\omega_c/\omega)^{-2} E_{a\pm}^2\right] , \qquad (2.16\,b)$$

$$\epsilon_{ai\pm} = -(\omega_p^2 b/\omega^3)_{(x=y=0)} \exp\left[-b\beta_{ob}(1-\omega_{oc}/2\omega)\sum_{\pm} (1\mp\omega_{oc}/\omega)^{-2} E_{a\pm}^2\right] , \qquad (2.17\,b)$$

$$\epsilon_{xr\pm} = \left\{\frac{\partial}{\partial(x^2/r_o^2)}\left(\frac{\omega_p^2}{\omega^2}\right) - \left(\frac{\omega_p^2}{\omega^2}\right)\frac{\partial}{\partial(x^2/r_o^2)}\left[\beta_b(1-\omega_c/2\omega)\sum_{\pm} (1\mp\omega_c/\omega)^{-2} E_{a\pm}^2\right] + \left(\frac{\omega_p^2}{\omega^2}\right)\beta_b(1-\omega_c/\omega)\sum_{\pm} (1\mp\omega_c/\omega)^{-2} E_{a\pm}^2 f_{x\pm}^{-2}\right\}_{(x=y=0)} \exp\left[-\beta_{ob}(1-\omega_{oc}/2\omega)\sum_{\pm} (1\mp\omega_c/\omega)^{-2} E_{a\pm}^2\right] , \qquad (2.18\,b)$$

$$\epsilon_{xi\pm} = \epsilon_{xr\pm}\left[\omega_p^2/\omega^2 \to \omega_p^2 b/\omega^3 ,\ \beta_b \to b\beta_b\right] , \qquad (2.19\,b)$$

$$\epsilon_{yr\pm} = \epsilon_{xr\pm}\left[x^2/r_0^2 \rightarrow y^2/r_0^2\,,\ f_{x\pm} \rightarrow f_{y\pm}\right], \qquad (2.20b)$$

$$\epsilon_{yi\pm} = \epsilon_{xi\pm}\left[x^2/r_0^2 \rightarrow y^2/r_0^2\,,\ f_{x\pm} \rightarrow f_{y\pm}\right], \qquad (2.21b)$$

$$\epsilon_{cr\pm} = \left(\omega_p^2/\omega^2\right)_{(x=y=0)} \beta_{ob}\left(1-\omega_{oc}/2\omega\right) \sum_{\pm} \left(1\mp\omega_{oc}/\omega\right)^{-2}$$

$$E_{a\pm}^2\, h_{\pm}\, \exp\left[-\beta_{ob}\left(1-\omega_{oc}/2\omega\right) \sum_{\pm} \left(1\mp\omega_{oc}/\omega\right)^2 E_{a\pm}^2\right], \qquad (2.22b)$$

$$\epsilon_{ci\pm} = \epsilon_{cr\pm}\left[\omega_p^2/\omega^2 \rightarrow \omega_p^2 b/\omega^3\,,\ \beta_b \rightarrow b\beta_b\right], \qquad (2.23b)$$

where $\beta_{ob} = \beta_b(x=y=0)$ and $\omega_{oc} = \omega_c(x=y=0)$. It should be noted that for $\omega_c > 2\omega$, the electron concentration in the presence of a Gaussian laser beam increases radially if the plasma-redistribution is caused by the ponderomotive force. In the present chapter it will be assumed that $\omega > \omega_p, \omega_c$.

2.1c: Electron-heating without thermal conduction

On longer time scales $(t > \tau_\epsilon \simeq M/m\nu)$, the plasma redistribution in the presence of a laser beam is governed by the nonuniform heating[4,29-35] of electrons. If the initial widths of the two modes of the laser beam are large, the thermal conduction effects[29] may be neglected. It can then be shown that[3,4,40]

$$N/N_o = \left[1 + \beta_c \sum_{\pm} (1 \mp \omega_c/\omega)^{-2} \vec{E}^*_{\pm} \cdot \vec{E}_{\pm}\right]^{s/2-1}, \quad (2.12c)$$

$$N\nu/N_o\nu_o = (N/N_o)^b (T/T_o)^{s/2}$$

$$= \left[1 + \beta_c \sum_{\pm} (1 \mp \omega_c/\omega)^{-2} \vec{E}^*_{\pm} \vec{E}_{\pm}\right]^{b\, s/2-b}$$

$$\left[1 + 2\beta_c \sum_{\pm} (1 \mp \omega_c/\omega)^{-2} \vec{E}^*_{\pm} \vec{E}_{\pm}\right]^{s/2}, \quad (2.13c)$$

where

$$\beta_c = M e^2 / 6 m^2 k_B T_o \omega^2, \quad (2.14c)$$

M is the mass of an ion or a neutral, and

$$s = -3 \text{ or } 1 \text{ or } 2 \quad (2.24)$$

depending upon whether the electron collisions are with ions or nondiatomic molecules or diatomic molecules[4,50]. Consequently

$$\epsilon_{a\pm} = 1 - (\omega_p^2/\omega^2)_{(x=y=o)} \left[1 + \beta_{oc} \sum_{\pm} (1 \mp \omega_{oc}/\omega)^{-2} E^2_{a\pm}\right]^{s/2-1} \quad (2.16c)$$

$$\epsilon_{ai\pm} = (\omega_p^2 \nu_o/\omega^3)_{(x=y=o)} \left[1 + \beta_{oc} \sum_{\pm} (1 \mp \omega_{oc}/\omega)^{-2} E^2_{a\pm}\right]^{b\, s/2-b}$$

$$\left[1 + 2\beta_{oc} \sum_{\pm} (1 \mp \omega_{oc}/\omega)^{-2} E^2_{a\pm}\right]^{s/2}, \quad (2.17c)$$

$$\epsilon_{xr\pm} = \left\{ \frac{\partial}{\partial(x^2/r_0^2)}\left(\frac{\omega_p^2}{\omega^2}\right) + \left(\frac{\omega_p^2}{\omega^2}\right)\left(\frac{s/2-1}{1+\beta_{oc}\sum_{\pm}(1\mp\omega_{oc}/\omega)^{-2}E_{a\pm}^2}\right)\right.$$

$$\left.\frac{\partial}{\partial(x^2/r_0^2)}\left[\beta_c\sum_{\pm}(1\mp\omega_c/\omega)^{-2}E_{a\pm}^2\right] - \beta_c\sum_{\pm}(1\mp\omega_c/\omega)^{-2}E_{a\pm}^2 f_{x\pm}^{-2}\right)\Big\}_{(x=y=0)}$$

$$\left[1+\beta_{oc}\sum_{\pm}(1\mp\omega_{oc}/\omega)^{-2}E_{a\pm}^2\right], \qquad (2.18c)$$

$$\epsilon_{xi\pm} = \left\{\frac{\partial}{\partial(x^2/r_0^2)}\left(\frac{\omega_p^2 y_0}{\omega^3}\right) + \left(\frac{\omega_p^2 y_0}{\omega^3}\right)\left(\frac{bs/2-b}{1+\beta_{oc}\sum_{\pm}(1\mp\omega_{oc}/\omega)^{-2}E_{a\pm}^2} + \right.\right.$$

$$\left.\frac{s}{1+2\beta_{oc}\sum_{\pm}(1\mp\omega_{oc}/\omega)^{-2}E_{a\pm}^2}\right)\left(\frac{\partial}{\partial(x^2/r_0^2)}\left[\beta_c\sum_{\pm}(1\mp\omega_c/\omega)^{-2}E_{a\pm}^2\right] -\right.$$

$$\left.\left.\beta_c\sum_{\pm}(1\mp\omega_c/\omega)^{-2}E_{a\pm}^2 f_{x\pm}^{-2}\right)\right\}_{(x=y=0)}\left[1+\beta_{oc}\sum_{\pm}(1\mp\omega_{oc}/\omega)^{-2}E_{a\pm}^2\right]^{bs/2-b}\left[1+2\beta_{oc}\sum_{\pm}(1\mp\omega_{oc}/\omega)^{-2}E_{a\pm}^2\right]^{s/2}, \qquad (2.19c)$$

$$\epsilon_{yx\pm} = \epsilon_{xx}\left[x^2/r_0^2 \to y^2/r_0^2,\ f_{x\pm} \to f_{y\pm}\right], \qquad (2.20c)$$

$$\epsilon_{yi\pm} = \epsilon_{xi}\left[x^2/r_0^2 \to y^2/r_0^2,\ f_{x\pm} \to f_{y\pm}\right], \qquad (2.21c)$$

$$\epsilon_{cr\pm} = \left(\omega_p^2/\omega^2\right)_{(x=y=0)}(1-s/2)\beta_{oc}\sum_{\pm}(1\mp\omega_{oc}/\omega)^{-2}E_{a\pm}^2 h_{\pm}$$

$$\left[1+\beta_{oc}\sum_{\mp}(1\mp\omega_{oc}/\omega)^{-2}E_{a\pm}^2\right]^{s/2-2}, \qquad (2.22c)$$

$$\epsilon_{ci\pm} = \left(\frac{\omega_p^2}{\omega^2}\right)\left(\frac{b-bs/2}{\left(1+\beta_{oc}\sum_{\pm}(1\mp\omega_{oc}/\omega)^{-2}E_{a\pm}^2\right)} - \frac{s}{\left(1+2\beta_{oc}\sum_{\pm}(1\mp\omega_{oc}/\omega)^{-2}E_{a\pm}^2\right)}\right)$$

$$\beta_{oc}\sum_{\pm}(1\mp\omega_{oc}/\omega)^{-2}E_{a\pm}^2 h_{\pm}\left[1+\beta_{oc}\sum_{\mp}(1\mp\omega_{oc}/\omega)^{-2}E_{a\pm}^2\right]^{bs/2-b}$$

$$\left[1+2\beta_{oc}\sum_{\pm}(1\mp\omega_{oc}/\omega)^{-2}E_{a\pm}^2\right]^{s/2}, \qquad (2.23c)$$

where $\beta_{oc} = \beta_c \ (x=y=o)$. It is to be noted that the expressions for $\epsilon_{x\,r,i\pm}$ and $\epsilon_{y\,r,i\pm}$ (as given by Eqs. 2.18 - 2.21) consist of three separate terms. The first term represents the nonuniformity in the initial electron temperature, the second term represents the nonuniformity[64] in the initial electron temperature and static magnetic field, and the third term represents the nonlinearity in (i.e. intensity-dependence of) the dielectric tensor. The dielectric functions $\epsilon_{c\,r,i\pm}$ (as given by Eqs.2.22 and 2.23) represent the direct coupling[70] between the two modes.

2.2: Laser Propagation

2.2.1: Wave equation

The electric field $\vec{E}$ of the laser beam is governed by the wave equation[1-4]

$$\nabla^2 \vec{E} - \nabla(\nabla \cdot \vec{E}) + \omega^2 c^{-2} \overleftrightarrow{\epsilon} \cdot \vec{E} = 0 \ . \qquad (2.25)$$

since the variations of the field along the z axis (i.e. along the static magnetic field) are more rapid than the variations in the x-y plane, the electromagnetic waves of the laser beam may be treated as transverse. It may then be assumed that[3,4]

$$\frac{\partial E_z}{\partial z} \simeq -\frac{1}{\epsilon_{\parallel}}\left[\epsilon_{xx}\frac{\partial E_x}{\partial x} + \epsilon_{xy}\frac{\partial E_y}{\partial x} + \epsilon_{yx}\frac{\partial E_x}{\partial y} + \epsilon_{yy}\frac{\partial E_y}{\partial y}\right], \tag{2.26}$$

where

$$\epsilon_{\parallel} = 1-(\omega_p^2/\omega^2)(N/N_0) - i(\omega_p^2\nu_0/\omega^3)(N\nu/N_0\nu_0), \tag{2.27}$$

$$\epsilon_{\pm} = \epsilon_{xx} \mp i\epsilon_{xy} = \epsilon_{yy} \pm i\epsilon_{yx}, \tag{2.28}$$

$$E_{\pm} = E_x \pm i E_y. \tag{2.29}$$

Multiplying the y component of Eq.2.25 by $\pm i$ and adding it to the x component of Eq.2.25 and using Eq.2.26, it is seen that the left and right circularly polarized electric fields $E_{\pm}$ satisfy the following equations[3,4].

$$\frac{\partial^2 E_{\pm}}{\partial z^2} + \frac{1}{2}\left(1+\frac{\epsilon_{\pm ar}}{\epsilon_{\parallel r}}\right)\left(\frac{\partial^2}{\partial x^2}+\frac{\partial^2}{\partial y^2}\right)E_{\pm} + \frac{\omega^2\epsilon_{\pm}E_{\pm}}{c^2}$$

$$= \frac{1}{2}\left(1-\frac{\epsilon_{\mp ar}}{\epsilon_{\parallel r}}\right)\left(\frac{\partial}{\partial x}\pm i\frac{\partial}{\partial y}\right)^2 E_{\mp}. \tag{2.30}$$

The terms on the right hand side arise because of the anisotropy generated by the static magnetic field, and they represent the direct coupling between the left and right circularly polarized modes. The indirect coupling

between the two modes arises because of the fact that the dielectric tensor component for one mode depends on the intensity of the other mode as much as on its own intensity.

The initial (z=0) electric fields of the two modes are taken as

$$E_{\pm}(z=0) = E_{0\pm} \exp\left[-x^2/2r_0^2 f_{0x\pm}^2 - y^2/2r_0^2 f_{0y\pm}^2\right] \exp(i\omega t), \tag{2.31}$$

where $r_0 f_{0x\pm}$ and $r_0 f_{0y\pm}$ are the initial beamwidths of the two modes along the X and Y axes respectively. The transverse electric field $\vec{E}_{\perp}$ (x=y=0) at t=z=0 may be assumed to be along the x axis so that $E_{0\pm}$ are real. If the beam diverges/converges slowly, the solutions of Eq.2.30 in the paraxial region may be expressed as

$$E_{\pm} = E_{a\pm} \exp\left[-x^2/2r_0^2 f_{x\pm}^2 - y^2/2r_0^2 f_{y\pm}^2 - h_{\pm} xy/2r_0^2\right]$$
$$\exp\left[i\omega t - i\omega c^{-1} \int \epsilon_{ar\pm}^{1/2} dz + i\theta_{\pm} - i\varphi_{x\pm} x^2/r_0^2\right.$$
$$\left. - i\varphi_{y\pm} y^2/r_0^2 - i\varphi_{c\pm} xy/r_0^2\right], \tag{2.32}$$

where the axial electric field amplitudes $E_{a\pm}$, beamwidth parameters $f_{x,y\pm}$, cross width parameters $h_{\pm}$, axial phases $\theta_{\pm}$ and offaxial phase-function coefficients

$\varphi_{x,y,c\pm}$ are z dependent functions to be determined. Substituting for $E_{\pm}$ from Eq.2.32 into Eq.2.30, and then equating the real and imaginary coefficients of x^0y^0, x^2/r_0^2, y^2/r_0^2 and xy/r_0^2 on both sides of the resulting equation (as an approximation to the Fourier-transfer technique), sixteen second order coupled differential equations for $E_{a\pm}$, $f_{x,y\pm}$, $h_{\pm}$, $\theta_{\pm}$ and $\varphi_{\pm}$ are obtained. In the WKB approximation, the second order terms are neglected[1-4,40,41] so that the equations reduce to the following:

$$\epsilon_{ar\pm}^{1/2}\frac{d\theta_{\pm}}{d\xi}-2\left(\frac{r_0^2\omega^2}{c^2}\right)\epsilon_{adr\pm}-\left(1+\frac{\epsilon_{ar\pm}}{\epsilon_{\parallel}}\right)\left(f_{x\pm}^{-2}+f_{y\pm}^{-2}\right)=0 \quad , \tag{2.33}$$

$$\epsilon_{ar\pm}^{1/2}\frac{d\ln E_{a\pm}^{1/2}}{d\xi}+\left(1+\frac{\epsilon_{ar\pm}}{\epsilon_{\parallel}}\right)(\varphi_{x\pm}+\varphi_{y\pm})+2\frac{d\epsilon_{ar\pm}}{d\xi}$$
$$+2\left(\frac{r_0^2\omega^2}{c^2}\right)\epsilon_{al\pm}=0 \quad , \tag{2.34}$$

$$\epsilon_{ar\pm}^{1/2}\frac{d\varphi_{x\pm}}{d\xi}-\left(1+\frac{\epsilon_{ar\pm}}{\epsilon_{\parallel}}\right)\left(f_{x\pm}^{-4}-\varphi_{x\pm}^2/2\right)+2\left(\frac{r_0^2\omega^2}{c^2}\right)\epsilon_{xR\pm}$$
$$=0 \quad , \tag{2.35}$$

$$\epsilon_{ar\pm}^{1/2}\frac{df_{x\pm}^{-2}}{d\xi}+\left(1+\frac{\epsilon_{ar\pm}}{d\xi}\right)f_{x\pm}^{-2}\varphi_{x\pm}-\left(\frac{r_0^2\omega^2}{c^2}\right)\epsilon_{xI\pm}$$
$$=0 \quad , \tag{2.36}$$

$$\epsilon_{ar\pm}^{1/2}\frac{d\varphi_{y\pm}}{d\xi}-\left(1+\frac{\epsilon_{ar\pm}}{\epsilon_{\parallel}}\right)\left(f_{y\pm}^{-4}-\varphi_{y\pm}^2/2\right)+2\left(\frac{r_0^2\omega^2}{c^2}\right)\epsilon_{yR\pm}$$
$$=0 \quad , \tag{2.37}$$

$$\epsilon_{ar\pm}^{1/2}\frac{df_{y\pm}^{-2}}{d\xi}+\left(1+\frac{\epsilon_{ar\pm}}{\epsilon_{11}}\right)f_{y\pm}^{-2}\varphi_{y\pm}-\left(\frac{r_0^2\omega^2}{c^2}\right)\epsilon_{yI\pm}=0, \qquad (2.38)$$

$$\epsilon_{ar\pm}^{1/2}\frac{d\varphi_\pm}{d\xi}+\left(1+\frac{\epsilon_{ar\pm}}{\epsilon_{11}}\right)\left[(f_{x\pm}^{-2}+f_{y\pm}^{-2})h_\pm+(\varphi_{x\pm}+\varphi_{y\pm})\varphi_{c\pm}\right]$$
$$+2\left(\frac{r_0^2\omega^2}{c^2}\right)\epsilon_{cR\pm}=0, \qquad (2.39)$$

$$\epsilon_{ar\pm}\frac{dh_\pm}{d\xi}+\left(1+\frac{\epsilon_{ar\pm}}{\epsilon_{11}}\right)\left[(f_{x\pm}^{-2}+f_{y\pm}^{-2})\varphi_{c\pm}+(\varphi_{x\pm}+\varphi_{y\pm})h_\pm\right]$$
$$-2\left(\frac{r_0^2\omega^2}{c^2}\right)\epsilon_{cI\pm}=0, \qquad (2.40)$$

where

$$\xi=z\,c/\omega r_0^2, \qquad (2.41)$$

$$\epsilon_{adr\pm}=(\mathcal{R}e\;\epsilon_{d\pm})_{(x=y=0)}, \qquad (2.42)$$

$$\epsilon_{aI\pm}=\epsilon_{ai\pm}+(\mathcal{I}m\;\epsilon_{d\pm})_{(x=y=0)} \qquad (2.43)$$

$$\epsilon_{xR\pm}=\epsilon_{xr\pm}+\left[\mathcal{R}e\,\partial\epsilon_{d\pm}/\partial(x^2/r_0^2)\right]_{(x=y=0)}, \qquad (2.44)$$

$$\epsilon_{xr\pm}=\epsilon_{xi\pm}+\left[\mathcal{I}m\,\partial\epsilon_{d\pm}/\partial(x^2/r_0^2)\right]_{(x=y=0)}, \qquad (2.45)$$

$$\epsilon_{yR\pm}=\epsilon_{yr\pm}+\left[\mathcal{R}e\,\partial\epsilon_{d\pm}/\partial(y^2/r_0^2)\right]_{(x=y=0)}, \qquad (2.46)$$

$$\epsilon_{yI\pm}=\epsilon_{yi\pm}+\left[\mathcal{I}m\,\partial\epsilon_{d\pm}/\partial(y^2/r_0^2)\right]_{(x=y=0)}, \qquad (2.47)$$

$$\epsilon_{cR\pm}=\epsilon_{cr\pm}+\left[\mathcal{R}e\,\partial\epsilon_{d\pm}/\partial(xy/r_0^2)\right]_{(x=y=0)}, \qquad (2.48)$$

$$\epsilon_{cI\pm}=\epsilon_{ci\pm}+\left[\mathcal{I}m\,\partial\epsilon_{d\pm}/\partial(xy/r_0^2)\right]_{(x=y=0)}, \qquad (2.49)$$

$$\epsilon_{d\pm} = E_{\pm}^{-1}\left(\frac{r_0^2\omega^2}{c^2}\right)^{-1}\left(1-\frac{\epsilon_{ar\pm}}{\epsilon_{11}}\right)\left(\frac{\partial}{\partial x}+i\frac{\partial}{\partial y}\right)^2 E_{\mp} \quad . \qquad (2.50)$$

The additional dielectric functions $\epsilon_{adr\pm}$, $\epsilon_{ar\pm}-\epsilon_{ai\pm}$, ... and $\epsilon_{cr\pm}-\epsilon_{ci\pm}$ which are abstract forms of the right hand side of Eq.2.30 represent the direct coupling[40] between the two modes.

Equations 2.36, 2.38 and 2.40 lead to

$$\varphi_{x\pm} = \left(\frac{r_0^2\omega^2}{c^2}\epsilon_{x\pm} - \epsilon_{ar\pm}^{1/2}\frac{d f_{x\pm}^{-2}}{d\xi}\right)\Big/ 2\left(1+\frac{\epsilon_{ar\pm}}{\epsilon_{11}}\right) f_{x\pm}^{-2} \,, \qquad (2.52)$$

$$\varphi_{y\pm} = \left(\frac{r_0^2\omega^2}{c^2}\epsilon_{y1\pm} - \epsilon_{ar\pm}^{1/2}\frac{d f_{y\pm}^{-2}}{d\xi}\right)\Big/ 2\left(1+\frac{\epsilon_{ar\pm}}{\epsilon_{11}}\right) f_{y\pm}^{-2} \,, \qquad (2.53)$$

$$\varphi_{c\pm} = \left[\frac{r_0^2\omega^2}{c^2}\epsilon_{cI\pm} - \epsilon_{ar\pm}^{1/2}\frac{dh_{\pm}}{d\xi} - \left(1+\frac{\epsilon_{ar\pm}}{\epsilon_{11}}\right)(\varphi_{x\pm}+\varphi_{y\pm})h_{\pm}\right] \Big/ \left[\left(1+\frac{\epsilon_{ar\pm}}{\epsilon_{11}}\right)\left(f_{x\pm}^{-2}+f_{y\pm}^{-2}\right)/2\right] \,. \qquad (2.54)$$

2.2.2: Beamwidth and crosswidth parameters

Substituting for $\varphi_{x\pm}, \varphi_{y\pm}$ and $\varphi_{c\pm}$ from Eqs. 2.52-2.54 into Eqs. 2.35, 2.37 and 2.39, the following equations for the beamwidth and cross width parameters are obtained

$$\frac{d^2 f_{x,y\pm}^{-2}}{d\xi^2} - \frac{3}{2 f_{x,y\pm}^{-2}}\left(\frac{d f_{x,y\pm}^{-2}}{d\xi}\right)^2 + \left(\frac{d \ln \epsilon_{ar\pm}^{1/2}}{d\xi} + \frac{2 r_0^2 \omega^2 \epsilon_{x,yI\pm}}{c^2 f_{x,y}^{-2} \epsilon_{ar\pm}}\right)\frac{d f_{x,y\pm}^{-2}}{d\xi}$$

$$+ \left(\frac{(1+\epsilon_{ar\pm}/\epsilon_{11})^2 f_{x,y\pm}^{-6}}{2\epsilon_{ar\pm}} - \frac{(1+\epsilon_{ar\pm}/\epsilon_{11})(r_0^2\omega^2/c^2) f_{x,y\pm}^{-2} \epsilon_{x,yR\pm}}{\epsilon_{ar\pm}}\right.$$

$$\left. - \frac{(r_0^2\omega^2/c^2)^2 \epsilon_{x,yI\pm}^2}{2 f_{x,y\pm}^{-2} \epsilon_{ar\pm}} - \frac{(r_0^2\omega^2/c^2)}{\epsilon_{ar\pm}^{1/2}} \frac{d\epsilon_{x,yI\pm}}{d\xi}\right) = 0 ,$$

(2.56, 2.56)

$$\frac{d^2 h_\pm}{d\xi^2} + \left(\frac{d \ln \epsilon_{ar\pm}^{1/2}}{d\xi} + \frac{(1+\epsilon_{ar\pm}/\epsilon_{11})(f_{x\pm}^{-2} + f_{y\pm}^{-2})}{\epsilon_{ar\pm}^{1/2}} - \frac{(d f_{x\pm}^{-2}/d\xi + d f_{y\pm}^{-2}/d\xi)}{(f_{x\pm}^{-2} + f_{y\pm}^{-2})}\right)\frac{d h_\pm}{d\xi}$$

$$+ \left[\frac{(1+\epsilon_{ar\pm}/\epsilon_{11})^2}{2\epsilon_{ar\pm}}\left(f_{x\pm}^{-4} + f_{y\pm}^{-4} + f_{x\pm}^{-2} f_{y\pm}^{-2}\right.\right.$$

$$\left. + 4\varphi_{x\pm}\varphi_{y\pm}\right) h_\pm - \frac{(1+\epsilon_{ar\pm}/\epsilon_{11})}{2\epsilon_{ar\pm}^{1/2}}\left(\epsilon_{xR\pm} h_\pm + \epsilon_{yR\pm} h_\pm\right.$$

$$\left. + f_{x\pm}^{-2}\epsilon_{cR\pm} + f_{y\pm}^{-2}\epsilon_{cR\pm} - 2\varphi_{x\pm}\epsilon_{cI\pm} - 2\varphi_{y\pm}\epsilon_{cI\pm}\right)$$

$$+ \frac{(r_0^2\omega^2/c^2)}{\epsilon_{ar\pm}^{1/2}} \frac{(d f_{x\pm}^{-2}/d\xi + d f_{y\pm}^{-2}/d\xi)}{(f_{x\pm}^{-2} + f_{y\pm}^{-2})} \epsilon_{cI\pm} - \frac{(r_0^2\omega^2/c^2)}{\epsilon_{ar\pm}^{1/2}} \frac{d\epsilon_{cI\pm}}{d\xi}$$

$$\left. - \frac{2(1+\epsilon_{ar\pm}/\epsilon_{11})}{\epsilon_{ar\pm}^{1/2}} \frac{(d f_{x\pm}^{-2}/d\xi + d f_{y\pm}^{-2}/d\xi)}{(f_{x\pm}^{-2} + f_{y\pm}^{-2})} (\varphi_{x\pm}\varphi_{c\pm} + \varphi_{y\pm}\varphi_{c\pm})\right] = 0 . \qquad (2.57)$$

Using Eqs. 2.52 and 2.53, Eq. 2.34 gives

$$E_{a\pm}^2 = E_{o\pm}^2 \exp\left[-\int_o^\xi \left(\epsilon_{aI\pm} + \epsilon_{xI\pm} f_{x\pm}^{-2}/2 + \epsilon_{yI\pm} f_{y\pm}^{-2}/2\right) d\xi\right] \cdot \left[\frac{\epsilon_{ar\pm(\xi=o)}^{1/2}}{\epsilon_{ac\pm}^{1/2}} \Big/ \frac{f_{x\pm} f_{y\pm}}{f_{ox\pm} f_{oy\pm}}\right] \quad (2.58)$$

Equations 2.55-2.57 can, in general, be solved numerically by employing the Runge-Kutta method[115]. The boundary conditions, corresponding to initially plane wavefronts for both the modes, are[4,40]

$$f_{x\pm}(\xi=o) = f_{ox\pm} \quad , \quad (2.59)$$

$$f_{y\pm}(\xi=o) = f_{oy\pm} \quad , \quad (2.60)$$

$$h_\pm(\xi=o) = 0 \quad ,$$

$$(df_{x\pm}/d\xi)_{(\xi=o)} = (df_{y\pm}/d\xi)_{(\xi=o)} = (dh_\pm/d\xi)_{(\xi=o)} = 0 \, . \quad (2.61)$$

2.2.3: Particular cases

In the following, the effects of axial inhomogeneity and absorption on laser self focusing will not be considered. Then the terms containing $d\epsilon_{ar\pm}/d\xi$, $\epsilon_{a1\pm}$ and $\epsilon_{x,y,c\,1\pm}$ in Eqs. 2.55-2.58 may be neglected. (The laser-induced inhomogeneity is generally negligible so that for an initially homogeneous plasma, $d\epsilon_{ar\pm}/d\xi \cong 0$.) In Eq. 2.57, the most important term besides $d^2h_\pm/d\xi^2$ is $\epsilon_{ar\pm}^{-1}(f_{x\pm}^{-2}+f_{y\pm}^{-2})\epsilon_{cR\pm}$; the other terms being quite small shall be neglected. Consequently, Eqs.2.55-2.58 reduce to

$$\frac{d^2f_{x,y\pm}^{-2}}{d\xi^2} = \frac{3}{2f_{x,y\pm}^{-2}}\left(\frac{df_{x,y\pm}^{-2}}{d\xi}\right) - \left(1+\frac{\epsilon_{ar\pm}}{\epsilon_{11}}\right)^2 \frac{f_{x,y\pm}^{-6}}{2\epsilon_{ar\pm}} + \left(1+\frac{\epsilon_{ar\pm}}{\epsilon_{11}}\right)\left(\frac{r_0^2\omega^2}{c^2}\right)\frac{f_{x,y\pm}^{-2}\,\epsilon_{x,yR\pm}}{\epsilon_{ar\pm}}, \tag{2.63, 2.64}$$

$$\frac{d^2h_\pm}{d\xi^2} = \left(1+\frac{\epsilon_{ar\pm}}{\epsilon_{11}}\right)\left(\frac{r_0^2\omega^2}{c^2}\right)\frac{(f_{x\pm}^{-2}+f_{y\pm}^{-2})\,\epsilon_{cR\pm}}{2\epsilon_{ar\pm}}, \tag{2.65}$$

$$E_{a\pm}^2 = E_{o\pm}^2\left(\frac{f_{ox\pm}\,f_{oy\pm}}{f_{x\pm}\,f_{y\pm}}\right). \tag{2.66}$$

In the absence of a static magnetic field, the left and right circularly polarized modes are identical[40,70], and

$$\frac{d^2 f_{x,y}^{-2}}{d\xi^2} - \frac{3}{2 f_{x,y\pm}^{-2}} \left(\frac{d f_{x,y\pm}^{-2}}{d\xi}\right)^2 - \frac{2 f_{x,y}^{-2}}{\epsilon_{a\pm}} \left(f_{x,y\pm}^{-6} - \frac{r_o^2 \omega^2}{c^2} \epsilon_{x,y\pm}\right), \tag{2.67}$$

$$h_\pm = 0 . \tag{2.68}$$

This case has already been analysed in detail in Chapter 1.

In the presence of a static magnetic field, $h_\pm \neq 0$ and $f_{x,y\pm}$ are all different unless

$$\left(1 + \frac{\epsilon_{oa\pm}}{\epsilon_{o\parallel}}\right) f_{ox,y\pm}^{-4} = \left(\frac{r_o^2 \omega^2}{c^2}\right) \epsilon_{o\,x,y\pm} , \tag{2.69}$$

where the subscript 0 here denotes $\xi = 0$. The above (Eq.2.69) modified condition for self trapping of both the modes is much more stringent than the condition $E_o^2 = E_{st}^2$ mentioned in Chapter 1. When the condition 2.69 is not satisfied, the direct coupling between the two modes leads to axial asymmetry of the intensity-distributions of the two modes, and the indirect coupling between the two modes leads to cross-focusing[40,70] and aperiodic oscillations of the two modes. Faraday rotation and ellipticity[70] can be easily evaluated once $f_{x,y\pm}$ and $h_\pm$ have been evaluated.

2.3: Results and Discussion

Using the Rungo-Kutta method[115], Eqs.2.63 - 2.65 have been solved for $f_{x,y\pm}$ and $h_{\pm}$ in the case of a collisionless plasma in which the redistribution is caused by the ponderomotive force. The dimensionless parameter $(\gamma_0^2\omega^2/c^2)$ has been chosen to be 400. The results have been presented in Figs. 2.1 - 2.7.

Figures 2.1 - 2.3 correspond to $\omega_c/\omega = 0.4$, $\omega_p^2/\omega^2 = 0.2$, $f_{ox,y\pm} = 1$ and $\beta_{ob} E_{o\pm}^2 = 10^{-5}$ for Fig.2.1, 0.1 for Fig.2.2 and 10 for Fig.2.3. It is seen that generally, but not necessarily $h_+ \simeq h_-$. The cross-width parameters $h_{\pm}$ are usually much smaller than $f_{x,y\pm}^{-2}$ and hence they may be neglected. However, they may be of interest in certain cases. When $h_{\pm} \neq 0$, $f_{x,y\pm}$ are all different. The differences between $f_{x,y\pm}$ are most significant when the beam converges. It is moreover seen that $|f_{x+}^{-2} - f_{y\pm}^{-2}| < |f_{x-}^{-2} - f_{y-}^{-2}| < |f_{x+}^{-2} - f_{x-}^{-2}|$. The presence of $h_{\pm}$ leads to axial asymmetry in the intensity profiles of the two modes.

In Figs. 2.4 - 2.7, the direct coupling between the two modes has been neglected so that $h_{\pm} = 0$.

Figure 2.4 corresponds to $\omega_c/\omega = 0.4$, $\omega_p^2/\omega^2 = 0.2$, $f_{ox+}^{-2} = 0.75$, $f_{oy+}^{-2} = 1.5$ for (A) and (C), 0.75 for (B) $f_{ox-}^{-2} = 0.75$ for (A), 1.5 for (B) and (C), $f_{oy-}^{-2} = 1.5$ for (A) and (B), 0.75 for (C), and $\beta_{ob} E_{o\pm}^2 = 0.3/\sqrt{8}$. The

curves show that the effect of any change in the initial beam-width is quite appreciable. When one mode is focused, the other one can be defocused if the initial beamwidths for the two modes are different. Similarly when a mode is focused along the X axis, it can be defocused along the Y axis if the initial beamwidths of the mode are different along the X and Y axes. Such a difference in behaviour can influence the process of Faraday rotation[70] very appreciably.

Figure 2.5 corresponds to $\omega_c/\omega = 0.4$, $\omega_p^2/\omega^2 = 0.2$, $f_{0x,y\pm} = 1$, and $\beta_{0b} E_{0\pm}^2 = 10^{-5}$ for (A), 0.1 for (B), 10 for (C), $\beta_{0b} E_{0-}^2 = 10$ for (A), 1 for (B), 0.1 for (C). The extent of influence of the indirect coupling on focusing/defocusing of the two modes is quite apparent from the graphs. Though $\beta_{0b} E_{0+}^2 \ll \beta_{0b} E_{0-}^2$ for (A), the + mode is focused much more than the - mode. This is because of the fact that the expressions for $\epsilon_\pm$ involve $(1 \mp \omega_c/\omega)$ in their denominators.

Figures 2.6 and 2.7 correspond to $\omega_c/\omega = 0.4 + 0.5\ x^2/r_0^2 + 0.5\ y^2/r_0^2$ for Fig.2.6, $0.4+0.2\ x^2/r_0^2 + 0.8\ y^2/r_0^2$ for Fig.2.7, $T_{0\pm} = T_{00} = 1$ for (A) and (B), $1 + 0.5 x^2/r_0^2 + 0.5\ y^2/r_0^2$ for (7C), $1 + 0.3\ x^2/r_0^2 + 0.7\ y^2/r_0^2$ for (8C) $\omega_p^2/\omega^2 = 0.2$ for (A) and (B), $0.2 + 0.5\ x^2/r_0^2 + 0.5\ y^2/r_0^2$

for (7C), $0.2 + 0.7\ x^2/r_o^2 + 0.3\ y^2/r_o^2$ for (8C), $f_{ox,y\pm} = 1$, and $\beta_{ob} E_{o\pm}^2 = 0.1$ for (A), 10 for (B), 1 for (C). It is seen that nonuniformities[64,65] in the electron concentration, electron temperature and static magnetic field can charge the behaviour of the two modes very appreciably. Aperiodicity in the oscillations of the beamwidth parameters is enhanced on account of the non-uniformities. The effect of radial nonuniformities is most apparent in the case of $\beta_{ob} E_{o\pm}^2 = 10$ which roughly corresponds to $E_o^2 > E_{stu}^2$ (where E_{stu}^2 is the upper self trapping intensity). Such an effect of radial nonuniformities on the plasma-parameters can be easily understood in terms of the external focusing which has been extensively investigated in the context of optical fibers.[58,111]

Figures 2.1 - 2.7

The mechanism of nonlinearity considered is the redistribution by the ponderomotive force. The dimensionless parameter $(r_0^2\omega^2/c^2)$ has been chosen to be 400 for all the figures. In Figs. 2.4 - 2.7, the direct coupling between the two modes has been neglected.

Fig.2.1 $f_{x,y\pm}^{-2}/f_{ox,y\pm}^{-2}$ and $\log|h_\pm|$ versus ξ for $\omega_t/\omega = 0.4$, $\omega_p^2/\omega^2 = 0.2$, $f_{ox,y\pm}^{-2} = 1$ and $\beta_{ob}E_{o\pm}^2 = 10^{-5}$. The dotted curve for $\log|h_\pm|$ means that $h_\pm$ is negative.

Fig.2.2 Same as in Fig.2.1 except that $\beta_{ob}E_{o\pm}^2 = 0.1$.

Fig.2.3 Same as in Fig.2.2 except that $\beta_{ob}E_{o\pm}^2 = 10$.

Fig.2.4 $f_{x,y\pm}^{-2}/f_{ox,y\pm}^{-2}$ versus ξ for $\omega_t/\omega = 0.4$, $\omega_p^2/\omega^2 = 0.2$, $f_{ox+}^{-2} = 0.75$, $f_{oy+}^{-2} = 1.5$ for (A & C) & 0.75 for (B), $f_{ox-}^{-2} = 0.75$ for (A) & 1.5 for (B & C), $f_{oy-}^{-2} = 1.5$ for (A & B) & 0.75 for (C), $\beta_{ob}E_{o\pm}^2 = 0.3/\sqrt{8}$.

Fig.2.5 $f_{x,y\pm}^{-2}/f_{ox,y\pm}^{-2}$ versus $\lambda\xi$ for $\omega_t/\omega = 0.4$, $\omega_p^2/\omega^2 = 0.2$, $f_{ox,y\pm} = 1$, $\beta_{ob}E_{o+}^2 = 10^{-5}$ for (A) & 0.1 for (B) & 10 for (C), $\beta_{ob}E_{o-}^2 = 10$ for (A) & 1 for (B) & 0.1 for (C). $\lambda = 1$ for

(A) & 30 for (B) & 10 for (G).

Fig.2.6 $f^{-2}_{x,y\pm} / f^{-2}_{ox,y\pm}$ versus $\lambda\xi$ for $\omega_c/\omega = 0.4 + 0.5\ x^2/r_o^2 + 0.5\ y^2/r_o^2$, $T_o/T_{oo} = 1$ for (A & B) & $1 + 0.5\ x^2/r_o^2 + 0.5\ y^2/r_o^2$ for (C), $\omega_p^2/\omega^2 = 0.2$ for (A & B) & $0.2 + 0.5\ x^2/r_o^2 + 0.5\ y^2/r_o^2$ for (C), $f^{-2}_{ox,y\pm} = 1$, $\beta_{ob} E^2_{o\pm} = 0.1$ for (A) & 10 for (B) & 1 for (C). $\lambda = 1$ for (A & C) & 0.1 for (B).

Fig.2.7 $f^{-2}_{x,y\pm} / f^{-2}_{ox,y\pm}$ versus $\lambda\xi$ for $\omega_c/\omega = 0.4 + 0.2\ x^2/r_o^2 + 0.8\ y^2/r_o^2$, $T_o/T_{oo} = 1$ for (A & B) & $1 + 0.3\ x^2/r_o^2 + 0.7\ y^2/r_o^2$ for (C), $\omega_p^2/\omega^2 = 0.2$ for (A & B) & $0.2 + 0.7\ x^2/r_o^2 + 0.3\ y^2/r_o^2$ for (C), $f^{-2}_{ox,y\pm} = 1$, $\beta_{ob} E^2_{o\pm} = 0.1$ for (A) & 10 for (B) & 1 for (C). $\lambda = 1$ for (A & B) & 0.5 for (C).

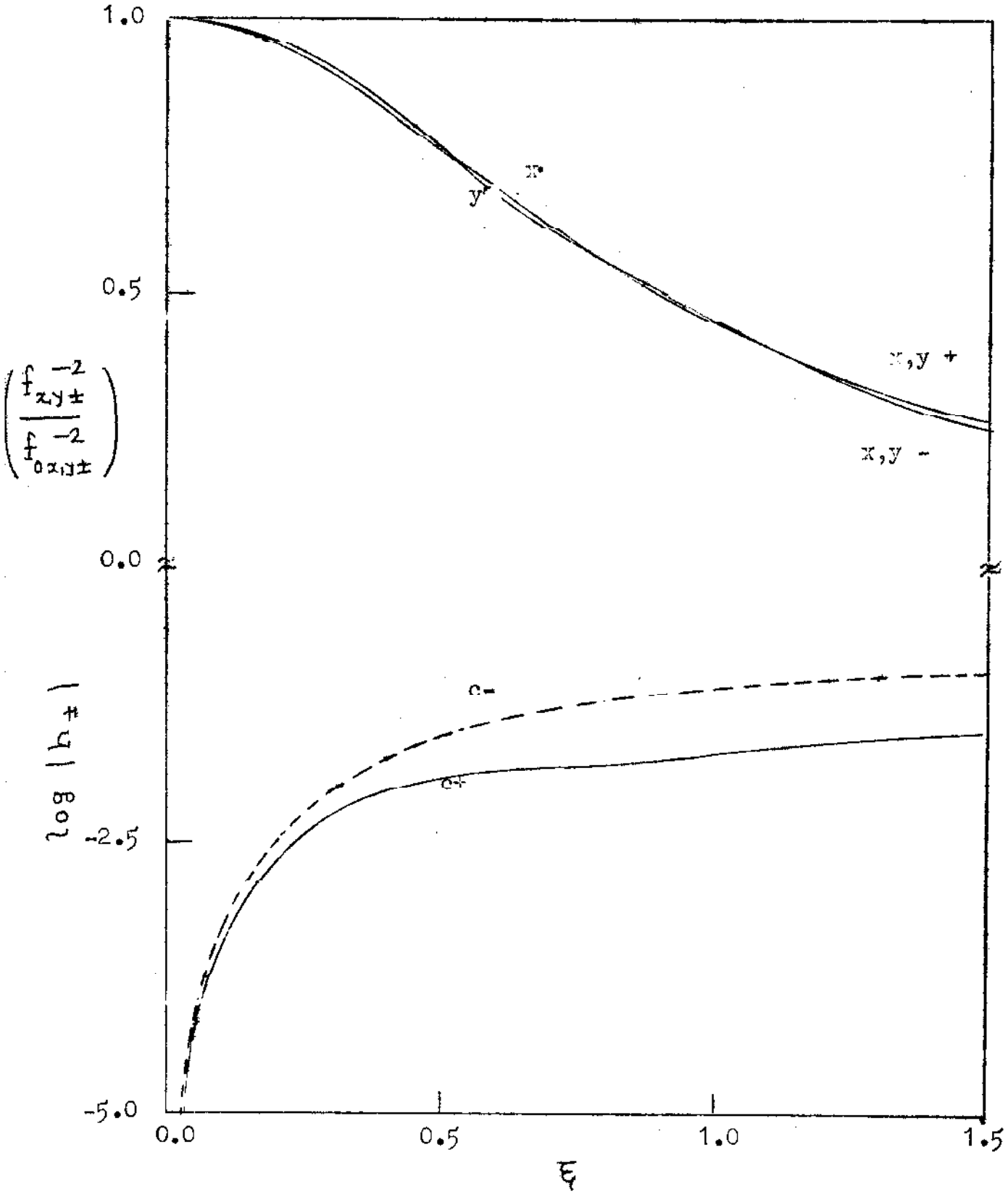
1.0
0.5
0.0
-2.5
-5.0
0.0
0.5
1.0
1.5
ξ
$\left(\frac{f^{-2}_{x,y\pm}}{f^{-2}_{0x,y\pm}}\right)$
log |γ±|
x,y +
x,y -
y+
x+
c-
c+

Fig. 2.1

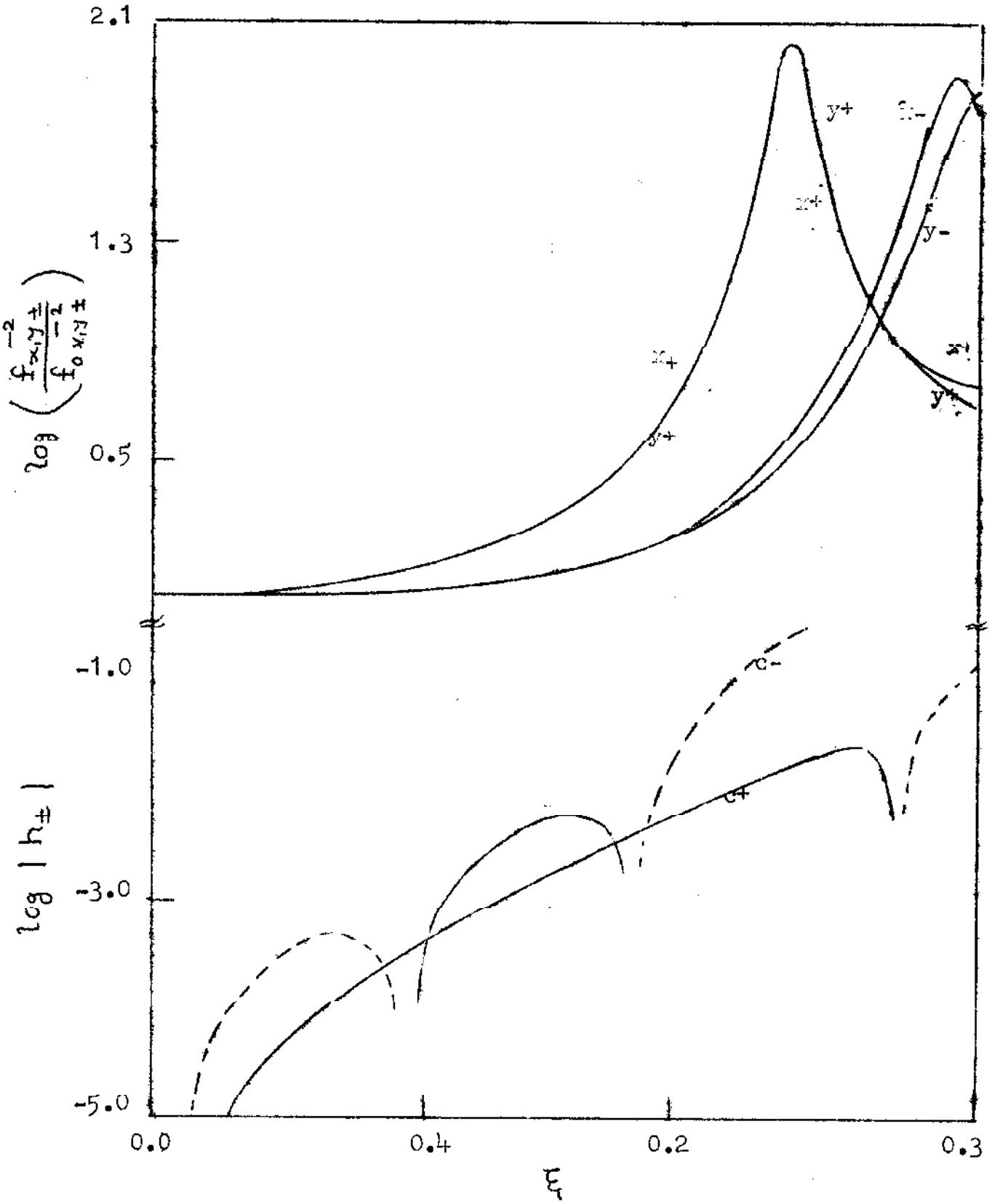

Fig. 2.2

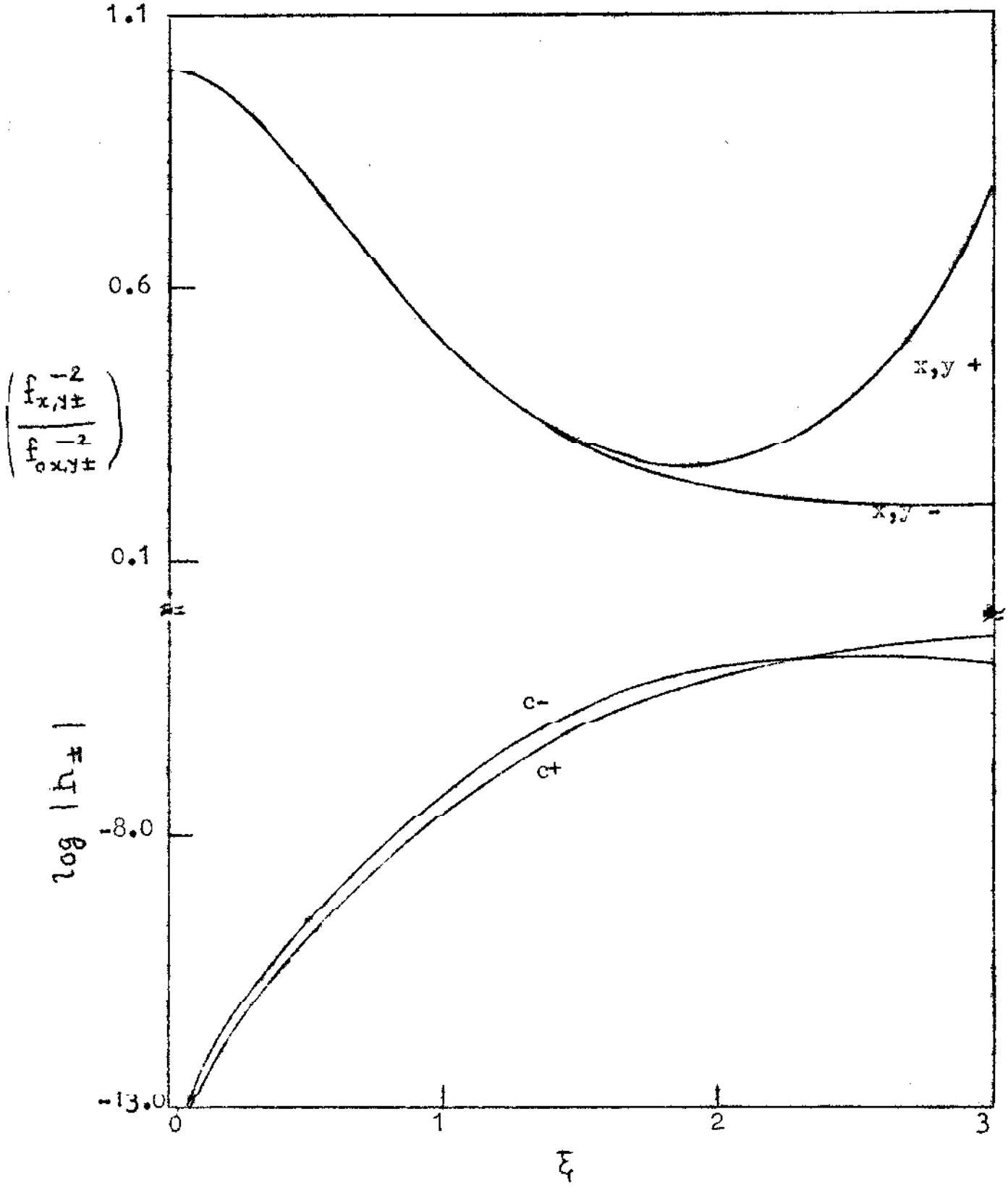
1.1
0.6
0.1
$\left(\frac{f^{-2}_{x,y\pm}}{f^{-2}_{0x,y\pm}}\right)$
x,y +
x,y -
c-
c+
log |$\psi_{\pm}$|
-8.0
-13.0
0
1
2
3
ξ

Fig. 2.3

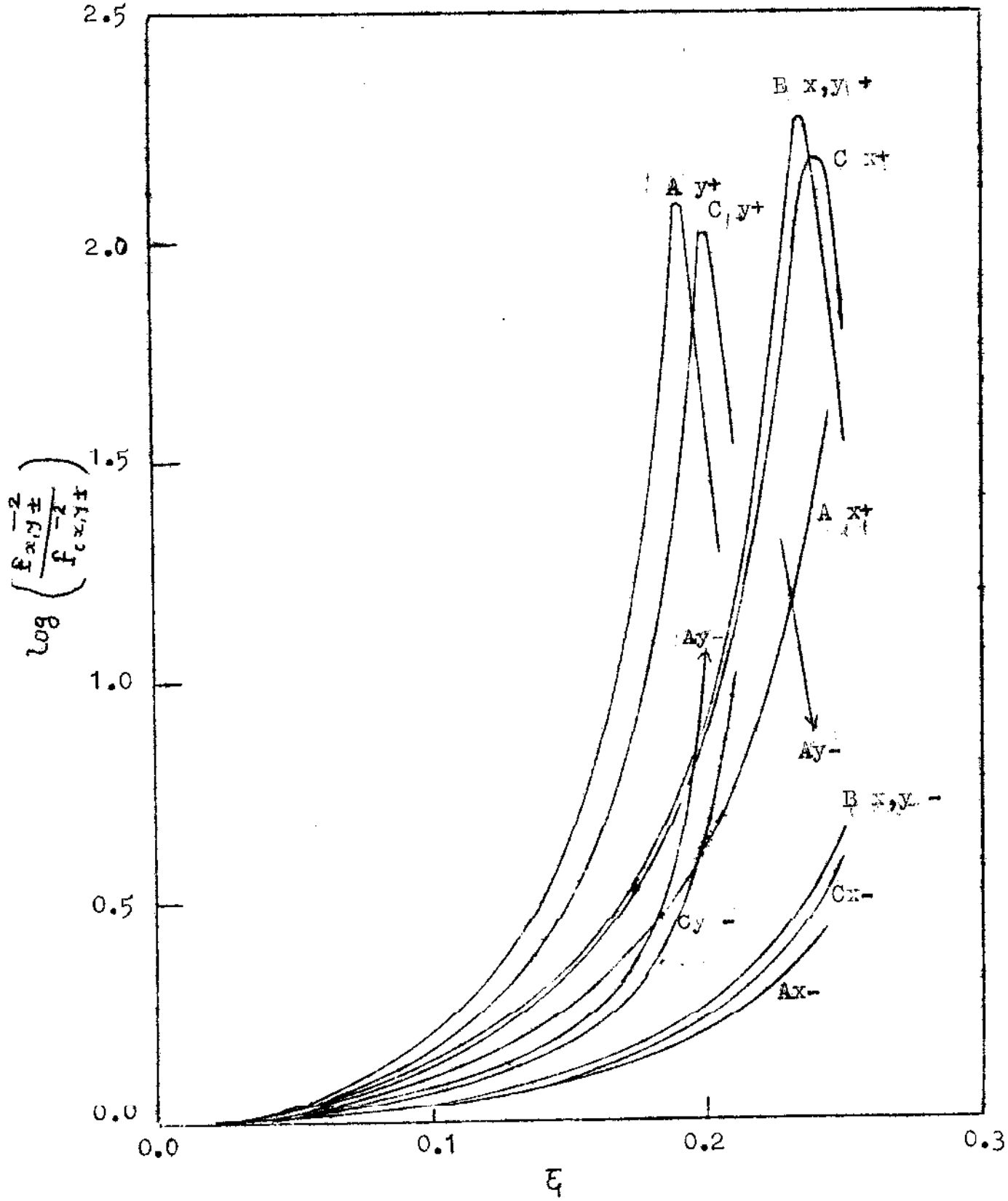
2.5
2.0
1.5
1.0
0.5
0.0
0.0
0.1
0.2
0.3
ξ
$\log\left(\frac{f_{x,y,\pm}^{-2}}{f_{c\,x,y\pm}^{-2}}\right)$
B x,y +
C x+
A y+
C y+
A x+
Ay-
Ay-
B x,y -
Cx-
Cy -
Ax-

Fig. 2.4

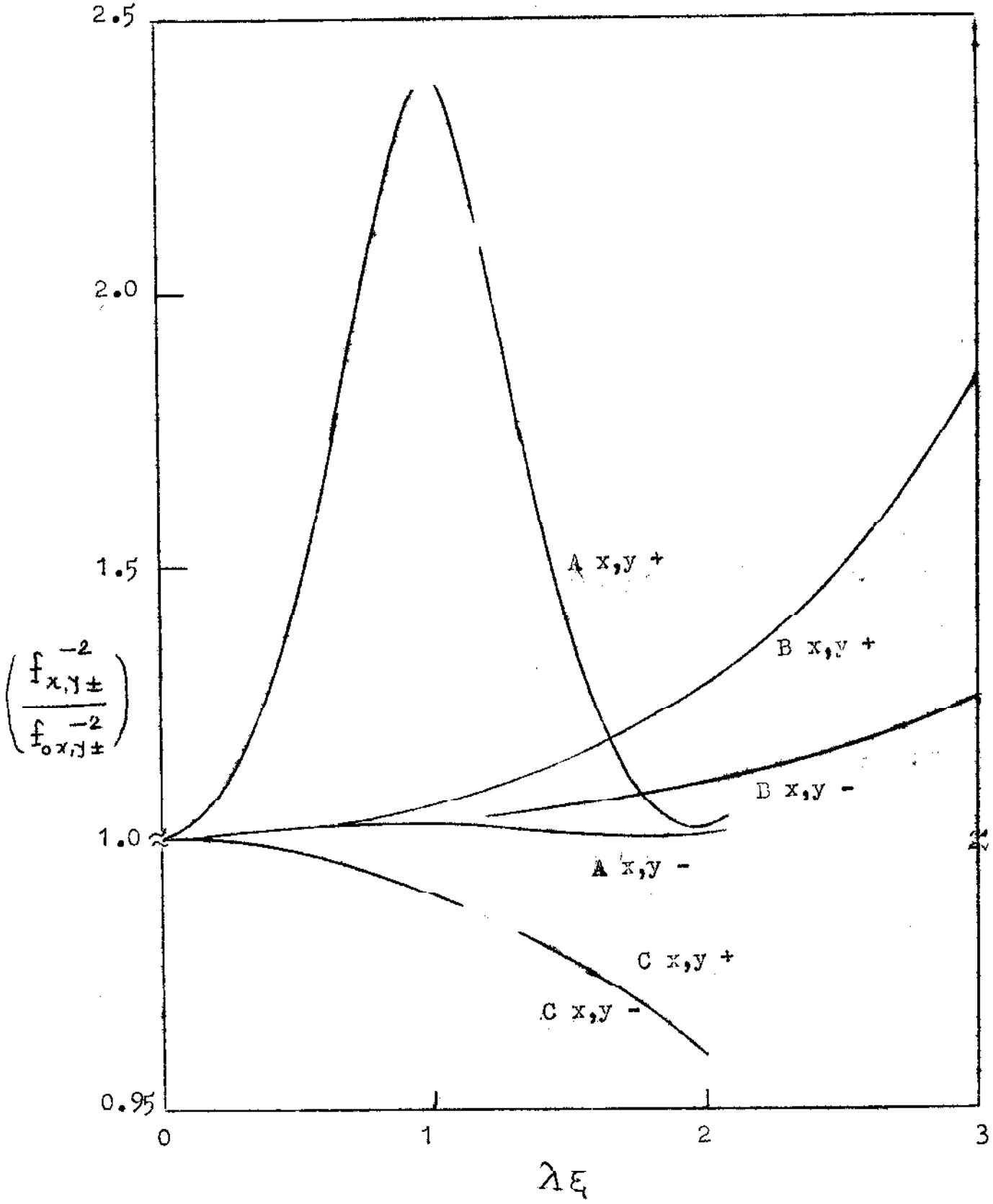
2.5
2.0
1.5
1.0
0.95
0
1
2
3
$\left(\frac{f^{-2}_{x,y\pm}}{f^{-2}_{o\,x,y\pm}}\right)$
$\lambda\xi$
A x,y +
B x,y +
B x,y -
A x,y -
C x,y +
C x,y -

Fig. 2.5

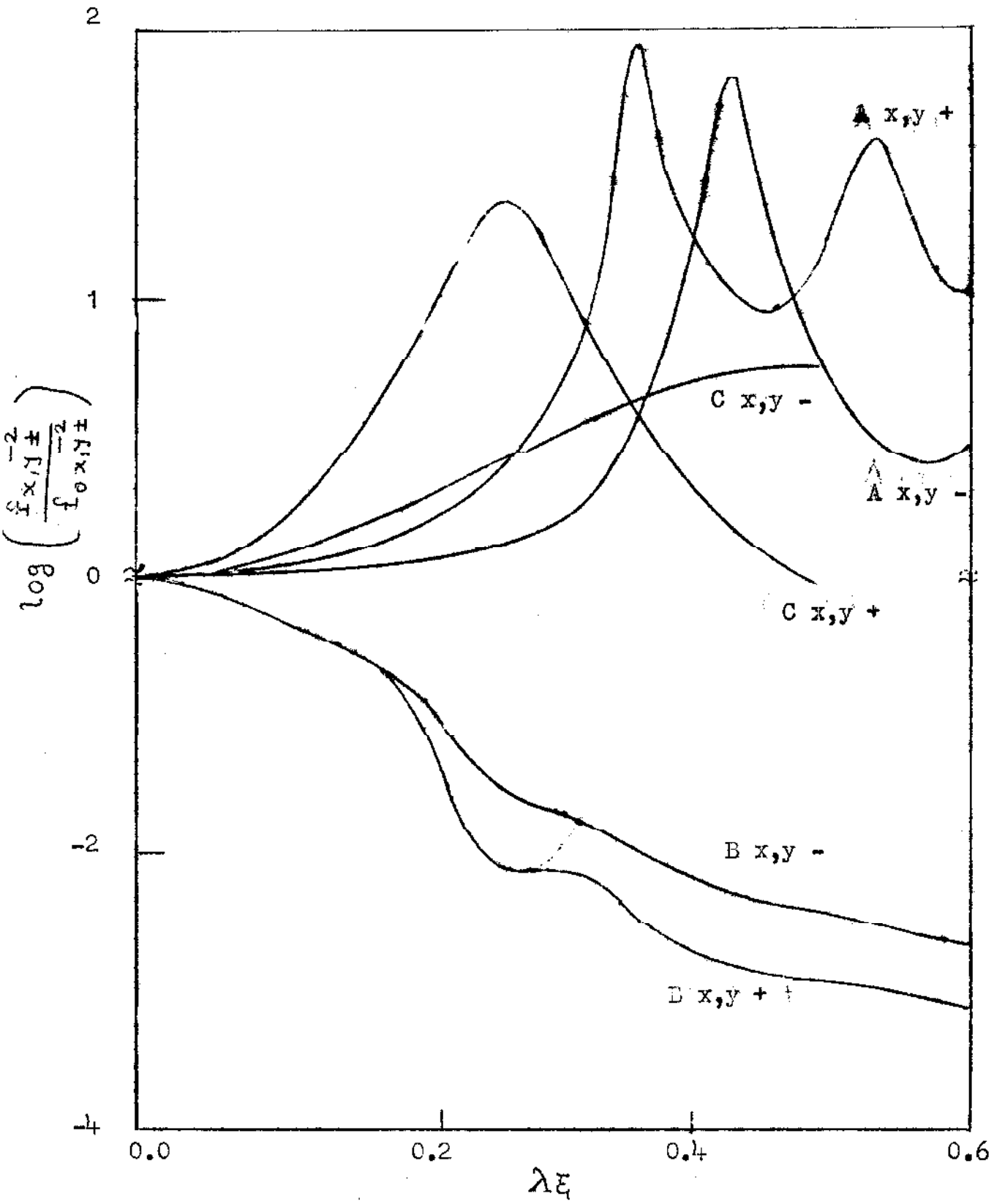

Fig. 2.6

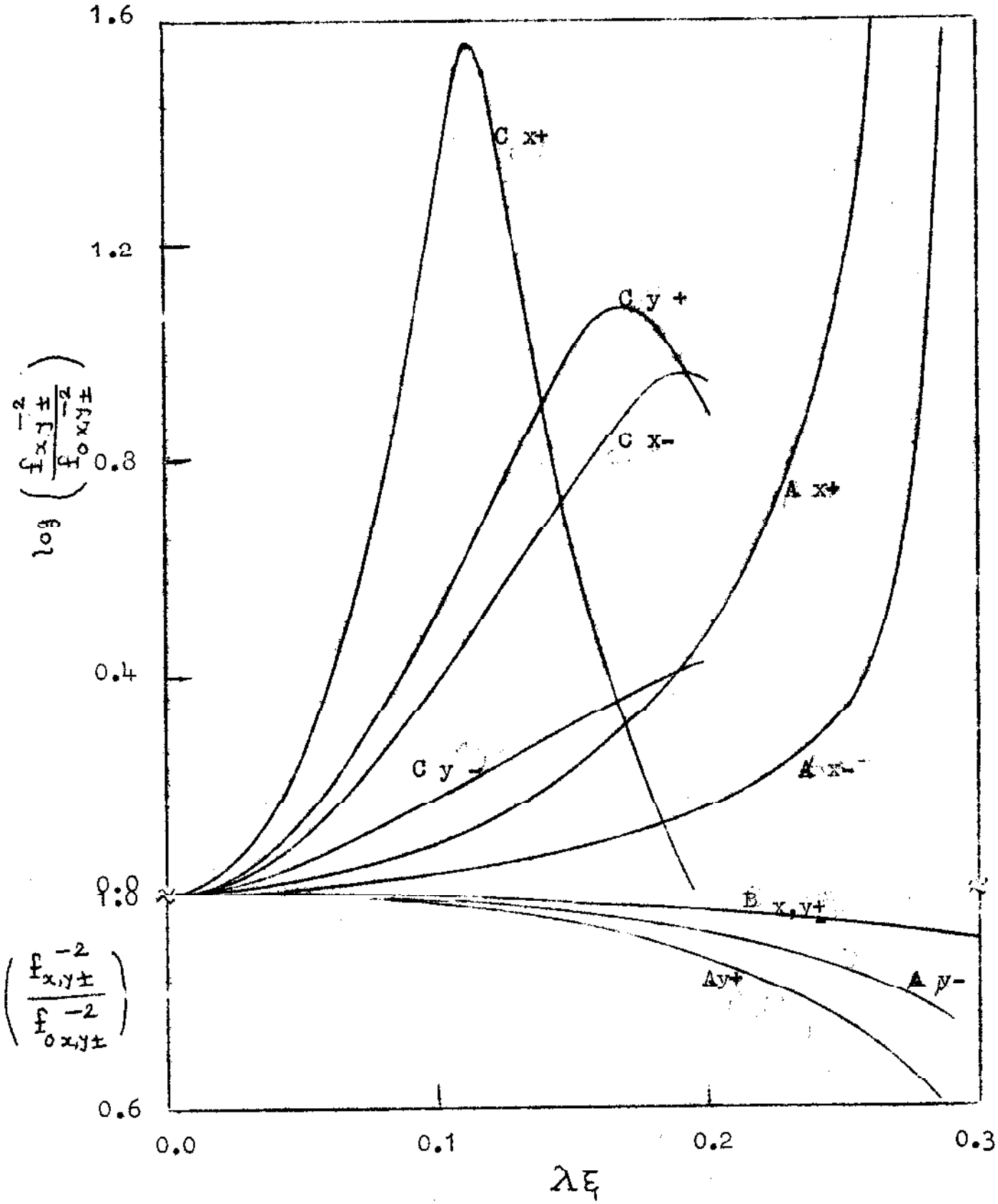
1.6
1.2
0.8
0.4
0.0
0.6
0.1
0.2
0.3
C x+
C y +
C x-
C y -
A x+
A x-
B x,y+
Ay+
A y-
$\log\left(\frac{f^{-2}_{x,y\pm}}{f^{-2}_{0\,x,y\pm}}\right)$
$\left(\frac{f^{-2}_{x,y\pm}}{f^{-2}_{0\,x,y\pm}}\right)$
$\lambda\xi$

Fig. 2.7

CHAPTER 3

TEMPORAL GROWTH OF A PARAMETRIC EXCITATION BY A SELF FOCUSED LASER BEAM

This chapter consists of two parts.

In Part 3A, a modified expression for the temporal growth rate of an arbitrary parametric excitation[6-10] by a self focused laser pump has been derived. In Sec.3.1, the relevant equations from the theory of self focusing[1-5] have been stated and then two dynamic equations for the signal and idler modes of an arbitrary parametric excitation[6-10] have been set up under the paraxial approximation. These two equations have been decoupled[74] by assuming the near self trapping[3] condition for the pump laser beam and a linearly varying phase mismatch for the parametric excitation. In Sec.3.2, the single eigenvalue equation[74,79] obtained upon decoupling has been solved under the WKB approximation. A modified analytical expression has been obtained for the 'growth rate parameter' from which the temporal growth rate of the parametric excitation can be easily determined. A graph has been plotted to show the variation of this parameter with the 'self focusing parameter'. In Sec.3.3, a discussion on characteristics of this graph, threshold intensity of the parametric excitation, validity of the assumed first-order approximation and quantization nature[79] of the temporal growth

rate has been presented. It is concluded that the temporal growth rate is a strong function of the radial intensity inhomogeneity of the pump laser beam. This strong dependence is not obtained when the pump laser beam is sharply defocused or sharply focused. The results in the case of back scattering and forward scattering are quite opposite in nature.

In Part 3B, the temporal growth rates of stimulated Raman and Brillouin scattering[7,8,75] of a laser beam in a plasma have been evaluated when the laser beam is self focused on account of the carrier-redistribution[4] caused by the collision-dominated heating of electrons. In Sec. 3.4, the relevant equations from the theory of self focusing have been stated. In Sec.3.5, the standard expressions[116] for the temporal growth rates of stimulated Raman and Brillouin scattering have been presented. In the local field approximation[87], the modifications in the expressions for the temporal growth rates (as discussed in Part 3A) may be neglected. In Sec.3.6, typical numerical results along with a discussion have been presented. The calculations predict a considerable spatial nonuniformity in the temporal growth rates of stimulated Raman and Brillouin scattering. The spatial dependence[7] of these growth rates and the propagation-distance dependence of the beam-width parameter of the pump laser beam are correlated. But

this correlation is not followed evenly, because on account of the electron heating and redistribution, the growth rates do not necessarily increase with the pump intensity.

Results of Parts 3A and 3B taken together imply that the temporal growth of any parametric excitation[7] is altered and becomes nonuniform if the pump laser beam is self focused.

PART 3A: MODIFIED EXPRESSION

3.1: Basic Equations

The dielectric constant of a nonlinear medium irradiated by a moderately intense laser beam is given by[1-5]

$$\epsilon = \epsilon_0 + \epsilon_{II} \vec{E}^* \cdot \vec{E} \quad , \tag{3.1}$$

where ϵ_0 and ϵ_{II} depend upon the medium parameters and the laser frequency ω. The electric field of a laser beam, with a radially Gaussian intensity profile and travelling along the z axis in the medium with the above-mentioned dielectric constant is given by[1-5]

$$\vec{E}(r,z,t) = \hat{E} \frac{E_0}{f(z)} \exp\left[-\frac{r^2}{2r_0^2 f^2(z)} + i\left(\Phi(r,z)+k\right)z - i\omega t\right]. \tag{3.2}$$

Here $k = \sqrt{\epsilon_0}\,\omega/c$ is the linear wave number;

$$\Phi(r,z) \simeq \varphi(z) + kr^2/2(z^2+z_{df}^2) \tag{3.3}$$

is the nonlinear part of the wavenumber, where

$$\varphi(z) = \left(k \epsilon_{II} E_0^4 / 4 \epsilon_0 - 1/k r_0^2\right)\left(z_{df}/z\right) \operatorname{arctan}\left(z/z_{df}\right), \qquad (3.4)$$

and

$$z_{df}^{-2} = z_d^{-2} - z_f^{-2} = 1/k^2 r_0^4 - \epsilon_2 E_0^2 / 2 \epsilon_0 r_0^2 \; ; \qquad (3.5)$$

and

$$f(z) = \left(1 + z^2/z_{df}^2\right)^{1/2} \qquad (3.6)$$

is the beamwidth parameter. The beam gets defocused, trapped or focused depending upon whether $z_{df}^{-2} >$, = or < 0.

The expression 3.2 for $\vec{E}$ (r, z, t) is valid only in the paraxial region ($r \ll r_0 f$) where Akhmanov at al.'s approach is valid. The expression 3.6 for f(z) restricts the validity of the present analysis to a laser beam of not very high intensity and to a small distance of propagation. The dielectric constant saturates[1-5] as the intensity $\vec{E}^* \cdot \vec{E}$ becomes very large. Consequently, an analytical expression for the beamwidth parameter f(z) is not available in the case of a laser beam of a very high intensity and a large distance of propagation.

Now let the electric vectors associated with the signal and idler modes (ℓ = 1, 2) excited by the forementioned pump laser beam, in the paraxial region ($r \ll r_0 f$) be given by[5-8,117]

$$\vec{E}_l(x\simeq 0, z, t) = \hat{E}_l\, E_0\, a_l(z)\, \exp\left[i(\varphi_l(z) + k_l)z + (g - i\omega_l)t \right]. \qquad (3.7)$$

Here the linear wavenumbers k_l and frequencies ω_l satisfy the conservation rules[5-8,117]

$$k_1 + k_2 = k \qquad (3.8)$$

and

$$\omega_1 + \omega_2 = \omega\,, \qquad (3.9)$$

whereas the nonlinear parts $\varphi_l(z)$ allow a mismatch

$$\Delta\varphi(z) = \varphi(z) - \left(\varphi_1(z) + \varphi_2(z)\right). \qquad (3.10)$$

Due to their coupling with the pump laser beam, the signal and idler modes gain in energy. The gain obviously depends upon the nature of the medium and the parametric excitation under consideration. The gain leads to: spatial variation of amplitudes of the signal and idler modes, shift in the frequencies of the two modes, and temporal growth of amplitudes of the two modes. These three consequences are described by the relative amplitude functions $a_l(z)$, imaginary part of the complex function g, and real part of g respectively. The form $\exp(\mathrm{Re}\, g \cdot t)$ for the temporal growth is based on the assumptions that the temporal growths of the two modes are

coupled so that they are the same, are exponential so that ($\mathcal{R}e\ g \cdot t$) occurs as an exponent, and are uniform so that g is independent of z. These assumptions are quite justified if the pump intensity is not very high so that saturation[7] of the parametric excitation does not come into picture.

The relative amplitude functions $a_1(z)$ satisfy, in the paraxial region and under the linearization approximation, the coupled rate equations[6-8,74,79]

$$\left(\frac{d}{dz} + \frac{g+\nu_1}{V_1}\right) a_1(z) = \frac{\Gamma_0}{V_1 f(z)}\, a_2^*(z)\, \exp\left(i\int \Delta\varphi(z)dz\right), \tag{3.11a}$$

$$\left(\frac{d}{dz} + \frac{g+\nu_2}{V_2}\right) a_2^*(z) = \frac{\Gamma_0}{V_2 f(z)}\, a_1(z)\, \exp\left(-i\int \Delta\varphi(z)dz\right). \tag{3.11b}$$

Here ν_1 and V_1 are the damping rates and the group velocities along the z axis, of the excited modes; and Γ_0 is the "homogeneous" coupling coefficient which varies linearly with E_0, the proportionality factor depending upon the parametric excitation under consideration. It has been assumed here that the laser induced spatial dependence of the parameters appearing in the expression for Γ_0 is negligible compared to that of f(z). The linearization approximation employed above is justified when the relative amplitude functions vary slowly in space.

In the first-order approximation, the pump laser beam will be assumed to be approximately self trapped[3,4] so that $z_{df}^{-2} \simeq 0$. Then f(z) is a slowly varying function of z, and hence while decoupling Eqs. 3.11, the term

$$\mathcal{U}(z) = \frac{d \ln f(z)}{dz} \tag{3.12}$$

may be neglected. Moreover, the mismatch function $\Delta\varphi(z)$ will be assumed[74] to be independent of z and set equal to $\Delta\varphi_o$. This is reasonable because in most of the cases of interest, the wavenumber mismatch is negligible or slowly/linearly varying function of z. It can now be shown that the transformations[79]

$$a_1(z) \exp\left(-i\,\Delta\varphi_o\, z/2\right) = a_2^*(z) \exp\left(i\,\Delta\varphi_o\, z/2\right)$$
$$= \Psi(z) \exp\left[-\left(\frac{g+\nu_1}{V_1} + \frac{g+\nu_2}{\bar{V}_2}\right)\frac{z}{2}\right] \tag{3.13}$$

can reduce Eqs.3.11 into a single equation

$$\left(\frac{d^2}{dz^2} + W(z)\right) \Psi(z) = 0 \quad , \tag{3.14}$$

where

$$W(z) = \frac{\Gamma_o^2}{V_1 \bar{V}_2 \left(1 + z^2/z_{df}^2\right)} - \left(\frac{g+\nu_1}{2V_1} + \frac{g+\nu_2}{2\bar{V}_2} + \frac{i\Delta\varphi_o}{2}\right)^2 , \tag{3.15}$$

and $\bar{V}_2 = -V_2$. For the more common case of backscattering

$\bar{V}_2$ is positive; V_1 having been assumed to be positive.

3.2: Growth Rate

Because of the assumed slow z dependence of f(z), W(z) is a slowly varying function of z, and hence a WKB solution[50,62,118] of Eq. 3.14 is reasonable. Thus

$$\Psi(z) \simeq C_{\pm} \left[W(z)\right]^{-1/4} \exp\left[\pm i \int \sqrt{W(z)}\, dz\right] , \qquad (3.16)$$

where $C_{\pm}$ are the constant coefficients determined by the boundary conditions. The turning points $z = \pm z_t$ where W(z) vanishes are

$$z_t = z_{df} \left[\left(\frac{g+\nu_1}{2V_1} + \frac{g+\nu_2}{2\bar{V}_2} + \frac{i\Delta\varphi_0}{2}\right)^2 \frac{\Gamma_0^2}{V_1 \bar{V}_2} - 1\right]^{1/2} . \qquad (3.17)$$

According to the WKB theory[50,118] of reflection inside a potential well, the eigenvalues g_n satisfy the condition

$$\int_0^{z_t} \sqrt{W_n(z)}\, dz = (2n+1)\pi/4 , \qquad (3.18)$$

where n is a non-negative integer[50,118]. This gives

$$B\left(1 - \left(\frac{g_n+\nu_1}{2V_1} + \frac{g_n+\nu_2}{2\bar{V}_2} + \frac{i\Delta\varphi_0}{2}\right)^2 \frac{V_1 \bar{V}_2}{\Gamma_0^2}\right)$$

$$= (2n+1)^2 (\pi/4)^2 V_1 \bar{V}_2 / \Gamma_0^2 z_{df}^2 , \qquad (3.19)$$

where the notation

$$B(x) \equiv \left[\int_0^{\pi/2} \left\{ (1 - x \sin^2\theta)^{-1/2} - (1 - x \sin^2\theta)^{1/2} \right\} d\theta \right]^2$$

$$\equiv \left[\mathbb{K}(x) - \mathbb{E}(x) \right]^2 \qquad (3.20)$$

has been used for convenience. Here $\mathbb{K}(x)$ and $\mathbb{E}(x)$ are the well known complete elliptic functions of the first and second kind[114,118].

Thus then results the following analytical expression for g_n whose real part is the temporal growth rate of the parametric excitation and imaginary part is the frequency shift.

$$(g_n \alpha + \beta) = \left[1 + B^{-1}(\gamma_n z_{df}^{-2}) \right]^{1/2}, \qquad (3.21)$$

where

$$\alpha = \left(\sqrt{\bar{\nu}_2 / \nu_1} + \sqrt{\nu_1 / \bar{\nu}_2} \right) / 2\Gamma_0 \quad , \qquad (3.22)$$

$$\beta = \left(\nu_1 \sqrt{\bar{\nu}_2 / \nu_1} + \nu_2 \sqrt{\nu_1 / \bar{\nu}_2} + i \Delta\varphi_0 \sqrt{\nu_1 \bar{\nu}_2} \right) / 2\Gamma_0 , \qquad (3.23)$$

$$\gamma_n = -(2n+1)^2 (\pi/4)^2 \nu_1 \bar{\nu}_2 / \Gamma_0^2 \quad , \qquad (3.24)$$

and B^{-1} stands for the inverse function corresponding to B. From physical reasoning (by carrying out the foregoing analysis for $z_{df}^{-2} = -z_{fd}^{-2}$), it is seen that $B^{-1}(-\gamma_n z_{df}^{-2}) = -B^{-1}(\gamma_n z_{df}^{-2})$. For convenience, the quantities $(\gamma_n z_{df}^{-2})$ and $(g_n\alpha + \beta)$ will be termed as 'self-focusing parameter' and 'growth rate parameter' respectively. In the absence of self-focusing, i.e. when the diffraction effect is balanced by the focusing-nonlinearity, $\gamma_n z_{df}^{-2} = 0$ and $(g_n\alpha + \beta) = 1$. The quantity

$$Q \equiv \left\{100(g_n\alpha + \beta - 1)(1 - Re\,\beta)/\left[(1 - Re\,\beta)^2 + (Im\,\beta)^2\right]\right\}$$

is the percentage increase in the temporal growth rate $(Re\ g_n)$ when the effect of self-focusing is taken into account.

In Fig.3.1, the 'growth rate parameter' $(g_n\alpha + \beta)$ has been plotted versus the 'self-focusing parameter' $(\gamma_n z_{df}^{-2})$. Note that the graph is separable into two parts, viz. upper and lower parts corresponding to $(g_n\alpha + \beta) > 1$ and < 1. The upper (/lower) part corresponds to the case of focusing (/defocusing) and backscattering i.e. $\bar{V}_2 > 0$ or of defocusing(/focusing) and forwardscattering i.e. $\bar{V}_2 < 0$.

3.3: Discussion

In the region $|\gamma_n z_{df}^{-2}| \simeq 0$, where the first order approximate theory may be quite reasonable, the graph $(g_n\alpha+\beta)$ versus $(\gamma_n z_{df}^{-2})$ has a remarkable slope. This means that in the near self-trapping condition, the temporal growth rate $(\mathcal{R}e\ g_n)$ varies very drastically with the 'self-focusing parameter' $(\gamma_n z_{df}^{-2})$. For example, in the case of focusing and backscattering (/defocusing and forwardscattering) with $(\gamma_n z_{df}^{-2}) = 0.1$, the graph gives $(g_n\alpha+\beta) = 1.059$ which implies 5.9 percent increase in its conventional value of unity calculated for $(\gamma_n z_{df}^{-2}) = 0$, or equivalently $\{5.9(1-\mathcal{R}e\beta)/[(1-\mathcal{R}e\beta)^2+(\mathcal{I}m\beta)^2]\}$ percent increase in the temporal growth rate $(\mathcal{R}e\ g_n)$. Similarly, in the case of defocusing and backscattering(/focusing and forwardscattering) with $(\gamma_n z_{df}^{-2})=-0.1$, the graph gives $(g_n\alpha+\beta) = 0.937$ which implies 6.3 percent decrease in its conventional value, or equivalently $\{6.3(1-\mathcal{R}e\beta)/[(1-\mathcal{R}e\beta)^2+(\mathcal{I}m\beta)^2]\}$ percent decrease in the temporal growth rate. Both of these cases thus lead to appreciable changes in the temporal growth rate. The values $\pm$ 0.1 for the 'self-focusing parameter' $(\gamma_n z_{df}^{-2})$ are realizable in a variety of cases. Thus the effect of self focusing (defocusing or focusing) on the temporal growth rate of the parametric excitation can be appreciable in a variety of experimentally realisable situations.

The threshold intensity I_{th} of the parametric excitation[6-8,117] under consideration is determined by setting the complex temporal growth rate function g_n equal to zero in Eq.3.21. This gives the transcendental equation

$$\frac{(\sqrt{I}\,\beta)}{\sqrt{I_{th}}} = \left[1 + B^{-1}\left(\frac{(I\gamma_n)}{I_{th}}\, z_{df}^{-2}\right)\right]^{1/2}. \qquad (3.25)$$

In the exact self-trapping case i.e. for $z_{df}^{-2} = 0$, this gives the usual result[6-8,117]

$$I_{th,c} = (1/4)\left|\, \nu_1\sqrt{\bar{V}_2/V_1} + \nu_2\sqrt{V_1/\bar{V}_2} + i\Delta\varphi_0\sqrt{V_1\bar{V}_2}\,\right|^2, \qquad (3.26)$$

which, as expected, is independent of the transverse intensity profile of the laser beam. Equation 3.25 can be solved for I_{th} by the usual graph-crossover technique. For example, on Fig.3.1, I_{th} corresponds to the crossover point of the already plotted graph of $\left[1+B^{-1}(\gamma_n z_{df}^{-2})\right]^{1/2}$ with a new graph of

$$\left[2(i\nu_1/\sqrt{V_1} + i\nu_2/\sqrt{\bar{V}_2} - \Delta\varphi_0)\, z_{df}\,/(2n+1)\pi\right](\gamma_n z_{df}^{-2})^{1/2}.$$

It is apparent that in the near self trapping condition, the threshold intensity varies appreciably with the parameters appearing in the expression for z_{df}^{-2}.

In Fig.3.1, it is seen that the growth rate parameter' $(g_n\alpha+\beta)$ has upper and lower saturation values $\sqrt{2}$ and 0 as the 'self-focusing parameter' $(\gamma_n Z_{df}^{-1})$ approaches $\pm\infty$. The upper (/lower) saturation corresponds to the case of complete focusing(/defocusing) and backscattering or complete defocusing(/focusing) and forward scattering. Hence the first order approximate theory meant for near self trapping region is not expected to remain valid in these saturation regions. In order to get rid of this limitation, the term $\mu(z) \equiv (d/dz)\ \ln f(z)$ should be incorporated in the foregoing theory. With this term included, it is seen that Eqs. 3.13-3.15 need to be replaced by

$$\frac{a_1(z)}{\psi_1(z)}\exp\left[\left(-\mu(z)-i\Delta\varphi_0\right)\frac{z}{2}\right]=\frac{a_2^*(z)}{\psi_2(z)}\exp\left[\left(-\mu(z)+i\Delta\varphi_0\right)\frac{z}{2}\right]$$

$$=\exp\left[-\left(\frac{g+\nu_1}{V_1}+\frac{g+\nu_2}{V_2}\right)\frac{z}{2}\right]\ , \qquad (3.27)$$

$$\left(\frac{d^2}{dz^2}+W_l(z)\right)\psi_l(z)=0\ , \qquad (3.28)$$

and

$$W_l(z)=\frac{\Gamma_0^2}{V_1\bar{V}_2\left(1+z^2/z_{df}^2\right)}-\left(\frac{g+\nu_1}{2V_1}+\frac{g+\nu_2}{2\bar{V}_2}+(-)^l\frac{\mu(z)}{2}+\frac{i\Delta\varphi_0}{2}\right)^2. \qquad (3.29)$$

The WKB. approximation is still reasonable in the intermediate region where z_{df}^{-2} and $(d\ \mu(z)/dz)$ are not very large. The foregoing first order approximate treatment is valid, i.e. the term $\mu(z)$ may be neglected, if and only if

$$\mu(z) \ll \left| \left(\frac{\nu_1}{V_1} + \frac{\nu_2}{V_2} + i\Delta\varphi_0 \right) \right| . \qquad (3.30)$$

This condition can be satisfied when the signal and idler modes are slowly propagating and easily attenuable in the region not far away from the self trapping of the pump laser beam.

The present investigation is valid in the paraxial region[1-5] and when $(d/dz)\ln\Gamma_0 \ll z_{df}^{-1}$ so that the spatial variation of Γ_0 may be neglected. The present investigation may be extended to include the nonparaxial region and spatial variation of Γ_0. But then the analysis would become much more complicated than the present one and analytical results would not be possible.

It is to be noted that the quantum number[6,74,79] n plays an important role in the expressions for γ_n and g_n, and that this n does not come into picture for a transversely homogeneous or a self trapped transversely inhomogeneous laser beam. It should be recalled that g_n is complex so that 'n^{th} temporal growth rate' corresponds to the parametric excitation at 'n^{th}

frequency shift[74,79].

It is thus concluded that the temporal growth rate of a parametric excitation varies significantly with the transverse intensity inhomogeneity of the pump laser beam, and hence the effect of self-focusing may not be neglected. The first order approximation employed here is valid when the signal and idler modes are slowly propagating and easily attenuable in the region not for away from the self trapping of the pump laser beam.

PART 3B: LOCAL CALCULATIONS

3.4: Self Focusing of the Pump

The electric field of the pump laser beam at z=0 is taken to be of the form

$$\vec{E}(r, z=0, t) = \hat{E}\, E_o \exp\left(-r^2/2r_o^2 - i\omega t\right), \qquad (3.31)$$

where $\hat{E}$ is the unit vector representing the polarization of $\vec{E}$ and r_o is the initial beamwidth. The time scale of variation of the initial axial intensity E_o^2 will be assumed to be much larger than the reciprocal of the electron collision frequency : ν^{-1}. The electron temperature then rises[3,4] to such an extent that the electron-ion redistribution due to the ponderomotive force may be neglected as compared to that due to the

nonuniform heating of electrons and that the redistribution process follows a steady state model[3,4]. By assuming the pump frequency ω to be much larger than the electron collision frequency ν and assuming the usual parametric approximation[6-8,117], any depletion of the pump intensity may be neglected.

Under these conditions, the nonlinear dielectric constant of the plasma is given by[3,4]

$$\epsilon = \epsilon_0 + \epsilon_{n.l.} \quad , \tag{3.32}$$

where

$$\epsilon_0 = 1 - \omega_{p0}^2 / \omega^2 \quad , \tag{3.33}$$

$$\epsilon_{n.l.} = \omega_{p0}^2/\omega^2 - \omega_p^2/\omega^2$$
$$= (\omega_{p0}^2/\omega^2)\ (1 + \beta \vec{E}^* \cdot \vec{E})^{-1}\ \beta \vec{E}^* \cdot \vec{E} \quad , \tag{3.34}$$

$$\omega_{p0}^2 = 4\pi N_0 e^2 / m \quad , \tag{3.35}$$

$$\beta = M e^2 / 12\, m^2 \omega^2 K_B T_0 \quad ; \tag{3.36}$$

N_0 is the electron (or ion) concentration in the absence of the pump, m is the electron mass, M is the ion mass, K_B is the Boltzmann constant and T_0 is the initial electron temperature.

The wave equation for $\vec{E}$, when solved under the

paraxial and WKB approximations, gives the following solution valid in the nonresonant ($\epsilon_0 \neq 0$) paraxial ($r \ll r_0 f$) region[1-5].

$$\vec{E}(r, z, t) = \hat{E}\, E_0\, f^{-1} \exp\left[-r^2/2r_0^2 f^2 + i k(S+z) - i\omega t\right], \tag{3.37}$$

where

$$k = \sqrt{\epsilon_0}\, \omega/c \tag{3.38}$$

is the linear wavenumber and $S(r, z)$, which may be expressed in terms of $f(z)$, is (z/k) times the nonlinear part of the wavenumber. On the basis of the analysis in Chapter 1, it can be shown that the beamwidth parameter $f(z)$ is governed by the equation[3,4]

$$f^3 \frac{d^2 f}{dz^2} = \frac{1}{k^2 r_0^4} - \frac{(\omega_{p0}^2/\omega^2)}{2\epsilon_0 r_0^2} \frac{\beta E_0^2}{(1+\beta E_0^2/2f^2)^2} \tag{3.39}$$

along with the boundary conditions

$$f(z=0) = 1 \qquad \text{and} \qquad (df/dz)_{(z=0)} = 0 . \tag{3.40}$$

It can be easily shown that there exist two values[40,41] of E_0^2 namely (cf. Chapter 1)

$$E_{st\mp}^2 = (2/\beta)\left[k^2 r_0^2 \omega_{p0}^2/2\epsilon_0\omega^2 - 1 \mp \left(k^4 r_0^4 \omega_{p0}^4/4\epsilon_0^2 r_0^4 - k^2 r_0^2 \omega_{p0}^2/\epsilon_0\omega^2\right)^{1/2}\right] \tag{3.41}$$

for which the beam gets self trapped (i.e. f=1 for all z). The beam experiences monotonic defocusing, oscillatory defocusing and oscillatory focusing when $E_o^2 < E_L^2 = c^2/\beta r_o^2 \omega_{po}^2$, $E_L^2 < E_o^2 < E_{st-}^2$ or $E_o^2 > E_{st+}^2$ and $E_{st-}^2 < E_o^2 < E_{st+}^2$ respectively[3,4].

3.5: Temporal Growth Rates

3.5.1: Stimulated Raman scattering (SRS)

For $\omega > 2\omega_p$, a pump photon can be scattered[7] as another photon polarized along some direction $\hat{E}_s$ by exciting a plasmon (quantum of electron plasma waves) of arbitrary wavenumber $\vec{k}_e$ and the corresponding frequency[116]

$$\omega_e = \omega_p \left(1 + 3 k_e^2 \lambda_D^2/2\right)^{1/2} , \qquad (3.42)$$

where the Debye length

$$\lambda_D = \left(K_B T_e / m \omega_p^2 \right)^{1/2} , \qquad (3.43)$$

$$T_e = T_o \left(1 + 2\beta \vec{E}^* \cdot \vec{E}\right) , \qquad (3.44)$$

$$\omega_p^2 = \omega_{po}^2 \left(1 + \beta \vec{E}^* \cdot \vec{E}\right)^{-1} . \qquad (3.45)$$

In a cold homogeneous plasma, the temporal growth rate of SRS of a uniform pump laser beam is given by[116]

$$\gamma(SRs) = \left\{ \left[1 + (\vec{k}-\vec{k_e})^2 c^2/\omega_p^2 \right]^{-1/2} \left[\vec{E}\cdot\hat{E}_s k_e e/ m\omega \right]^2 + (\Gamma_2-\Gamma_p)^2/4 \right\}^{1/2} - (\Gamma_2+\Gamma_p)/2, \quad (3.46)$$

where

$$\Gamma_2 = \nu_c \omega_p^2 / 2\omega^2 \quad (3.47)$$

is the collisional damping rate of the scattered electromagnetic waves, and

$$\Gamma_p = (\pi^{1/2} \omega_p / 2 k_e^3 \lambda_D^3) \exp(-3/4 - k_e^2 \lambda_D^2/2) + \nu_{ec} \quad (3.48)$$

is the Landau plus collisional damping rate of electron plasma waves[51].

3.5.2: Stimulated Brillouin scattering (SBS)

For $\omega > \omega_p$, a pump photon can be scattered[7] as another photon polarized along some direction $\hat{E}_s$ by exciting a phonon (quantum of ion acoustic waves) of arbitrary wavenumber $\vec{k_i}$ and the corresponding frequency[116]

$$\omega_i = \omega_p (m/M)^{1/2} (1 + 1/k_i^2 \lambda_D^2)^{-1/2}. \quad (3.49)$$

In a cold homogeneous plasma, the temporal growth rate of SBS of a uniform pump laser beam is given by[116]

$$\gamma(SBS) = \left\{ (\omega_p/\omega)(m/M)^{1/2} (1 + 1/k_i^2 \lambda_D^2)^{1/2} \left[\vec{E} \cdot \hat{E}_s \, k_i e / m\omega(1 + k_i^2 \lambda_D^2) \right]^2 + (\Gamma_2 - \Gamma_a)^2/4 \right\}^{1/2} - (\Gamma_2 + \Gamma_a)/2 \, , \qquad (3.50)$$

where

$$\Gamma_a = (T_e/T_0)^{3/2} \exp(-3/2 - T_e/2T_0) + k_i c_s (\pi m/8M)^{1/2} + \nu_{ic} \qquad (3.51)$$

is the Landau plus collisional damping rate of ion acoustic waves, and

$$c_s = (K_B T_e / M)^{1/2} \qquad (3.52)$$

is the ion-acoustic speed[51].

3.5.3: Local field approximation

The expressions for the temporal growth rates of SRS and SBS in the case of a hot plasma are slightly different[116] from the expressions 3.46 and 3.50. However, in the first-order approximation, the modifications in the expressions on account of thermal effects in the

plasma can be neglected.

As shown in the Part 3A, the expressions for the temporal growth rates of SRS and SBS in the case of a nonuniform pump (or inhomogeneous plasma) are different[6,86] from the expressions 3.46 and 3.50. However, when the beamwidth and self-focusing length of the pump are much larger than the wavelengths involved in the scattering, the modifications in the expressions on account of non-uniformity in the pump can be neglected[87]. Thus, in the first order approximation, the temporal growth rates of SRS and SBS at a particular region in the plasma are given by using the local parameters[87] in the expressions 3.46 and 3.50 respectively.

3.6: Results and Discussion

For illustration, the following parameters have been chosen:-

$N_o = 10^{18}$ cm^{-3} for SRS and 5×10^{18} cm^{-3} for SBS,

$M/m = 2000$,

$K_B T_o = 1.38\times10^{-9}$ erg,

$\nu_c = \nu_{ec} = \nu_{ic} \ll \omega$,

$\omega = 1.84\times10^{14}$ rad/sec,

$r_o = 0.005$ cm ,

$\hat{E}_s = \hat{E}$

$\vec{k}_e = \vec{k}_i = \hat{z}\ 100$ /cm.

These parameters yield

$E^2_{st-} = 2.484 \times 10^7$ erg.cm^{-3} for SRS and 4.880×10^6 erg.cm^{-3} for SBS;

$E^2_{st+} = 1.913 \times 10^{11}$ erg.cm^{-3} for SRS and 9.742×10^{11} erg.cm^{-3} for SBS.

The initial axial intensity E^2_o will be allowed to take the following five different values in each case.
(1) $E^2_o = E^2_{st-}/2$, (2) $E^2_o = E^2_{st-}$, (3) $E^2_o = (E^2_{st-} + E^2_{st+})/2$,
(4) $E^2_o = E^2_{st+}$, (5) $E^2_o = 2E^2_{st+}$.

These parameters have been so chosen that the modifications required in the expressions for the temporal growth rates, on account of the nonuniformity in the pump laser beam (and induced nonuniformity in the plasma), are negligible[87] so that the use of the expressions 3.46 and 3.50 along with the local field parameters is justified. The values of E^2_o have been chosen as above with the aim to illustrate all the manifestations of the phenomenon of self-focusing (cf. Chapter 1).

The beamwidth parameters f versus z for SRS and SBS have been plotted in Figs. 3.2 and 3.3. The temporal growth rates γ_o at r=0 versus z for SRS and SBS have been plotted in Figs. 3.4 and 3.5. The temporal growth rates γ_1 at r = 0.01 cm versus z for SRS and SBS have been plotted in Figs. 3.6 and 3.7. In view of

the paraxial approximation[1-5] employed, the graphs of Figs. 3.6 and 3.7 can be claimed to be correct only approximately.

Some of the general observations from Figs.3.2-3.7 are as follows. For $E_o^2 = E_{st-}^2$ or E_{st+}^2, $f(z) = 1$ and $\gamma_1(z) = \gamma_1(o) < \gamma_0(z) = \gamma_0(o)$ in such a way that γ (for $E_o^2 = E_{st-}^2$) $< \gamma$ (for $E_o^2 = E_{st+}^2$). For $E_{st-}^2 < E_o^2 < E_{st+}^2$, f and γ_1 oscillate between their values at z=0 and certain minimum values, whereas γ_0 oscillates between its value at z=0 and a certain maximum value. For $E_o^2 < E_{st-}^2$ or $E_o^2 > E_{st+}^2$, f and γ_1 oscillate between their values at z=0 and certain maximum values, whereas γ_0 oscillates between its value at z=0 and a certain minimum value. The conclusion that γ_1 has similar variation with z as f whereas γ_0 behaves oppositely can be explained as follows. The temporal growth rate increases with the pump intensity and the electron/ion concentration, which in turn, decreases and increases respectively with f. In the paraxial region, the effect of change of the pump intensity dominates and γ_0 decreases with f. In the offaxial region, on the other hand, the effect of change of the electron/ion concentration dominates and hence γ_1 increases with f.

However, the forementioned correlation is not followed evenly. In Fig.3.5, the graph for $E_o^2=(E_{st-}^2+E_{st+}^2)/2$

has two peaks rather than a single peak within one oscillatory unit of length. In the same figure, the position of the graph for $E_o^2 = 2E_{st+}^2$ is inverted as compared to its position expected in view of the foregoing correlation. This odd behaviour does not appear in a collisionless[3,4] plasma in which the electron-heating does not take place[87]. It may therefore be concluded that the increase in the electron temperature, induced by the laser beam, has an effect to complicate the functional dependence of the temporal growth rates, particularly that of γ (SBS).

The temporal growth rates of SRS and SBS oscillate with the propagation distance z and moreover decrease or increase with the radial coordinate r. To have a numerical appreciation of this spatial nonuniformity, the following particular case may be useful. For $E_o^2 = (E_{st-}^2 + E_{st+}^2)/2$, the ratios $\gamma_{0\,max}/\gamma_{0(z=o)}$, $\gamma_{1(z=o)}/\gamma_{0(z=o)}$, $\gamma_{1\,min}/\gamma_{0(z=o)}$ are respectively 1.192, 0.32, 0.08 for SRS and 1.001, 0.96, 0.55 for SBS. These ratios are appreciably different from unity and thereby indicate appreciable nonuniformity in the temporal growth rates of SRS and SBS.

The time scale of variation of the initial axial intensity E_o^2 has been assumed here to be much larger than the reciprocal of the electron collision frequency ν^{-1}. When it be not so, the electron-heating does not take place

and the redistribution takes place due to the ponderomotive force[4,40] rather than the nonuniform heating of electrons. Sodha et al.[87] have analysed the temporal growths of SRS, SBS, two-plasmon decay and plasmon-phonon decay in such a "collisionless" plasma. They have, however, considered only a limited range of values of E_o^2 so that not all of the manifestations of the phenomenon of self-focusing are examined. Due to the absence of electron-heating and restricted range of the parameters involved, their[87] results do not show any odd behaviour as seen in the present analysis. Their results as well as results of the present analysis show that the temporal growth rates of SRS and SBS are enhanced if $E_{st-}^2 < E_o^2 < E_{st+}^2$. This result is consistent with Cotter et al.'s[119] result that SRS is enhanced by external focusing of the pump and Sodha et al.'s[85] result that SRS is enhanced by self-focusing of the pump.

Figures 3.1 - 3.7

Fig.3.1 'Growth rate parameter' $(g_n\alpha + \beta)$ versus 'self focusing parameter' $(\gamma_n z_{df}^{-2})$.

In Figs. 3.2 - 3.7, the number at the tip of a graph denotes the initial pump intensity as follows: (1) $E_o^2 = E_{st-}^2/2$, (2) $E_o^2 = E_{st-}^2$, (3) $E_o^2 = (E_{st-}^2 + E_{st+}^2)/2$, (4) $E_o^2 = E_{st+}^2$, (5) $E_o^2 = 2E_{st+}^2$.

Fig.3.2 Beamwidth parameter f versus z for SRS.

Fig.3.3 Beamwidth parameter f versus z for SBS.

Fig.3.4 Temporal growth rate γ_o at r=0 versus z for SRS.

Fig.3.5 Temporal growth rate γ_o at r=0 versus z for SBS.

Fig.3.6 Temporal growth rate γ_1 at r=0.01 cm versus z for SRS.

Fig.3.7 Temporal growth rate γ_1 at r=0.01 cm versus z for SBS.

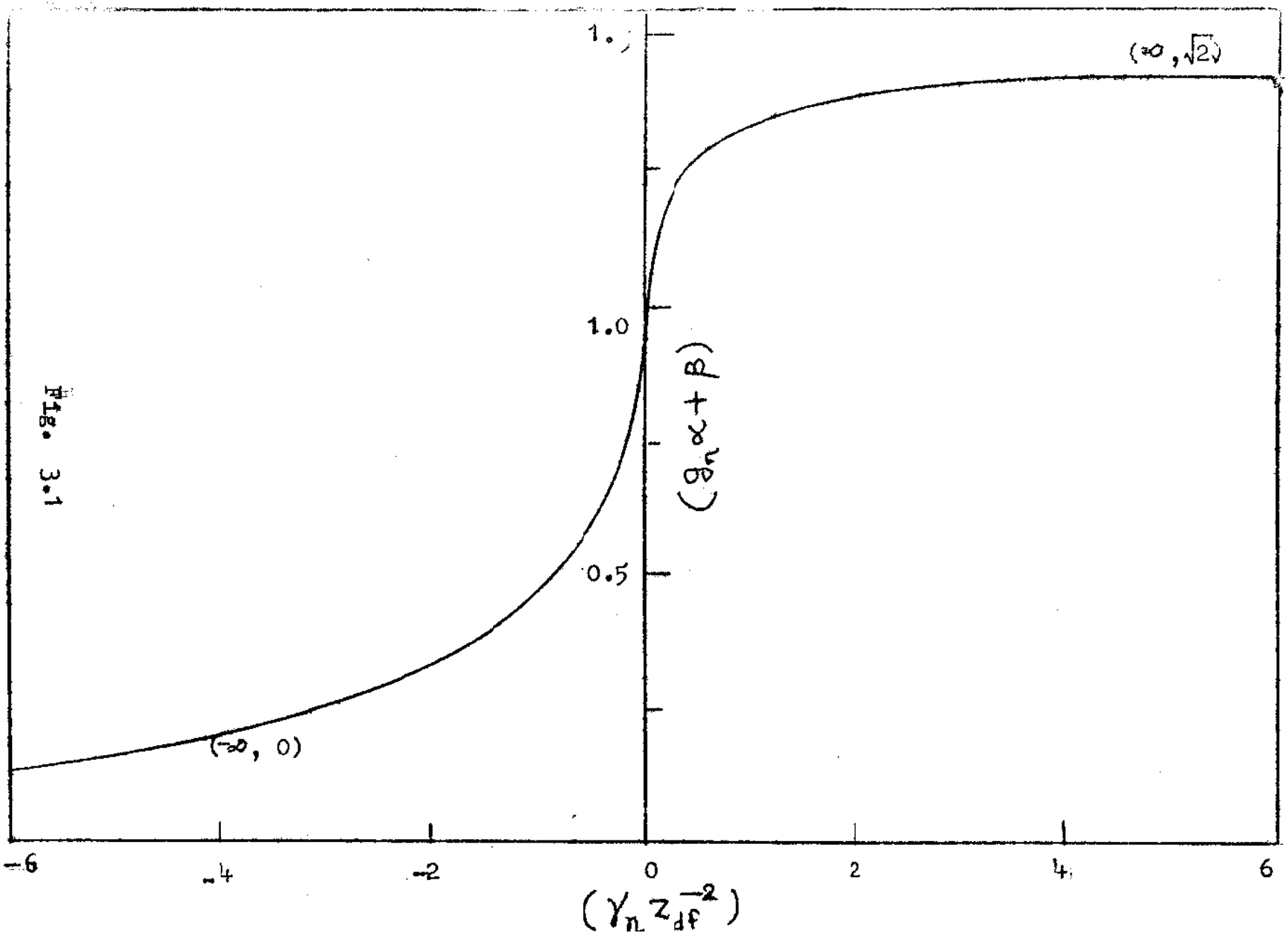

Fig. 3.1

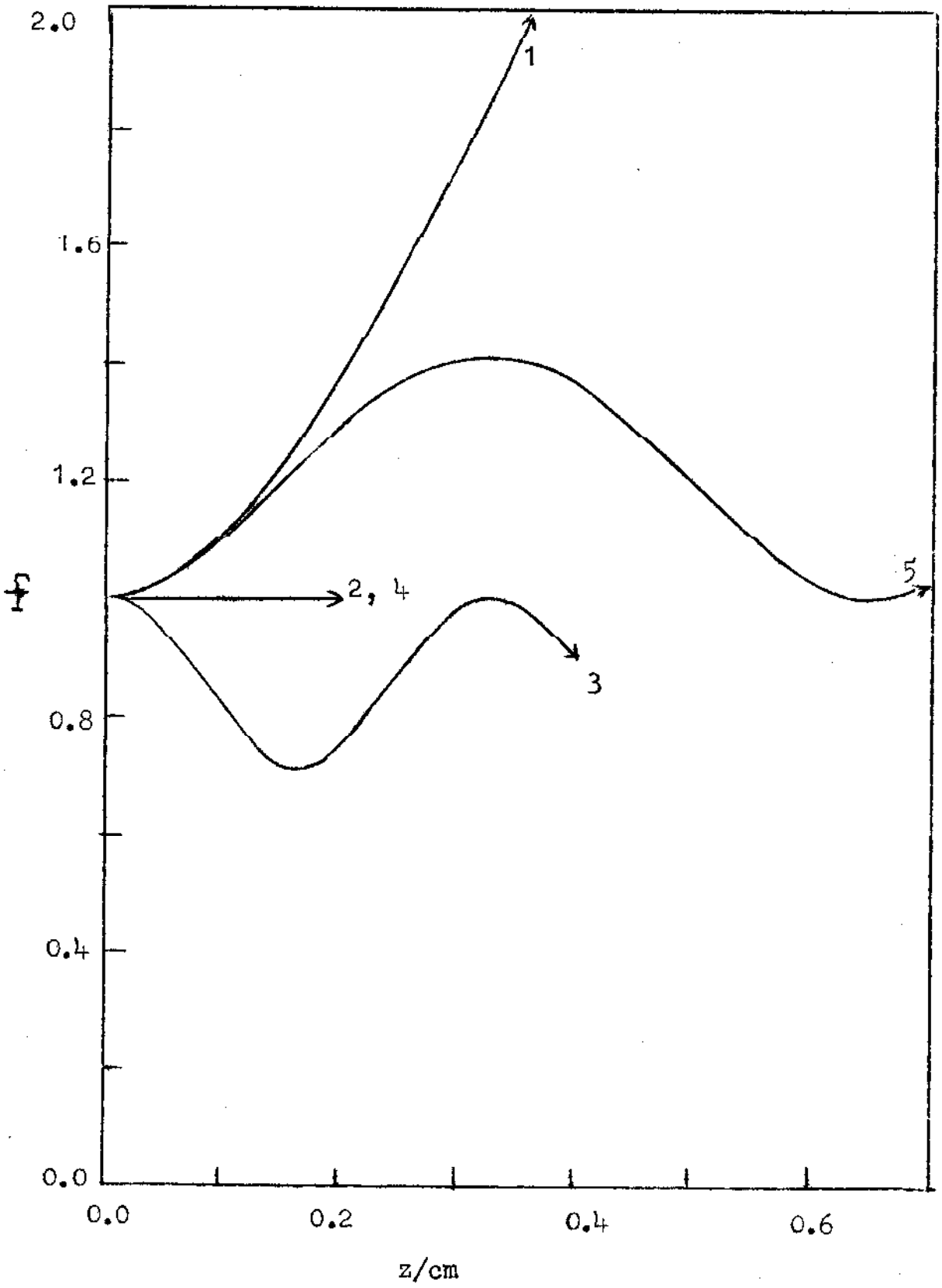

Fig. 3.2

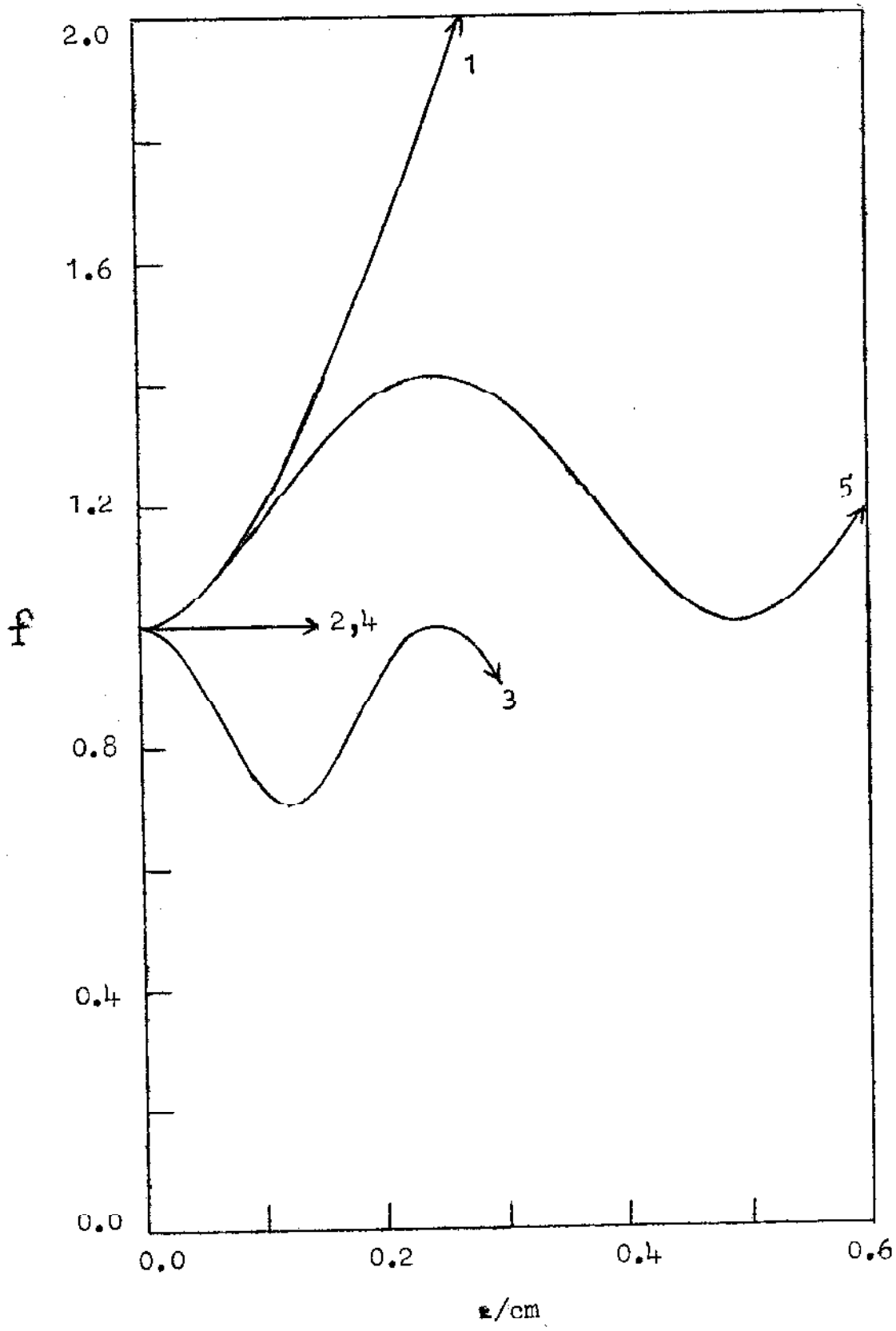

Fig. 3.3

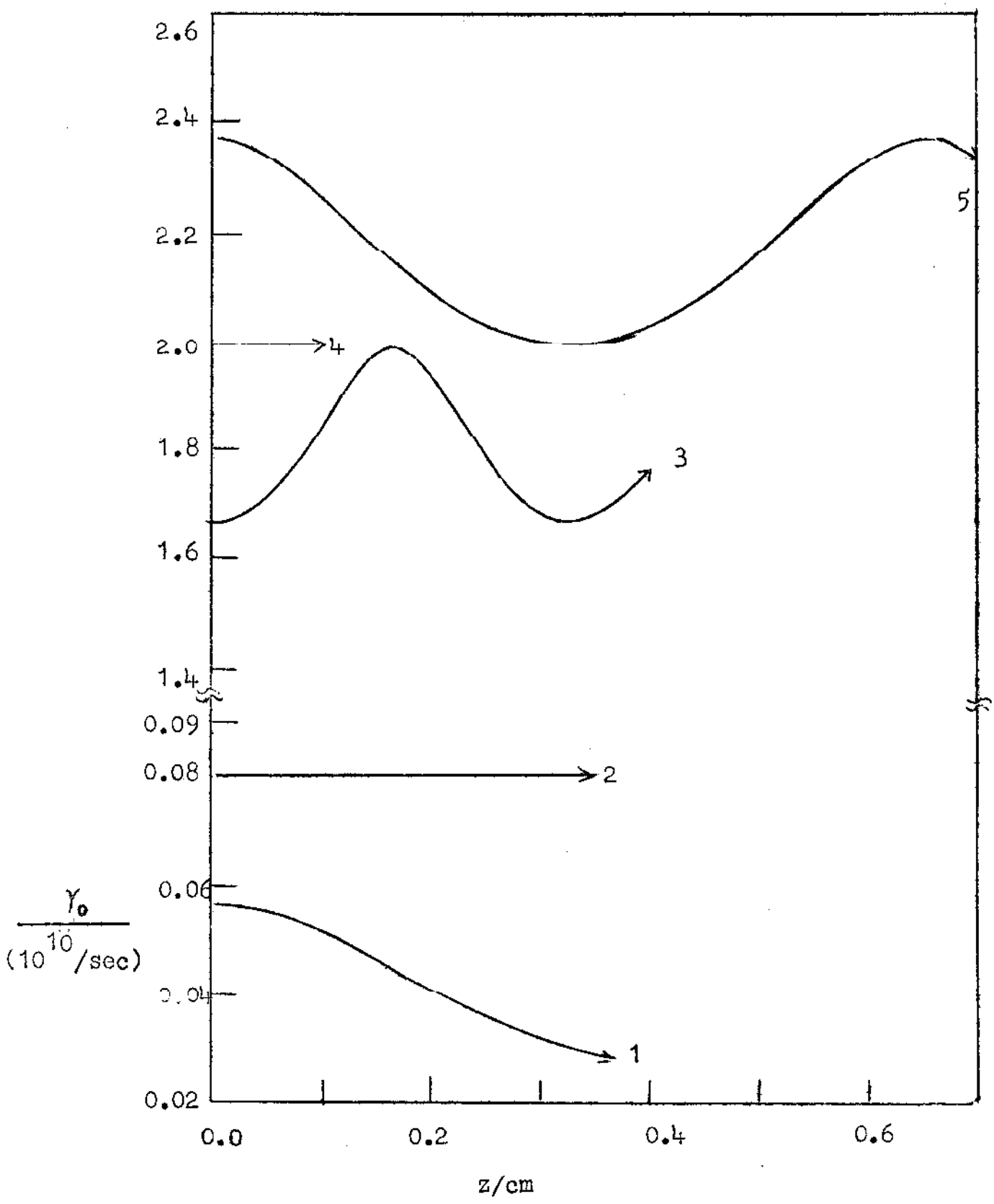
2.6
2.4
2.2
2.0
1.8
1.6
1.4
0.09
0.08
0.06
0.04
0.02
0.0
0.2
0.4
0.6
z/cm
$\frac{\gamma_0}{(10^{10}/\text{sec})}$
1
2
3
4
5

Fig. 3.4

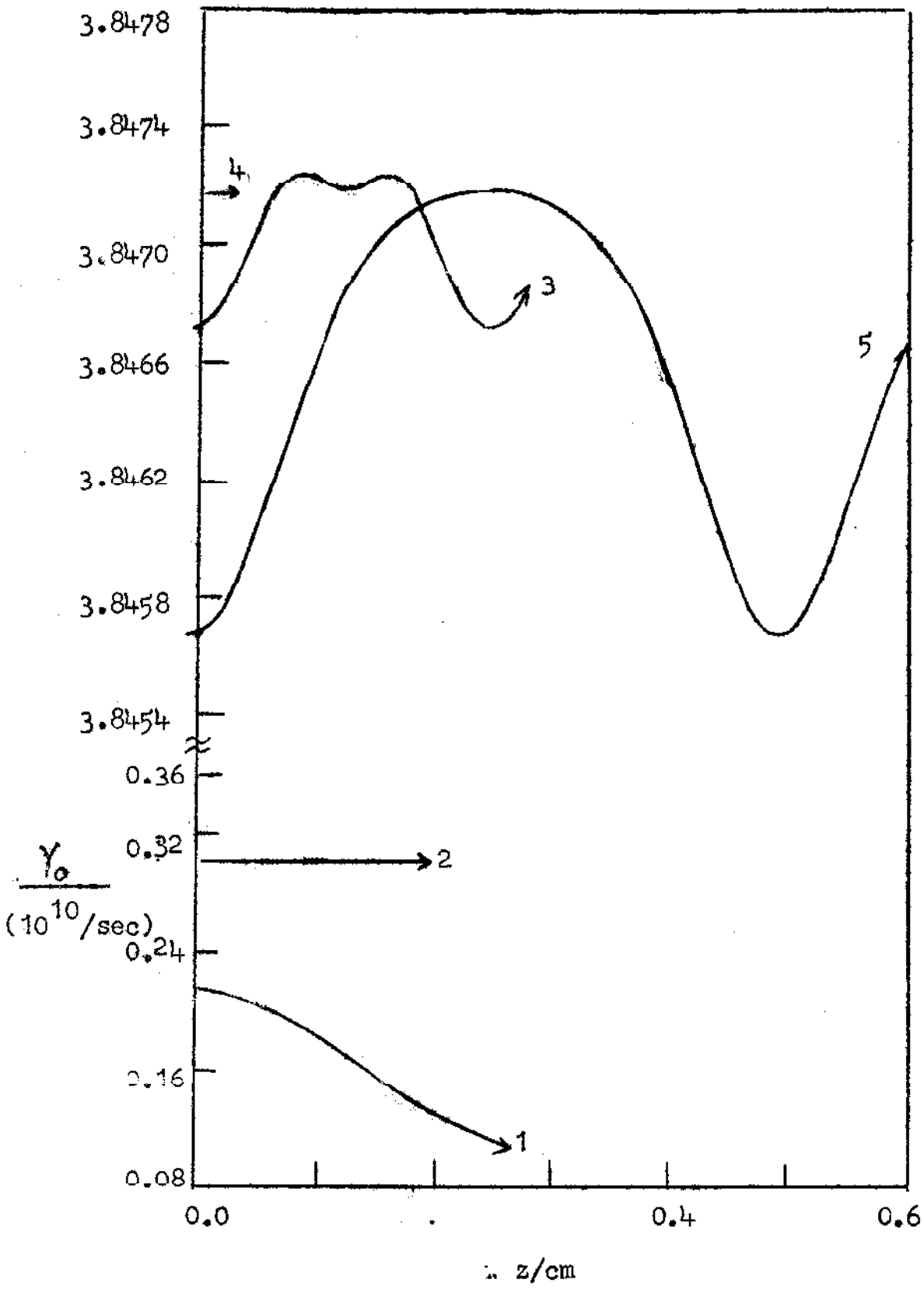
3.8478
3.8474
3.8470
3.8466
3.8462
3.8458
3.8454
0.36
0.32
0.24
0.16
0.08
$\frac{Y_o}{(10^{10}/sec)}$
0.0
0.4
0.6
z/cm
1
2
3
4
5

Fig. 3.5

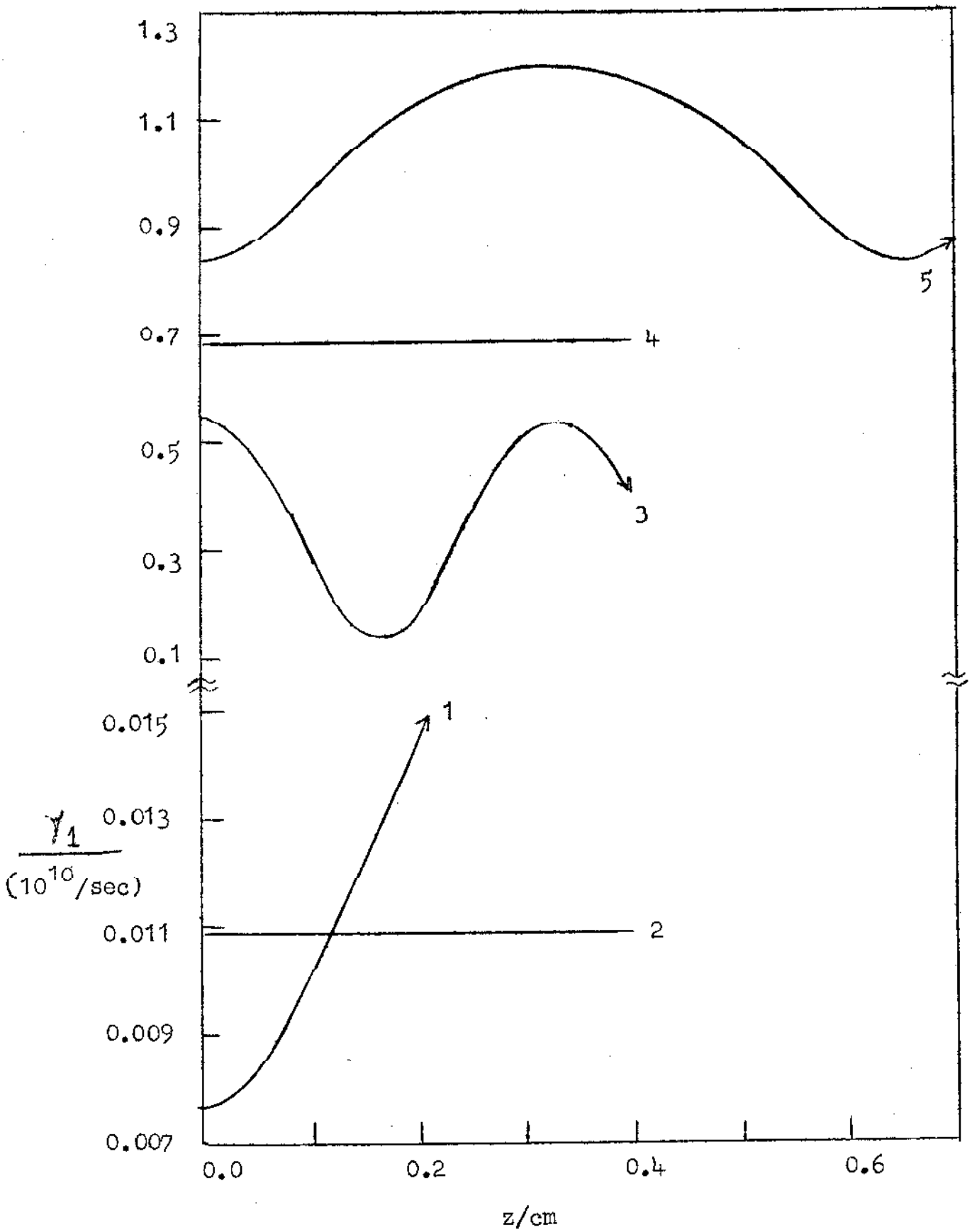
1.3
1.1
0.9
0.7
0.5
0.3
0.1
0.015
0.013
0.011
0.009
0.007
γ_1
$(10^{10}/sec)$
1
2
3
4
5
0.0
0.2
0.4
0.6
z/cm

Fig. 3.6

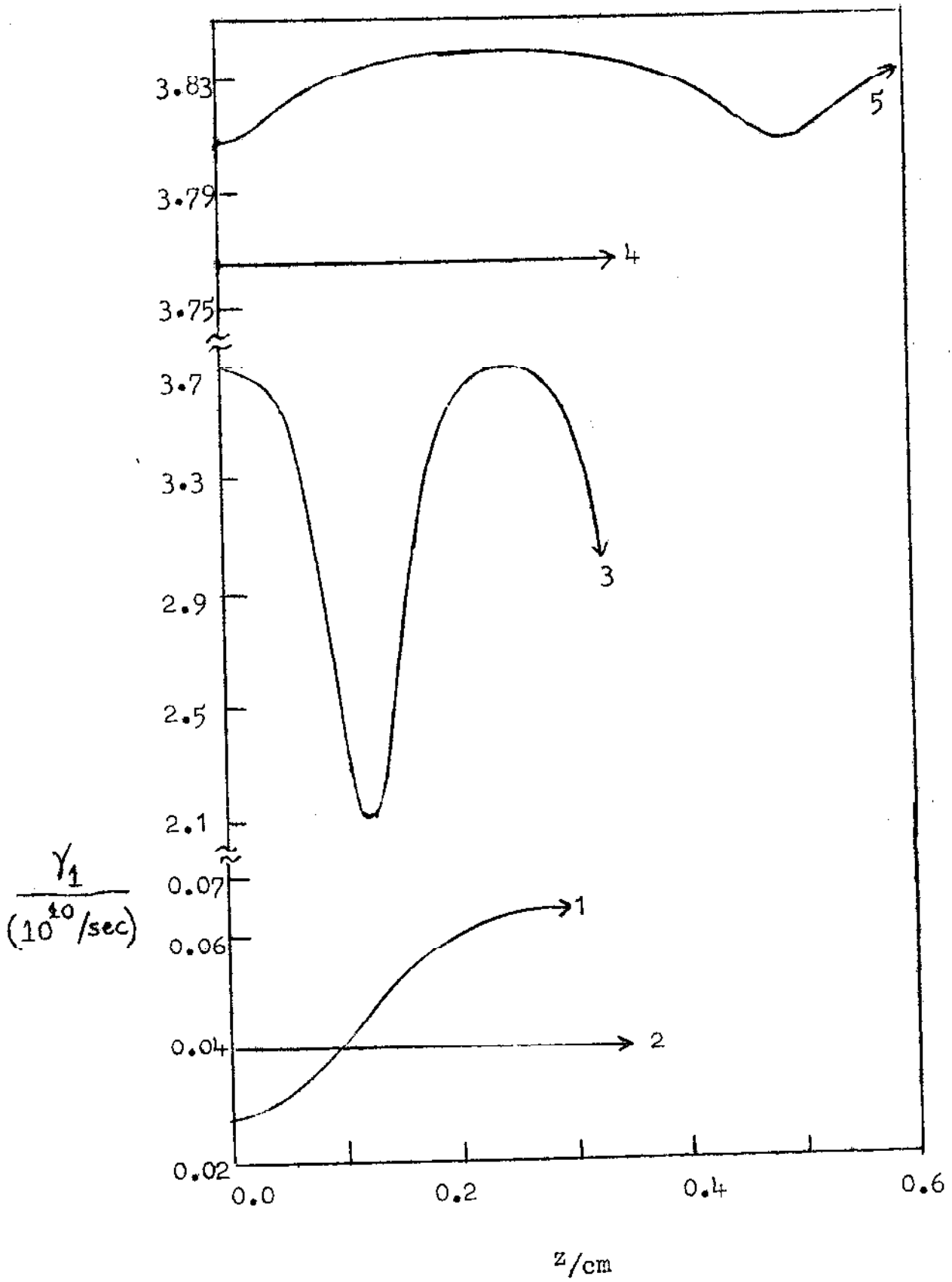
3.83
3.79
3.75
3.7
3.3
2.9
2.5
2.1
0.07
0.06
0.04
0.02
0.0
0.2
0.4
0.6
1
2
3
4
5
$\frac{\gamma_1}{(10^{10}/\text{sec})}$
z/cm

Fig. 3.7

CHAPTER 4

ION ACOUSTIC SOLITONS IN AN ELECTROMAGNETICALLY IRRADIATED MAGNETOPLASMA

This chapter presents an analysis of the influence of an electromagnetic beam and an axial static magnetic field on the ion acoustic solitons in a plasma. The analysis is based primarily on Zakharov and Kuznetsov's[107] investigation on the magnetically induced shape-distortion of an ion acoustic soliton and on Kaw and Nishikawa's[108] investigation on the interaction of an ion acoustic soliton with an electromagnetic beam. In Sec.4.1, an equation for the ion velocity has been derived. In Sec.4.2, the equation has been solved in the small velocity case[108] to obtain the solution representing a propagating filamentary electromagnetic beam. In Sec.4.3, the equation for the ion velocity has been reduced to a modified KdV equation by assuming that the ion motion is confined to some specific direction. In Sec.4.4, the modified KdV equation has been solved in the perturbation approximation and assuming the static magnetic field and electromagnetic field to be weak. In Sec.4.5, a particular case has been considered in which the electromagnetic beam is radially Gaussian and undergoes self focusing[1-5] on account of the ponderomotive force[3,4] on electrons. In Sec.4.6, numerical results along with a discussion have been presented.

It is inferred from the present chapter that the presence of a static magnetic field changes[107] the transverse shape of the solitons. A homogeneous electromagnetic beam does not destabilize the solitons; it reduces the amplitude, but not the velocity, of the solitons. However, any inhomogeneity in the electromagnetic field intensity does destabilize the ion acoustic solitons; albeit not to an appreciable extent for typical cases. The present analysis explains the observed[109,110] reduction in the amplitude of ion acoustic solitons in the presence of RF fields, but it does not explain the observed[109,110] reduction in the width and velocity of the solitons. To interpret the experimental observations completely, it would be necessary to solve the modified KdV equation without the perturbation approach employed in the present chapter.

4.1: Basic Equations

The electric field $\vec{E}(\vec{r}, t)$ of an electromagnetic beam propagating in a plasma obeys the wave equation[3,4]

$$\left(\frac{\partial^2}{\partial t^2} - c^2\nabla^2 + \omega_p^2\right)\vec{E} = 0 \,. \qquad (4.1)$$

Here the square of the local plasma frequency is written as

$$\omega_p^2(\vec{r},t) = 4\pi n_e(\vec{r},t)\, e^2/m = \omega_{po}^2\, n_e(\vec{r},t)/n_o$$

$$= \omega_{po}^2\left(1+\delta n_e(\vec{r},t)/n_o\right) = \omega_{po}^2 + \delta\omega_p^2(\vec{r},t), \tag{4.2}$$

where n_o is the equilibrium electron concentration and $n_e(\vec{r}, t)$ is the perturbed electron concentration. The solution of Eq. 4.1 may be expressed as

$$\vec{E}(\vec{r},t) = \hat{x}\,\mathcal{E}(\vec{r},t)\exp\left(ikz - i\omega t + i\theta(\vec{r},t)\right), \tag{4.3}$$

where the field envelope $\mathcal{E}(\vec{r}, t)$ and the phase $\theta(\vec{r}, t)$ are real quantities and obey the coupled equations

$$\left[\frac{\partial^2}{\partial t^2} - c^2\nabla^2 + 2\omega\left(\frac{\partial\theta}{\partial t}\right) + 2c^2k\left(\frac{\partial\theta}{\partial z}\right) - \left(\frac{\partial\theta}{\partial t}\right)^2 + c^2(\nabla\theta)^2 + \delta\omega_p^2\right]\mathcal{E} = 0, \tag{4.4}$$

$$\left[\left(\frac{\partial^2\theta}{\partial t^2}\right) - c^2(\nabla^2\theta) - 2\left\{\omega\frac{\partial}{\partial t} + c^2k\frac{\partial}{\partial z} - \left(\frac{\partial\theta}{\partial t}\right)\frac{\partial}{\partial t} + c^2(\nabla\theta)\cdot\nabla\right\}\right]\mathcal{E} = 0\ ; \tag{4.5}$$

the linear wavenumber is defined as

$$k = \left(\omega^2 - \omega_{po}^2\right)^{1/2}/c\ . \tag{4.6}$$

The slowly varying electric field due to the beam and ion acoustic solitons will be represented[96] as usual by $(-\nabla\varphi)$. On neglecting the electron inertia and

assuming the isothermal equation of state (i.e. $P_e = n_e K_B T_e$), the force equation in the quasi-steady state gives[108]

$$e\nabla\varphi - K_B T_e \nabla(\ln n_e) - (e^2/2m\omega^2)\nabla\mathcal{E}^2 = 0 . \qquad (4.7)$$

Here, the pressure of the static magnetic field $H_o \hat{z}$ has been neglected under the assumption that $\omega_c \ll \omega$, where $\omega_c = |e|H_o/mc$ is the electron cyclotron frequency. Equation 4.7 yields the Boltzmann distribution[108]

$$n_e = n_o \exp\left(e\varphi/K_B T_e - \mathcal{E}^2 e^2/2m\omega^2 K_B T_e\right). \qquad (4.8)$$

(Deviation from the assumed isothermality of the electrons will introduce half integral[103] powers of φ in the power series expansion of n_e.). Poisson's equation then becomes

$$\nabla^2\varphi = 4\pi n_e\left\{n_o \exp\left[e\varphi/K_B T_e - \mathcal{E}^2 e^2/2m\omega^2 K_B T_e - n\right]\right\}, \qquad (4.9)$$

where $n(\vec{r}, t)$ is the ion-concentration at $(\vec{r}, t)$. The continuity, momentum and pressure equations for ions are[103]

$$\frac{\partial n}{\partial t} + \nabla\cdot(n\vec{V}) = 0 , \qquad (4.10)$$

$$\frac{\partial\vec{V}}{\partial t} + (\vec{V}\cdot\nabla)\vec{V} = -\frac{e}{M}\nabla\varphi + \vec{V}\times\vec{\omega}_H - \frac{T}{nT_{ef}}\nabla p , \qquad (4.11)$$

and

$$\frac{\partial p}{\partial t} + (\vec{v}\cdot\nabla)p + \gamma p\,\nabla\cdot\vec{v} = 0 \quad . \qquad (4.12)$$

Here $\vec{v}(\vec{r}, t)$, M, $\vec{\omega}_H = \hat{z}H_o\,(e)/Mc$, T and $p(\vec{r}, t)$ are the velocity, mass, cyclotron frequency, temperature and pressure of the ions respectively. In the present case of isothermal electrons, the free electron temperature T_{ef} is the same as T_e. In Eq.4.12, $\gamma = p/nK_BT = 3$ for adiabatic ion motion.

For long wavelength [$\lambda \gg$ Debye length $\lambda_D = (K_BT_e / 4\pi n_o e^2)^{1/2}$] and weak nonlinearity ($\delta n_e \ll n_o$), Eq. 4.9 yields

$$\frac{e\varphi}{K_BT_e} \simeq (1+\lambda_D^2\nabla^2)\left[\frac{\varepsilon^2e^2}{2m\omega^2K_BT_e} + \frac{\delta n_e}{n_o} - \frac{1}{2}\left(\frac{\delta n_e}{n_o}\right)^2\right] . \qquad (4.13)$$

The ion fluid will be assumed to be cold[96] so that $\nabla p = 0$ and Eq. 4.12 is not required. Eliminating φ from Eq.4.11 by using Eq. 4.13, the following equation is obtained for the ion velocity.

$$\frac{\partial\vec{v}}{\partial t} + \nabla\left\{(1+\lambda_D^2\nabla^2)\left[\frac{\varepsilon^2e^2}{2Mm\omega^2} + \frac{K_BT_e}{M}\frac{\delta n_e}{n_o} - \frac{K_BT_e}{2M}\left(\frac{\delta n_e}{n_o}\right)^2\right] - \frac{v_a^2}{2}\right\} = \vec{v}\times\vec{\omega}_H \quad . \qquad (4.14)$$

Note that this equation does not have a 'divergence form'[107]. It therefore implies that the ion momentum is, in general,

not conserved. Consequently, unlike in the case of absence of a static magnetic field, a soliton solution can exist only if the ion motion is confined to some particular direction[107]. Also note that Eq.4.14 is coupled with Eqs. 4.10, 4.4 and 4.5. It is necessary to get rid of this coupling between the equations, in order to make the problem solvable.

4.2: Small Velocity Case

It is instructive to consider first a particular case investigated by Kaw and Nishikawa[108]. Let $H_o=0$. When the density perturbations are small (i.e. $n_e \simeq n_o$) and the field envelope $\mathcal{E}$ does not vary appreciably with time, the electron density perturbations $\delta n_e(\vec{r},t)$ follow the equation

$$\left[\partial^2/\partial t^2 - (K_B T_e/M)\nabla^2\right] \delta n_e \simeq (K_B T_e/M)\nabla^2 \mathcal{E}^2 . \qquad (4.15)$$

This equation describes an ion wave propagating in a direction depending upon the ponderomotive force due to the electromagnetic beam. Solutions corresponding to the solitons propagating with a constant velocity $\vec{U}$ (with $U \ll c$) are obtained by introducing a new variable[108]

$$\vec{R} = \vec{r} - \vec{U}t \quad . \qquad (4.16)$$

Equation 4.15 then gives

$$\delta n_e = -\varepsilon^2/(1-U^2M/K_B T_e), \qquad (4.17)$$

and Eq.4.5, to the first order approximation, yields

$$\theta = \omega \vec{R}\cdot\vec{U}/(c^2-U^2). \qquad (4.18)$$

Substituting the expressions 4.17 and 4.18, Eq. 4.4 gives

$$\left\{\nabla^2 - \left(\frac{2\omega Uk - 2\omega^2U^2/c^2}{c^2-U^2}\right) + \frac{\omega_{po}^2\varepsilon^2}{n_0(1-U^2M/K_BT_e)(c^2-U^2)}\right\}\varepsilon = 0. \qquad (4.19)$$

Equation 4.19 is a type of nonlinear Schrödinger equation[11-15]. Consider only the one dimensional version of it, and put

$$\nabla^2 = \frac{\partial^2}{\partial y^2}, \quad \vec{U} = \hat{y}U \quad \text{and} \quad \vec{R} = \hat{y}Y = \hat{y}(y-Ut). \qquad (4.20)$$

Then the solution of Eq.4.19, under the boundary condition that the solution and its first derivative vanish at $R \to \pm\infty$, may be written as

$$\varepsilon = \left[2(2\omega Uk - 2\omega^2U^2/c^2)(1-U^2M/K_BT_e)(n_0/\omega_{po}^2)\right]^{1/2} \cdot \operatorname{sech}\left[\left(\frac{2\omega Uk - 2\omega^2U^2/c^2}{c^2-U^2}\right)^{1/2} Y\right]. \qquad (4.21)$$

This solution represents a propagating filamentary electromagnetic beam[108].

4.3: Modified KdV Equation

In order to simplify Eq.4.14, it will be assumed that the waves described by this equation travel only in some specific direction, say $\hat{\ell}$. This arbitrary direction $\hat{\ell}$ may be the direction of the static magnetic field[107] or the y axis[108] depending upon whether $H_0^2 \gg \mathcal{E}^2$ or $H_0^2 \ll \mathcal{E}^2$. It will be moreover assumed that the electric field intensity $\mathcal{E}^2$ is already known so that it need not be derived along with Eq.4.14, and that $\lambda_D^2 \nabla^2 \mathcal{E}^2 \ll \mathcal{E}^2$. Following the arguments given by Zakharov and Kuznetsov[107], it can be shown that

$$\frac{\partial V_\ell}{\partial t} + c_s \frac{\partial}{\partial \ell} \left\{ \frac{V_\ell^2}{2c_s} + \left[1 + \frac{\lambda_D^2}{2} \frac{\partial^2}{\partial \ell^2} + \frac{\lambda_H^2 + \lambda_D^2}{2} \nabla_{\perp \ell}^2 \right] V_\ell + \frac{\mathcal{E}^2 e^2 c_s}{2 m \omega^2 k_B T_e} \right\} = 0 , \qquad (4.22)$$

where the ion speed $c_s \equiv (k_B T_e / M)^{1/2}$ and

$$\lambda_H = \hat{\ell} \cdot \hat{H}_0 \, c_s / \omega_H . \qquad (4.23)$$

The analysis is greatly simplied by employing the following dimensionless variables[96] which form a coordinate

system moving with velocity $c_s \hat{l}$.

$$\xi = \frac{l - c_s t}{\lambda_D} \quad , \quad \vec{\xi}_\perp = \frac{\vec{r} - \vec{r}\cdot\hat{l}}{(\lambda_H^2 + \lambda_D^2)^{1/2}} \quad ,$$

$$\tau = \frac{t\,\omega_{pi}}{2} = t(\pi n_0 e^2/M)^{1/2} \quad , \quad u = \frac{V_l}{2c_s}$$

and $$\gamma^2 = \frac{e^2\mathcal{E}^2}{4m\omega^2 k_B T_e} \quad . \qquad (4.24)$$

Then Eq. 4.22 can be written in the dimensionless form

$$\frac{\partial u}{\partial \tau} + \frac{\partial}{\partial \xi}\left(u^2 + \nabla_\xi^2 u + \gamma^2\right) = 0 \quad . \qquad (4.25)$$

4.4: Perturbation Analysis

No analytical solution of Eq. 4.25 exists. However, the KdV equation[96]

$$\frac{\partial W}{\partial \tau} + \frac{\partial}{\partial \xi}\left(W^2 + \frac{\partial^2 W}{\partial \xi^2}\right) = 0 \qquad (4.26)$$

does have an analytical solution: the soliton solution[1-5,96]

$$W = (3\mu/2)\,\mathrm{sech}^2\left[\chi \mu^{1/2}/2\right] , \qquad (4.27)$$

where $\chi \equiv (\xi - \mu\tau)$ and μ is a parameter determining the amplitude, velocity and width of the soliton. It may be assumed that it is possible to transform Eq. 4.25 into Eq. 4.26. This is possible if (but not only if) the

following conditions are satisfied:

$$\frac{\partial W}{\partial \tau} = \frac{\partial u}{\partial t} \quad , \tag{4.28}$$

$$W = u + \Psi \quad , \tag{4.29}$$

and

$$\Psi^2 + 2u\Psi + \frac{\partial^2 \Psi}{\partial \xi^2} = \nabla_{\perp \xi}^2 u + \gamma^2 \, . \tag{4.30}$$

In the first order approximation, it will be assumed that $\partial^2\Psi/\partial\xi^2 = \nabla_{\perp\xi}^2 u = 0$, so that Eq. 4.30 in conjunction with Eqs. 4.28 and 4.29, gives

$$W = U_1 + \Psi_1 = (U_1^2 + \gamma^2)^{1/2} \quad , \tag{4.31}$$

so that

$$U_1 = (W^2 - \gamma^2)^{1/2} \, . \tag{4.32}$$

The electromagnetic field intensity will be assumed to be so small that $\gamma^2 \ll U_1^2$. Then

$$\Psi_1 \simeq \gamma^2 / 2W \, . \tag{4.33}$$

In the second order approximation, Eq. 4.30 will be written as

$$\Psi_2^2 + 2U_2\Psi_2 = \Gamma^2 \quad , \tag{4.34}$$

where

$$\Gamma^2 = \gamma^2 + \nabla_{\perp\xi}^2 U_1 - \frac{\partial^2 \Psi_1}{\partial \xi^2}$$

$$\simeq \gamma^2 + \nabla_{\perp\xi}^2 (W^2 - \gamma^2)^{1/2} - \frac{\partial^2 \gamma^2}{\partial \xi^2} / 2W . \quad (4.35)$$

Equation 4.34 yields

$$U_2 = (W^2 - \Gamma^2)^{1/2} . \quad (4.36)$$

4.5: Self Focusing

In the presence of an inhomogeneous electromagnetic beam, the electrons of the plasma experience a ponderomotive force[24-28] and a beam with radially decreasing intensity thereby gets self focused[1-5] as already discussed in the previous chapters on laser self focusing. The radial intensity profile of the beam will be considered to be Gaussian, and only the ponderomotive force will be considered as the nonlinear mechanism leading to the self focusing. The nonlinear saturation[3,4,28] of the dielectric constant will be neglected. It can then be shown that γ^2 may be expressed in the form

$$\gamma^2 = \gamma_0^2 \exp(-\rho^2/f^2) , \quad (4.37)$$

where $\rho \equiv (x^2+y^2)^{1/2} / r_o$, r_o = mean beamwidth at z=0, and the beamwidth parameter f(z) (for $\rho \ll 1$ and $z < z_f$) is given by

$$f^2 \simeq 1 - z^2/z_f^2 , \qquad (4.38)$$

$$z_f^2 = r_o^2 (\omega^2 - \omega_{po}^2)/(\omega_{po}^2 \gamma_o^2/2 - c^2/r_o^2) . \qquad (4.39)$$

The ion acoustic waves will be assumed to be travelling in the direction of propagation of the electromagnetic beam, i.e. $\hat{\ell} = \hat{z}$. The static magnetic field $\vec{H}_o$ will be considered to be longitudinal, i.e. $\vec{H}_o = \hat{z}H_o$, so that

$$\lambda_H^2 - c_s^2/\omega_H^2 = c^2 M \kappa_B T_e / e^2 H_o^2 . \qquad (4.40)$$

Hence

$$\nabla_{\perp\xi}^2 (W^2-\gamma^2)^{1/2} = \frac{(\lambda_H^2+\lambda_D^2)}{r_o^2 \rho} \frac{\partial}{\partial \rho} \rho \frac{\partial}{\partial \rho} (W^2-\gamma^2)^{1/2}$$

$$= \frac{(\lambda_H^2+\lambda_D^2)\gamma^2}{r_o^2 f^2 (W^2-\gamma^2)^{1/2}} \left[2 - \frac{2\rho^2}{f^2} - \frac{\rho^2\gamma^2}{f^2(W^2-\gamma^2)} \right] , \qquad (4.41)$$

and

$$\frac{\partial^2 \gamma^2}{\partial \xi^2} = \lambda_D^2 \frac{\partial^2 \gamma^2}{\partial z^2} - \frac{2\lambda_D^2 \gamma^2 \rho^2}{z_f^2 f^4}\left[\left(\frac{\rho^2}{f^2} - 2\right)\frac{2z^2}{f^2 z_f^2} - 1\right] . \tag{4.42}$$

4.6: Results and Discussion

In the perturbation analysis, the magnetically induced transverse inhomogeneity of the ion acoustic solitons has been neglected in the absence of the electromagnetic field. This type of inhomogeneity was earlier studied by Zakharov and Kuznetsov[107] and was shown not to destabilize the ion acoustic solitons. The present treatment is valid for the static magnetic field small enough to allow the approximation $\nabla_{\perp\xi}^2 U_{(\gamma=0)} = 0$. Given this, it is seen from Eq. 4.32 that the presence of a homogeneous electromagnetic field does not destablize the ion acoustic solitons; it reduces the amplitude, but not the velocity, of the solitons. On the other hand, any inhomogeneity in the electromagnetic field intensity destabilizes the ion acoustic solitons; the ion acoustic waves are in the strictest sense no longer solitary waves, since they now depend not only on $\chi = (\xi - u\tau)$ but also on ξ separately. A positive spatial gradient in the electromagnetic field enhances the amplitude of the ion acoustic solitons.

In order to illustrate the above analytical results, the graphs of U_2 have been plotted in Figs. 4.1-4.3 for

the following parameters:

$n_o = 10^{17}\ cm^{-3}$,

$T_e = 10^4\ ^oK$,

$H_o = 100$ Gauss,

$M/m = 2000$,

$\mu = 0.3$,

$\mathcal{E}_o^2 = 10^4\ erg/cm^3$,

$r_o = 5$ cm,

$\omega = 10^{13}$ rad/sec.

Figures 4.1 - 4.3 give U_2 versus X, Z and ζ respectively. These graphs, as expected, indicate that U_2 falls off at the focal point and increases with the radial distance. For the typical parameters chosen, it is seen, however, that in most of the regions, the solitons are not perturbed appreciably and hence the destablization is not significant. This implies the inherent stability of the solitons against external perturbations[93,94].

Figures 4.1 - 4.3

Fig.4.1 U_2 versus X = ($\xi - \mu\tau$).
ς = 1 for (A) & 0 for (B & C).
z/r_o = 0 for (A & B) & 2.8 for (C).

Fig.4.2 U_2 versus z/r_o.
ς = 1 for (A & C) and 0 for (B & D & E).
X = 0 for (A & B) & 1 for (C & D) & 2 for (E).

Fig.4.3 U_2 versus ς .
z/r_o = 0 for (A & C & D & F) & 2.8 for (B & E).
X = 0 for (A & B) & 1 for (C) & 2 for (D & E) & 4 for (F).

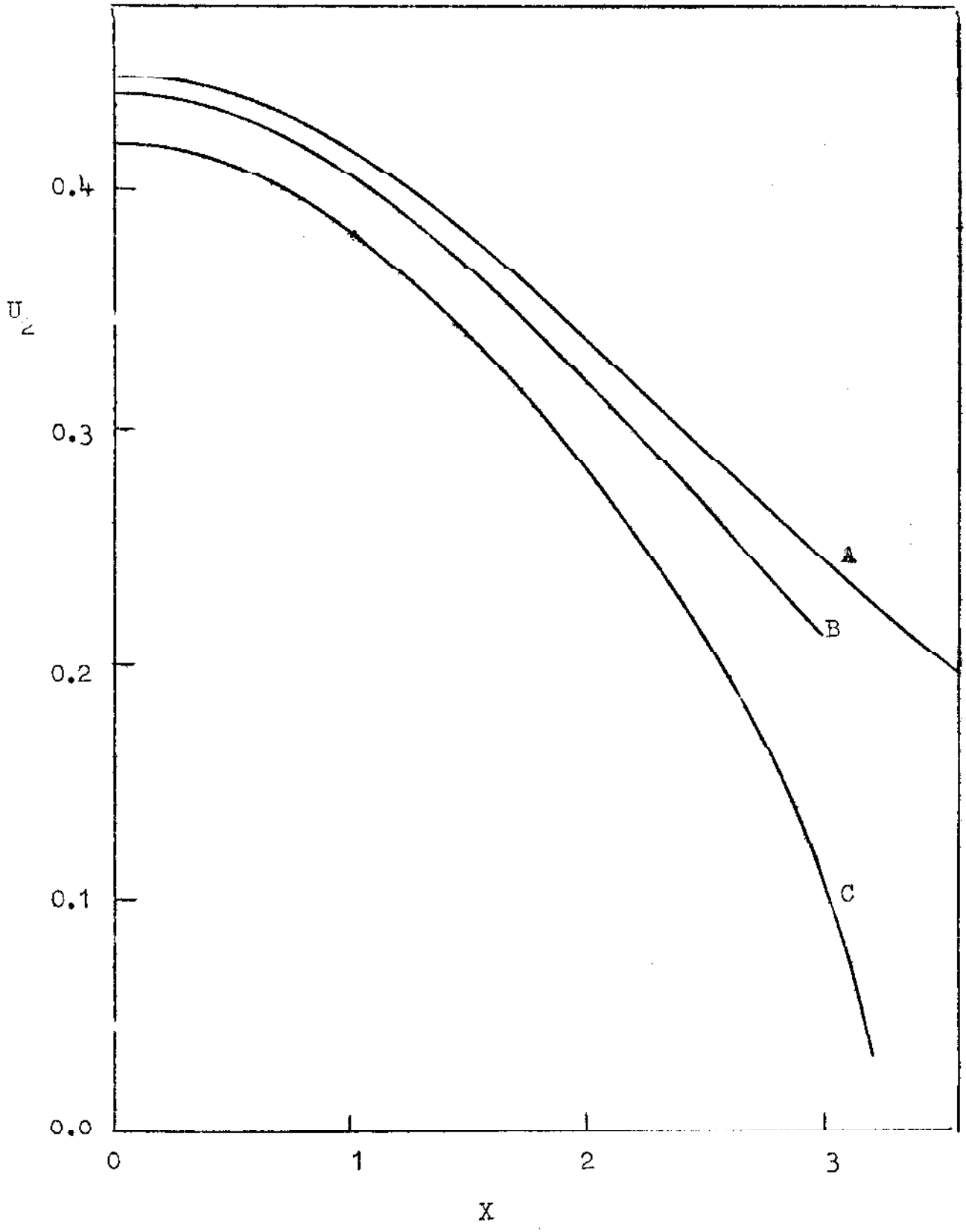

Fig. 4.1

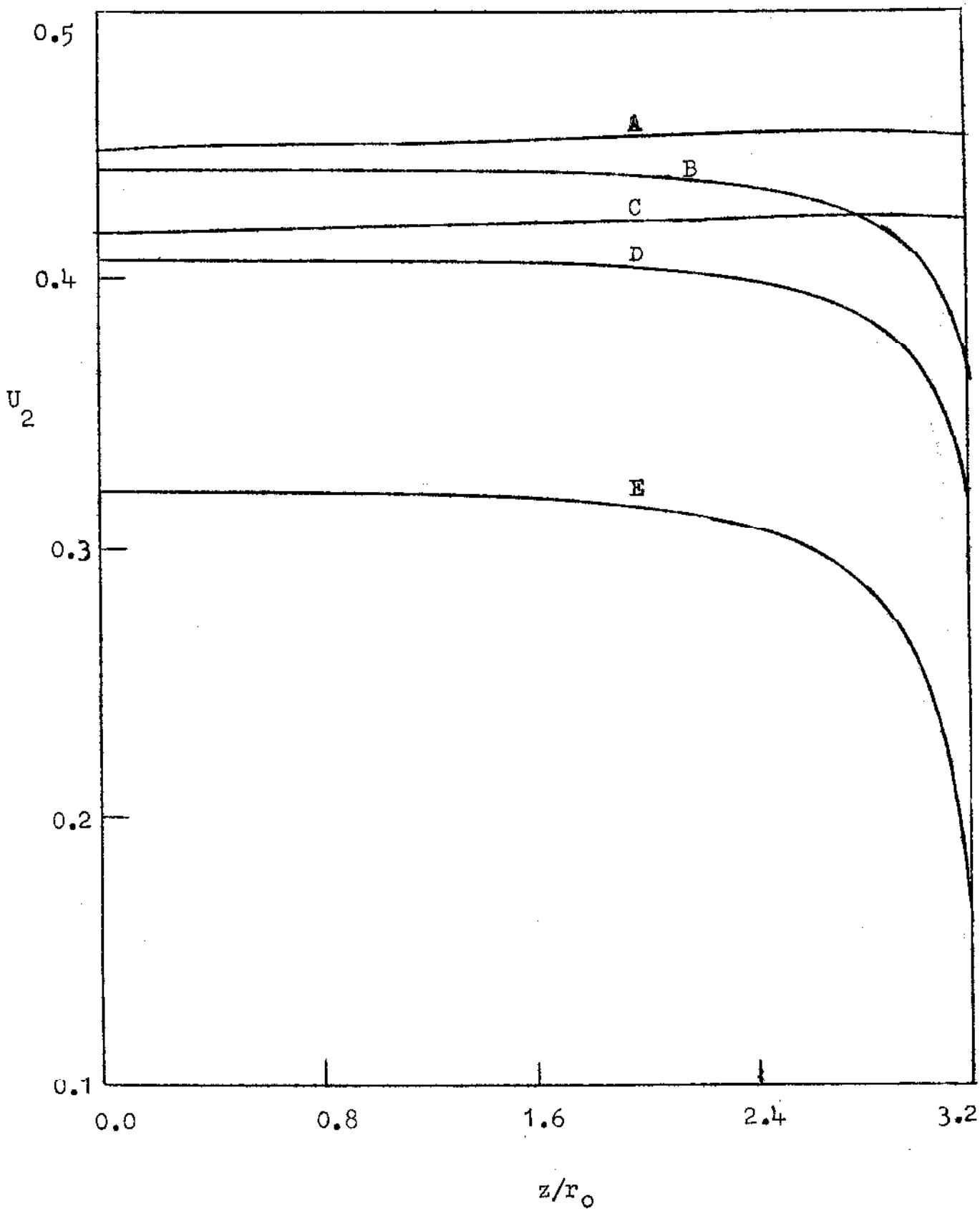

Fig. 4.2

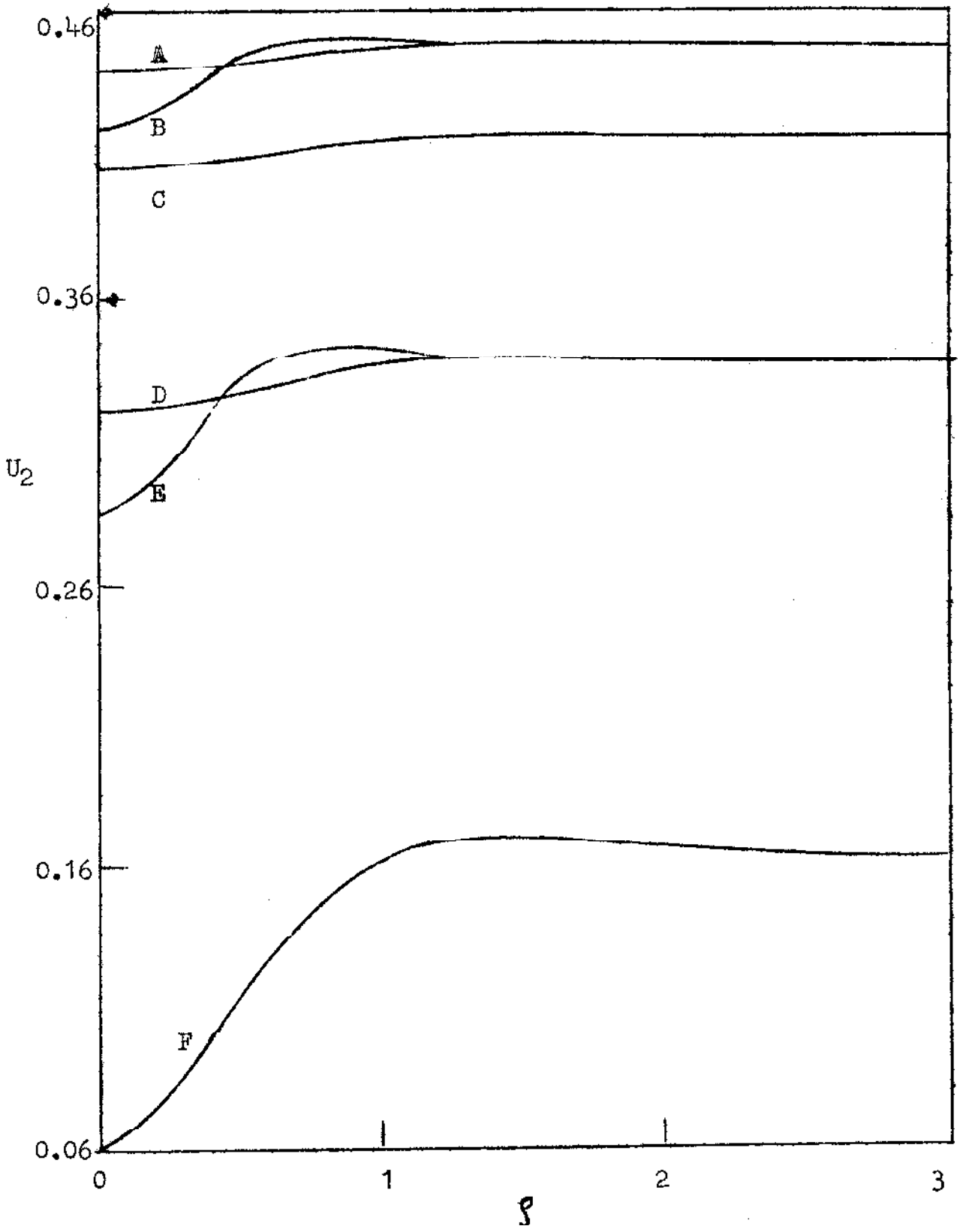

Fig. 4.3

BIBLIOGRAPHY

1. S.A.Akhmanov, R.V.Khokhlov & A.P.Sukhorukov: Laser Handbook Vol.2, eds. F.T.Arecchi & E.O. Schulz-DuBois, North Holland (1972) 1151.

2. O.Svelto: Progress in Optics Vol.12, ed. E.Wolf, North Holland (1974) 1.

3. M.S.Sodha, A.K.Ghatak & V.K.Tripathi: Self Focusing of Laser Beams in Dielectrics, Plasmas and Semiconductors, Tata McGraw Hill (1974).

4. M.S.Sodha, A.K.Ghatak & V.K.Tripathi: Progress in Optics Vol.13, ed. E.Wolf, North Holland (1976)169.

5. Y.R.Shen: Prog. Quant. Electronics 4 (1975) 1.

6. K.Nishikawa & C.S.Liu: Advances in Plasma Physics Vol.6, eds. A.Simon & W.B.Thompson, John-Wiley (1976) 3.

7. J.M.Dawson & A.T.Lin: Univ. of California Los Angeles Report No.PPG-191 (1974).

8. S.Jorna: Phys.Fluids 17 (1974) 765.

9. M.Porkolab: Physica 82C (1976) 86.

10. R.N.Franklin: Rep.Prog.Phys. 40 (1977) 1369.

11. N.J.Zabusky & M.D.Kruskal: Topics in Nonlinear Mathematics, ed. M.D.Kruskal, Springer-Verlag (1968).

12. A.E.Scott, F.Y.F.Chu & D.W. McLaughlin: Proc. IEEE 61 (1973) 1443.

13. V.I.Karpman: Nonlinear Waves in Dispersive Media, Pergamon (1975).

14. A.Hasegawa: Plasma Instabilities and Nonlinear Effects, Springer-Verlag (1975).

15. V.G.Makhankov: Phys.Reports 35 (1978) 1.

16. N.J.Zabusky ed.: Topics in Nonlinear Physics, Springer-Verlag (1968).

17. Y.R.Shen: Rev.Mod.Phys. 48 (1976) 1.

18. A.I.Akhiezer, I.A.Akhiezer, R.V.Polovin, A.G.Sitenko & K.N.Stepanov: Plasma Electrodynamics Vol.2 Nonlinear Theory and Fluctuations, Pergamon (1975).

19. H.Hora: Laser Plasmas and Nuclear Energy, Plenum (1975).

20. D.J.Thome & F.W.Perkins: Phys.Rev.. Lett. 32 (1974) 1234.

21. J.F.Drake & Y.C.Lee: Phys.Fluids 19 (1976) 1772.

22. E.O.Kane: Laser Interaction and Related Plasma Phenomena Vol.4, eds. H.J.Schwarz & H. Hora, Plenum (1977).

23. K.H. Spatschek: J.Plasma Phys. 18 (1977)293.

24. H.Hora: Phys.Fluids 12 (1969) 182.

25. J.D.Lindl & P.K.Kaw: Phys.Fluids 14 (1971) 371.

26. P.Kaw, G.Schmidt & T.Wilcox: Phys.Fluids 16 (1973) 1522.

27. L.C.Johnson & T.K.Chu: Phys.Rev.Lett. 32 (1974) 517.

28. C.E.Max: Phys.Fluids 19 (1976) 74.

29. G.A.Askaryan & V.A.Pagosyan: (Sov.Phys.JETP ZHETF 60 (1971) 1295.

30. M.S.Sodha, S.Prasad & V.K.Tripathi: App.Phys. 3 (1974) 213.

31. B.G.Eremin, A.G.Litvak & B.K.Poluyakhtov: Izv. Vuz. Radiofiz. 15 (1972) 1132.

32. M.S.Sodha, R.K.Khanna & V.K.Tripathi: Opto Electronics 5 (1973) 533.

33. M.S.Sodha, R.K.Khanna & V.K.Tripathi: J.Phys.D. App.Phys. 7 (1974) 2188.

34. M.S.Sodha, S.C.Kaushik & A.Kumar: App.Phys. 7 (1975) 187.

35. N.M.Tomlijanovich: Phys.Fluids 18 (1975) 741.

36. V.N.Lugovoi & A.M.Prokhorov: Sov.Phys.Uspekhi 16 (1974) 658.

37. V.N.Lugovoi: Sov.Phys.JETP 38 (1974) 439.

38. J.F.Lam, B.Lippmann & F.Tappert: Phys.Fluids 20 (1977) 1976.

39. D.Subbarao: Private communications.

40. M.S.Sodha & V.K.Tripathi: Laser Interaction and Related Plasma Phenomena Vol.4, eds. H.J.Schwarz & H.Hora, Plenum (1977).

41. M.S.Sodha & V.K.Tripathi: Phys.Rev. A16 (1977) 2101.

42. A.J.Alcock: Laser Interaction and Related Plasma Phenomena Vol.1, eds. H.J.Schwarz & H.Hora, Plenum (1971) 155.

43. B.G.Eremin & A.G.Litvak: Sov.Phys.JETP-PR 13 (1971) 430.

44. C.Yamanaka, T.Yamanaka, J.Mizui & N.Yamaguchi: Phys.Rev.A 11 (1975) 2138.

45. V.A.Isaev , V.N.Kruglov, V.A.Mirnov & B.K.Poluyakhtov: Fiz.Plasmy 3 (1977) 607.

46. S.C.Kaushik & R.Sen: J.Phys.D. App.Phys. 8 (1975) 1975.

47. M.S.Sodha, S.C.Kaushik, R.P.Sharma & V.K.Tripathi: Optica Acta 23 (1976) 321.

48. M.D.Feit & J.A.Fleck Jr.: App.Phys.Lett. 28 (1976) 121.

49. M.D.Feit & J.A.Fleck Jr.: App.Phys.Lett. 29 (1976) 234.

50. V.L.Ginzburg: The Propagation of Electromagnetic Waves in Plasmas, Pergamon (1970).

51. A.I.Akhiezer, I.A.Akhiezer, R.V.Polovin, A.G.Sitenko & K.N.Stepanov: Plasma Electrodynamics Vol.1 Linear Theory, Pergamon (1975).

52. V.A.Isaev, V.N.Kruglov & B.K.Poluyakhtov: Sov.Phys. JETP 44 (1976) 532.

53. H.L.Rutkowski: Experimental Study of a Laser Heated Solenoid (Ph.D. Diss.) Uni. of Washington (1975).

54. J.M.Chapman: Propagation of a Trapped Laser Beam in a Plasma Column (Ph.D. Diss.) Uni. of Washington (1977).

55. R.L.Stenzel: Phys.Rev.Lett. 35 (1975) 574.

56. W.Bekelman & R.L.Stenzel: Phys.Rev.Lett. 39 (1975) 1708.

57. C.J.K.Virmani, R.G.Gupta & V.K.Tripathi: Optik 40 (1974) 431.

58. D.Marcuse: Light Transmission Optics, Van Nostrand-Reinhold (1972).

59. S.Y.Yuen: App.Phys.Lett. 30 (1977) 223.

60. I.P.Shkarofsky, T.W.Johnston & M.P.Bachynski: The Particle Kinetics of Plasmas, Addison-Wesley (1966).

61. L.Spitzer Jr.: Physics of Fully Ionized Gases, Interscience (1962).

62. H.Margenau & G.M.Murphy: The Mathematics of Physics and Chemistry Vol.1, Van Nostrand (1955).

63. L.A.Pipes: Applied Mathematics for Engineers and Physicists, McGraw Hill (1958).

64. L.C.Steinhauer & H.G.Ahlstrom: Phys.Fluids 18 (1975) 541.

65. M.Kristiansen & M.O.Hagler: Nucl.Fusion 16 (1976) 999.

66. B.S.Tanenbaum: Plasma Physics, McGraw Hill (1967).

67. S.Ichimaru: Basic Principles of Plasma Physics A Statistical Approach, W.A.Benjamin (1973).

68. H.Washimi: J.Phys.Soc.Japan 34 (1973) 1373.

69. N.G.Loter, D.R.Cohn, W.Halverson & B.Lax: J.App.Phys. 46 (1975) 3302.

70. M.S.Sodha, R.P.Sharma, S.Kumar & V.K.Tripathi: Optica Acta 23 (1976) 305.

71. W.H.Manheimer & E.Ott: Phys.Fluids 17 (1974) 1413.

72. F.F.Chen: Laser Interaction and Related Plasma Phenomena Vol.3A, eds. H.J.Schwarz & H.Hora, Plenum (1974).

73. F.W.Perkins & J.Flick: Phys.Fluids 14 (1971) 2012.

74. M.N.Rosenbluth: Phys.Rev.Lett. 29 (1972) 565.

75. C.S.Liu, M.N.Rosenbluth & R.B.White: Phys.Fluids 17 (1974) 1211.

76. C.S.Liu: Advances in Plasma Physics Vol.6, eds. A.Simon & W.B.Thompson, John-Wiley (1976) 121.

77. J.J.Schuss: Phys.Fluids 20 (1977) 1121.

78. P.Guzdar, P.Kaw, Y.Satya, A.Sen, A.K.Sundaram & R.K.Varma: Plasma Physics and Controlled Nuclear Fusion Research 1974 Vol. 2, Proc. Fifth Conf. Tokyo, IAEA (1975).

79. M.Y.Yu, P.K.Shukla & K.H.Spatschek: Phys.Rev.A 12 (1975) 656.

80. S.S.Jha & S.Srivastava: Phys.Rev. A11 (1975) 378.

81. A.J.Palmer: Phys.Fluids 14 (1972) 2714.

82. P.Lallemand & N.Bloembergen: Phys.Rev.Lett. 15 (1965) 1010.

83. S.A.Korolyov, Z.A.Baskakova & B.V.Smirnov: Opt. Spect. 32 (1975) 195.

84. M.S.Sodha, R.K.Khanna & V.K.Tripathi: Phys.Rev. A12 (1975) 219.

85. M.S.Sodha, R.P.Sharma & S.C.Kaushik: J.App. Phys. 47 (1976) 3518.

86. T.A.Davydova & K.P.Shamrai: Plasma Phys.18 (1976) 947.

87. M.S.Sodha, S.C.Kaushik & R.P.Sharma: J.Plasma Phys. 18 (1977) 551.

88. V.E.Zakharov & A.B.Shabat: Sov.Phys. JETP 34 (1972) 62.

89. T.M.Makhviladze & M.E.Sarychev: Sov.Phys. JETP 44 (1976) 471.

90. Y.C.Lee, C.S.Liu, H.H.Chen & K.Nishikawa: Plasma Physics and Controlled Nuclear Fusion Research 1974 Vol.3, Proc.Fifth Conf.Tokyo, IAEA (1975) 207.

91. R.Rajaraman: Phys.Reports 21 (1975) 227.

92. R.Jackiw: Phys.Rev. D11 (1975) 1486.

93. M.B.Fogel, S.E.Trullinger, A.R.Bishop & J.A. Krumhansl: Phys.Rev.Lett. 36 (1976) 1411.

94. K.Nakajima, Y.Sawada & Y.Onodera: J.App.Phys. 46 (1975) 5272.

95. N.A.Krall & A.W.Trivelpiece: Principles of Plasma Physics, McGraw Hill (1973).

96. R.C.Davidson: Methods in Nonlinear Plasma Theory, Academic (1972).

97. S.Watanabe: J.Plasma Phys. 13 (1975) 217.

98. S.Watanabe: J.Plasma Phys. 14 (1975) 353.

99. I.Alexeff: Recent Advances in Plasma Physics, ed. B.Buti, Indian Academy of Sciences (1977) 131.

100. K.H.Spatschek, P.K.Shukla & M.Y.Yu: Phys.Lett 54A (1975) 419.

101. T.Ogino & S.Takeda: J.Phys.Soc.Japan 39 (1975) 1365.

102. J.Satsuma: J.Phys.Soc.Japan 40 (1976) 286.

103. S.G.Tagare: J.Plasma Phys. 14 (1975) 1.

104. K.Nishikawa & P.K.Kaw: Phys.Lett. 50A (1975) 455.

105. K.Ko & H.H.Kuehl: Phys.Rev.Lett. 40 (1978) 233.

106. T.Ikuta: J.Phys.Soc.Japan 41 (1976) 2105.

107. V.E.Zakharov & E.A.Kuznetsov: Sov.Phys.JETP 39 (1974) 285.

108. P.K.Kaw & K.Nishikawa: J.Phys.Soc.Japan 38 (1975) 1753.

109. P.I.John, Y.C.Saxena & R.P.Dahiya: Phys.Lett. 60A (1977) 119.

110. Y.C.Saxena: Recent Advances in Plasma Physics, ed. B.Buti, Indian Academy of Sciences (1977) 145.

111. M.S.Sodha & A.K.Ghatak: Inhomogeneous Optical Waveguides, Plenum (1977).

112. R.E.Aamodt & M.C.Vella: Phys.Rev.Lett. 39 (1977) 1273.

113. M.S.Sodha, P.Chandra & V.K.Tripathi: App.Phys. 11 (1976) 299.

114. M.Abramovitz & I.A.Stegun: Handbook of Mathematical Functions, Dover (1964).

115. J.B.Scarborough: Numerical Mathematical Analysis, JohnsHopkins (1966).

116. C.S.Liu & P.K.Kaw: Advances in Plasma Physics Vol.6, eds. A. Simon & W.B.Thompson, John Wiley (1976) 83.

117. A.Yariv: Quantum Electronics, John Wiley (1975).

118. P.M.Morse & F.H.Feshbach: Methods of Theoretical Physics, McGraw Hill (1953).

119. D.Cotter, D.G.Hanna & R.Wyatt: App.Phys. 8 (1975) 333.

BIODATA

L.A. Patel was born in Shertha on September 8, 1952. He obtained his school-education in Sardhav and Patan, and Pre-University-education in Ahmedabad. He received his B.Sc. degree from M.S.University, Baroda in 1973, and M.Sc. degree from Indian Institute of Technology, New Delhi in 1975. Since July 1975, he is a Ph.D. research scholar at I.I.T. New Delhi. He has obtained Govt. Open Merit School Scholarship (1962-69), National Merit Scholarship (1969-70) and National Science Talent Search Scholarship (1970 onwards), and has won three prizes for science-essay writing. He is a student member of the American Physical Society and the Institute of Electrical and Electronics Engineers.

REPRINTS/PREPRINTS

(List of Relevant Publications has been given in the Preface)

J. Plasma Physics (1977), *vol.* 18, *part* 3, *pp.* 381–389
Printed in Great Britain

Ion-acoustic solitons in an electromagnetically irradiated magnetoplasma

By L. A. PATEL
Department of Physics, Indian Institute of Technology,
New Delhi-110029, India

(Received 23 September 1976 and in revised form 12 April 1977)

We have investigated how the presence of an electromagnetic beam and a static magnetic field influences the ion-acoustic solitons in a plasma. A modified KdV equation is derived in which the electromagnetic field plays the role of a source term. By using the perturbation analysis technique, it is shown that a homogeneous electromagnetic beam does not destabilize the ion-acoustic solitons; it reduces the amplitude, but not the velocity, of the solitons. However, any inhomogeneity in the electromagnetic field intensity does destabilize the ion-acoustic solitons; albeit not to an appreciable extent for typical cases.

J. Phys. D: Appl. Phys., Vol. 11, 1978. Printed in Great Britain.

Effect of self-focusing on scattering of a laser beam in a collisional plasma

Lalit A Patel
Department of Physics, Indian Institute of Technology, New Delhi-110029, India

Received 22 July 1977

Abstract. The temporal growth rates of stimulated Raman and Brillouin scattering of a self-focused laser beam in a collisional plasma have been evaluated. The calculations predict a considerable spatial nonuniformity in the scattering because of the temperature and density gradients induced in the plasma on account of the nonuniformity of the pump laser beam.

J. Plasma Physics (1978), *vol.* 19, *part* 2, *pp.* 301–312
Printed in Great Britain

Self-focusing of a laser pulse in a transient plasma

By M. S. SODHA, D. P. TEWARI AND L. A. PATEL

Department of Physics, Indian Institute of Technology,
New Delhi-110029, India

(Received 5 September 1977 and in revised form 21 November 1977)

Following Akhmanov's approach, self-focusing of a laser pulse in a transient plasma has been studied. The beamwidth parameter and hence the laser intensity and the frequency shift (time derivative of the phase) have been evaluated as a function of time and the distance of propagation. It is seen that the time dependence of the axial intensity changes appreciably as the pulse propagates. The present investigation is restricted to a pulse whose incident intensity has Gaussian radial dependence.

Optical and Quantum Electronics **10** (*1978*) *189–194*

Temporal growth of a parametric excitation by a self-focused laser beam

LALIT A. PATEL
Department of Physics, Indian Institute of Technology, New Dehli–110029, India

Received 31 March 1977; revised 4 October 1977

The effect of self-focusing of the pump laser beam on the temporal growth of a parametric excitation has been investigated in the paraxial region. The two equations for the signal and idler modes have been decoupled by assuming the near self-trapping condition and a linearly varying phase mismatch. By employing the WKBJ approximation, it is found that the growth rate is a strong function of the radial intensity inhomogeneity of the pump laser beam. The condition for validity of the first-order approximate theory employed here has been derived.

Effect of nonlinear absorption on self-focusing of a laser beam in a plasma[a)]

M. S. Sodha, L. A. Patel, and R. P. Sharma

Department of Physics, Indian Institute of Technology, New Delhi-110029, India
(Received 16 December 1977; accepted for publication 7 February 1978)

Considering both the real and imaginary parts of the dielectric constant to be intensity dependent, we have investigated the self-focusing of a Gaussian laser beam in a plasma. The mechanism or nonlinearity considered herein is the ponderomotive force or heating mainly determined by collisions of electrons with heavier particles. An equation for the beamwidth parameter and an expression of the axial intensity have been obtained in the WKB(J) and paraxial approximations. It is seen that the effect of nonlinear absorption on self-focusing is significant. Consideration of nonlinearity in absorption predicts focusing of a laser beam (under certain conditions) even when the linear-absorption approximation would predict defocusing of the beam. The results reduce to the corresponding analytical results reported earlier, when the intensity dependence of the dielectric constant is neglected. The technique adopted in the present investigation for solving the wave equation in the presence of nonlinear absorption is equally applicable to media other than a plasma.

PACS numbers: 42.65.Jx, 52.40.Db

 0021-8979/78/4907-3707$01.10

Optik 50 (1978) No. 3, 243–247

Self induced transparency of a two-frequency pulse

Lalit A. Patel

Department of Physics, Indian Institute of Technology, New Delhi-110029, India

Received 17 October 1977

Abstract

The two modes of a two frequency electromagnetic pulse are parametrically coupled in a medium which is resonantly absorbing at these two frequencies. It is found that the pulse can pass undistorted provided the initial electric-field-amplitude E_{l0} be large enough, and the effective refractive index $(\eta_l + 4\pi\hbar\omega_l n_l/\eta_l \bar{E}^2_{l0})$ be the same for both the modes.